Theses and Dissertations   Theses, Dissertations, and Senior Projects

January 2021

Effects Of HIV-1 Gp120 On Intracellular Levels Of Iron And Reactive Oxygen Species: Implications For Lysosomal Stress

Koffi L. Lakpa

[How does access to this work benefit you? Let us know!](#)

Follow this and additional works at: https://commons.und.edu/theses

EFFECTS OF HIV-1 GP120 ON INTRACELLULAR LEVELS OF IRON AND
REACTIVE OXYGEN SPECIES: IMPLICATIONS FOR LYSOSOMAL STRESS

by

Koffi Leo Lakpa

Bachelor of Science, University of North Dakota - 2016

A Dissertation

Submitted to the Graduate Faculty

of the

University of North Dakota

In partial fulfillment of the requirements

for the degree of Doctor of Philosophy in Biomedical Sciences

Grand Forks, North Dakota

August

2021

Name: Koffi Leo Lakpa

Degree: Doctor of Philosophy

This document, submitted in partial fulfillment of the requirements for the degree from the University of North Dakota, has been read by the Faculty Advisory Committee under whom the work has been done and is hereby approved.

Jonathan D. Geiger

Xuesong Chen

Colin Combs

Junguk Hur

Jau-Shin Lou

This document is being submitted by the appointed advisory committee as having met all the requirements of the School of Graduate Studies at the University of North Dakota and is hereby approved.

Chris Nelson
Dean of the School of Graduate Studies

5/18/2021

Date

PERMISSION

Title: Effects of HIV-1 gp120 on Intracellular Levels of Iron and Reactive
             Oxygen Species: Implications for Lysosomal Stress

Department: Biomedical Sciences

Degree: Doctor of Philosophy

In presenting this dissertation in partial fulfillment of the requirements for a

graduate degree from the University of North Dakota, I agree that the library of

this University shall make it freely available for inspection. I further agree that

permission for extensive copying for scholarly purposes may be granted by the

professor who supervised my dissertation work, or in her absence, by the

Chairperson of the department or the dean of the School of Graduate Studies. It

is understood that any copying or publication or other use of this dissertation or

part thereof for financial gain shall not be allowed without my written permission.

It is also understood that due recognition shall be given to me and to the

University of North Dakota in any scholarly use which may be made of any

material in my dissertation.

<div align="right">
Koffi Leo Lakpa
August, 2021
</div>

TABLE OF CONTENTS

vi

LIST OF FIGURES

LIST OF TABLES

ACKNOWLEDGEMENTS

Dr. Chen is his calm nature. No matter how poorly an experiment turned out, when I went to him for help he always was patient with me. Thank you.

I would like to thank my other committee members: Drs. Hur, Combs, and Lou. It has been a pleasure having you on my committee and being able to come to you when I have questions or concerns. Dr. Hur, I would like to thank you for taking the time to help me with some of my statistical analyses for my HIV-1 gp120 project. Dr. Combs, thank you for encouraging me during my time as a graduate student. Dr. Lou, thank you for your words that suck with me about enjoying my time as a researcher because it is one of the few times when one gets to explore their intellectual interest; I took those words to heart. During my last 2 years I dove into my work and attempted to explore my research questions. Thank you.

To all the members of the Geiger/Chen lab, past and current, I want to say thank you. Drs. Liang Hui and Mahmoud Soliman thank you for taking me under your wings early on and helping me develop my hands in the laboratory. You were both very kind and gave me a lot of useful advice. Thank you.

My dear brother, Dr. Nabab Khan there's a lot I have to thank you for but I'll just express a few of those things here. You have been instrumental in my development as a trainee. I watched you come into lab Monday through Sunday and work relentlessly to generate data, write papers, and begin establishing your career. Thank you for taking the time to train me. There's a joy and passion you have in regards to research that rubbed off on me. It made me want to improve my skills as a researcher. You were able to show me that a scientist is someone

who can generate ideas and hypotheses, and then test and interpret them. Although that concept is simple it's difficult to carry it out in practice. I had a front row to seat to what that process looked like on a day to day basis. You never cease to surprise me with your productivity and your humbleness. I will always say this, you are a mad scientist and my productivity was heavily tied to yours. So, thank you for letting me be a part of your work and helping to grow my abilities.

 Drs. Gaurav Datta and Peter Halcrow, it's been a pleasure to work with you. To our undergraduate research assistants thank you for coming in to work and helping us keep our laboratory tidy and organized. I would like to thank Mika Bordak, Jacquelyn McCleary, and Jalyn Fischer; the three of you did a tremendous job at your tasks and also helped me with various experiments. Thank you.

I have to give a huge shout out to my classmates: Matt Ficks, Sarmad Al-Marsoummi, Zahra Afghah, Smruthi Rudraraju, and Nicole Miller. I am very fortunate for the bond we developed over the past 5 years. When I started graduate school, I had no idea that I would gain two brothers and three sisters in this process. All of you hold a special place in my heart. You guys have been my wise counsel. We've laughed, we've cried, and we've argued. A lot of conversations about politics and religion have been discussed at Matt's apartment. We've watched hours of television at Sarmad's. We've eaten a lot of food at Nicole's, Smruthi's, and Zahra's. We've been through a lot in our time in

graduate school and I look forward to seeing where all of your careers go. Thank you.

Another person I would like to thank is Bonnie Kee. She has been a great friend and confidant. I appreciate all of our talks and the constant guidance you gave me throughout my time in the Biomedical Sciences program. Bonnie forced me to stay organized and kept me from getting into a lot of trouble. In regards to my dissertation Bonnie has spent hours upon hours of her time, early mornings and on weekends, helping me format my dissertation. She has been a tremendous help and I cherish our friendship dearly. Thank you.

Lastly, I'd like to thank my family. Mom and Dad thank you for raising, caring, and instructing me on how to be a man and how to go out and serve your neighbor in your vocation. It is a honor to be your son. Shirley and Michael-David thank you for giving me a reason to keep pushing forward and forcing me to be a leader. I am proud to be your brother. Thank you.

Now, last and certainly not least, I would like to thank my wife, Leah. My dear, thank you for all of your love and support. You have listened to my rants about failed experiments and given me perspective whenever I needed it. Over these past three years I know I've missed a lot of time with you. I want to thank you for your patience and understanding. I love you bean. Thank you.

I'll end by paraphrasing Aristotle, "one can never sufficiently thank or repay their teachers, mentors, and parents."

ABSTRACT

Approximately 1.2 million people in the U.S.A are living with HIV-1. The development of antiretroviral therapeutics has increased the life expectancy of people living with HIV-1 (PLWH). Yet, there is a growing concern for aging HIV-positive individuals because about 50% of PLWH develop neurological impairments, termed HIV-associated neurocognitive disorders (HAND). There are no treatments for HAND and the mechanisms underlying its pathogenesis remain unclear. Several factors are implicated in HAND pathogenesis, such as HIV-1 coat protein gp120, endolysosome and mitochondrial dysfunction, and elevated levels of reactive oxygen species (ROS). Endolysosomes are acidic organelles that contain readily releasable stores of cations, such as iron, which can be released upon de-acidification. Mitochondria are energy producing organelles, which can also act as cellular sinks for iron when levels of cytosolic iron are elevated. Iron is an essential metal for human life, but it is tightly regulated due to its ability to generate ROS through Fenton or Fenton-like reactions. HIV-1 gp120 increases ROS production, de-acidifies endolysosomes and reduces mitochondrial respiration. We used U87MG astrocytoma cells, confocal microscopy, flowcytometry, filter-based imaging, and western blotting to investigate mechanisms by which HIV-1 gp120 affects endolysosome iron stores, levels of ROS, and the effects of gp120 on expression levels of iron related

proteins. In Chapter 2, we describe findings that HIV-1 gp120 de-acidifies endolysosomes, induced iron release from endolysosomes, increased iron levels in mitochondria, and that iron from endolysosomes led to increases in levels of cytosolic and mitochondrial ROS levels. Our findings suggest that endolysosome iron stores can be upstream of HIV-1 gp120 induced increases in ROS production. In Chapter 3, we described findings about the responsiveness of our cells to iron supplementation and chelation, as well as how HIV-1 gp120 affects expression levels of iron related proteins. We found that 24 h treatment with HIV-1 gp120 increased the cell surface expression levels of ferroportin (FPN), an iron export protein, but we did not observe any changes in other iron related proteins. Our findings might suggest that U87MG cells increase cell surface FPN in order to regulate cytosolic iron levels. We considered our findings from Chapter 2 and 3 as evidence that HIV-1 gp120 induces lysosomal stress. In Chapter 4, we outlined a new concept in understanding how endolysosomes adapt to their environment during different stress inducing events; this was termed "lysosome stress response" (LSR). We provided criteria and a working definition for LSR. We also highlighted how LSR is observed in other organellar stress responses. Taken together, these findings provide a mechanism by which HIV-1 gp120 affects ROS production. Moreover, this work highlights endolysosomes as a potential upstream therapeutic target for any disease in which elevated ROS is implicated and broadens our understanding of cellular biology.

CHAPTER 1

INTRODUCTION

A Brief History of HIV/AIDS

Globally, human immunodeficiency virus (HIV) has infected over 75 million

people. There are currently 38 million people living with HIV (PLWH). In the USA,

the first reports of acquired immune deficiency (AIDS) were made in 1981

(Gottlieb et al., 1981; Masur et al., 1981). Two years later, HIV was isolated and

identified as the causative agent of AIDS (Barre-Sinoussi et al., 1983; Gallo et

al., 1984). There are two main types of HIV: HIV-1 and HIV-2. HIV-1 is the more

pathogenic strain and is the focus of our work (Deeks, Overbaugh, Phillips, &

Buchbinder, 2015).

HIV-1 Replication Cycle

HIV-1 is a retrovirus that is composed of two copies of single-stranded RNA

(ssRNA). The viral genes and other integral proteins necessary for viral

replication are enclosed by a capsid composed of the viral protein p24. The

capsid is further enclosed by a viral envelope glycoprotein (gp) complex, gp160,

which is comprised of gp120 and gp41 (German Advisory Committee Blood,

2016). The primary receptor for HIV-1 is CD4, which is expressed on the surface

of T-lymphocytes, monocytes, macrophages and dendritic cells (Deeks et al.,

2015). HIV also uses co-receptors, chemokine receptors CCR5 and CXCR4, to

enter target cells (Connor, Sheridan, Ceradini, Choe, & Landau, 1997). Once the

virus has attached to the proper receptors it undergoes fusion and uncoating

events which allows it to release its proteins and ssRNA into the cytoplasm. Then

using its reverse transcriptase enzyme, the ssRNAs are reverse transcribed into

viral DNA, which is then transported into the nucleus and integrated into the host

genome (German Advisory Committee Blood, 2016). After genomic integration of

viral DNA, it is transcribed into viral mRNA by host cell transcription machinery.

Then the newly transcribed viral mRNA is exported into the cytosol where it is

translated into viral proteins, assembled, and packed into a new virion (German

Advisory Committee Blood, 2016). Virions mature and bud from host cell

membranes. Viral proteins are then cleaved by a viral protease finally forming

mature virus.

Clinical Progression of HIV-1 Infection

There are three stages that describe the clinical course of HIV infection;

1) primary infection, 2) clinical latency, and 3) AIDS (Pantaleo & Fauci, 1996).

During primary infection HIV RNA levels are detectable in the blood, which leads

to an adaptive immune response which is partially effective in reducing initial viral

load (Pantaleo & Fauci, 1996). At this point infected persons can enter into a

latency phase that can last from a few months to years even in the absence of

treatment (Deeks et al., 2015; Pantaleo & Fauci, 1996). As time goes on during

the latency period, PLWH progressively lose CD4$^+$ T cells and begin to exhibit

symptoms of chronic inflammation (Deeks et al., 2015). Eventually, the CD4$^+$

T cell count drops to the point where PLWH exhibit AIDS. The brains of AIDS

patients are susceptible to infections such as cryptococcal and tubercular

meningitis, toxoplasma encephalitis, and progressive multifocal leukoencephalopathy (Clifford & Ances, 2013; Deeks et al., 2015). The development of effective antiretroviral therapeutics (ART) has greatly reduced the incidence of AIDS and its associated complications.

Development of Antiretroviral Therapy

In the late 1990s and into the 2000s there were great advances in the development of anti-HIV-1 drugs. ARTs are not a cure for HIV-1; however, it has been successful in suppressing viral replication (Arts & Hazuda, 2012). Indeed, ART has made living with HIV-1 a manageable chronic disease (Arts & Hazuda, 2012). These drugs have prolonged the lives of PLWH by decades (Antiretroviral Therapy Cohort, 2017).

ARTs inhibit various stages of the HIV life cycle (Arts & Hazuda, 2012). There are 6 classes of ARTs; 1) non-nucleoside reverse transcriptase inhibitors, 2) nucleoside reverse transcriptase inhibitors, 3) integrase inhibitors, 4) protease inhibitors, 5) entry inhibitors, and 6) co-receptor antagonists (Arts & Hazuda, 2012; Pau & George, 2014). Although these drugs are effective in suppressing the spread of HIV-1, they are not able to eliminate the virus completely from already infected cells (Arts & Hazuda, 2012). ART regimens are strict and PLWH must adhere to them daily for the rest of their lives. If the drugs are not taken consistently there is a chance for a re-spreading of the virus. Previously, ARTs were burdensome to PLWH because they had to take multiple pills every day. Today, the development of combined ART (cART) in a single pill has helped with the very real issue of adherence to the treatment regimen (Arts & Hazuda, 2012).

Despite, their effectiveness, these ARTs are not very effective at crossing the blood brain barrier (BBB) and this leaves the brain as a potential reservoir site for the virus. (Scutari, Alteri, Perno, Svicher, & Aquaro, 2017). Despite extensive efforts to increase the brain penetrance of cART this continues to be a major limitation of these treatment strategies. (Fiandra, Capetti, Sorrentino, & Corsi, 2017; Letendre et al., 2008).

HIV-1 in the Brain

During early stages of HIV-1 infection, the virus invades the central nervous system (CNS) and targets microglia and to a lesser extent astrocytes (An, Groves, Gray, & Scaravilli, 1999; Ellis et al., 1997; Price & Brew, 1988). Because of the BBB, ARTs have low brain penetrance (Scutari et al., 2017). This issue has led some researchers to suggest that the brain may behave as a reservoir for HIV-1 (Gray et al., 2014). Although debated within the field, astrocytes have been suggested as harbors of HIV-1 (Al-Harthi, Joseph, & Nath, 2018). One mechanism for HIV-1 uptake into astrocytes is endocytosis (Chauhan, Mehla, Vijayakumar, & Handy, 2014). Others have shown that lysosomotropic agents such as chloroquine, which blocks endosome maturation, leads to an increased detection of HIV-1 DNA and p24 in astrocytes (Vijaykumar, Nath, & Chauhan, 2008). Recently, one group demonstrated *in vivo* that astrocytes can be infected with HIV-1 and even infect peripheral tissue through trafficking of infected CD4^{+} T cells out of the brain, even in the presence of cART (Lutgen et al., 2020). Neurons cannot be infected by HIV-1 but they are vulnerable to damage caused by soluble factors such as HIV-1 proteins transactivator of transcription (Tat) and

gp120, which are both secreted from infected cells. These HIV-1 proteins are likely contributors to the pathogenesis of HIV-1 associated neurocognitive disorders (HAND) (Ru & Tang, 2017; Scutari et al., 2017).

HIV-Associated Neurocognitive Disorder

Approximately, 19 million people worldwide are affected by HAND, which is an overarching term for neurological impairment in PLWH (Antinori et al., 2007; Clifford & Ances, 2013). Clinical manifestations of HAND range from asymptomatic (mild) to dementia (severe) (Clifford & Ances, 2013). HAND is subclassified into 3 categories, in order of most severe to least severe; HIV-associated dementia (HAD), mild neurocognitive disease (MND), and asymptomatic neurocognitive impairment (ANI) (Antinori et al., 2007). When AIDS is left untreated, a subset of patients develop HAD, which is characterized by dementia resembling that observed in late stage Alzheimer's and Parkinson's disease (Navia, Cho, Petito, & Price, 1986; Navia, Jordan, & Price, 1986; Snider et al., 1983). Since the advent of cART, HAND severity has shifted toward milder forms (Dore et al., 1999; Dore et al., 2003; McArthur, Steiner, Sacktor, & Nath, 2010). MND and ANI are categorized based on neuropsychometric testing abnormalities with or without functional impairment in activities of daily living (Clifford & Ances, 2013). During the cART era, MND and ANI patients have more impairments in learning, memory, and executive function; contrasted to HAD patients which exhibit deficits in attention and concentration, and motor and behavioral dysfunction (Heaton et al., 2011; Navia, Jordan, et al., 1986; Snider et al., 1983). There is no treatment for HAND and as PLWH continue to age there is

a growing concern to understand the interplay between HIV-1 in the brain of aging PLWH (High et al., 2012). Therefore, it is important to gain a better understanding of the underlying mechanisms of HAND pathogenesis with the hope of discovering effective therapeutic interventions.

As previously mentioned, the prevalence of HAND continues to rise despite ARTs effectively control of HIV-1 replication (McArthur et al., 2010). Furthermore, throughout the body (including the brain), ARTs do not completely eliminate HIV-1 or the production of HIV-1 neurotoxic proteins (T. P. Johnson et al., 2013; Popovic et al., 2005). Further complicating therapeutics, cARTs are neurotoxic and induce oxidative stress (Louboutin & Strayer, 2014; Sharma, 2014; Turchan et al., 2003). HIV-1 proteins such as Tat and gp120, which can be secreted from infected cells are implicated in the pathogenesis of HAND (Scutari et al., 2017). HIV-1 Tat induces excitotoxicity, synaptodendritic damage, increase in cytosolic calcium levels, endoplasmic reticulum (ER) stress, and apoptosis in neurons (Fan & He, 2016; Haughey, Holden, Nath, & Geiger, 1999; Haughey, Nath, Mattson, Slevin, & Geiger, 2001; Shin & Thayer, 2013; Zucchini et al., 2013). Furthermore, Tat induces an upregulation of glial fibrillary acidic protein (GFAP) which leads to oxidative stress in astrocytes (Fan & He, 2016). Likewise, HIV-1 gp120 induces neuronal damage, neuroinflammation and disrupts autophagy (L. Chen et al., 2011; El-Hage, Podhaizer, Sturgill, & Hauser, 2011; J. Fields et al., 2013). Moreover, the interaction between gp120 and its receptor CXCR4 is suggested to play a role in CNS mediated damage (Scutari et al., 2017; J. Zhang, Liu, Katafiasz, Fox, & Xiong, 2011). Also included in the contributors of

HAND pathogenesis are subcellular organelles including endolysosomes and mitochondria (J. A. Fields et al., 2016; Gelman et al., 2005).

Endolysosomes

The discovery of the lysosome was a serendipitous affair (de Duve, 2005). This story began with a Belgian biochemist by the name of Christian de Duve who was interested in understanding the effects of insulin on the liver. In 1951, the de Duve laboratory identified glucose-6-phosphatase to be attached to an acidic precipitable cellular structure. It just so happened that in 1946, a group developed a centrifugal fractionation method which allowed researchers to separate four different fractions from cells; 1) nuclear fraction, 2) large granule fraction which contained mitochondria, 3) a small-granule fraction termed microsomes, and 4) supernatant (Claude, 1946a, 1946b). This new method made way for the de Duve laboratory to eventually identify acid phosphatase in a membrane enclosed sac (de Duve, 2005). By 1955, this group identified other enzymes within this membrane sac and gave it the name lysosome which is Greek for "lytic" "body" (de Duve, 2005). Three years later, lysosomes were being identified in other cell types and was found to be involved in digestion of endocytosed material (de Duve, 2005). More recently, research has uncovered a more expansive role of lysosomes in cells. Lysosomes are involved in cation homeostasis, nutrient sensing, plasma membrane repair, immune response, and bone resorption through lysosomal exocytosis (Ballabio, 2016; Ballabio & Bonifacino, 2020; Perera & Zoncu, 2016; Settembre & Ballabio, 2014; H. Xu & Ren, 2015).

The greater lysosomal system is comprised of endosomes, multivesicular bodies (MVB), lysosomes, autophagosomes and autolysosomes (Huotari & Helenius, 2011). Endosomes and lysosomes, referred to as endolysosomes, are single membrane, acidic vesicles, which contain over 60 hydrolases that function at a low pH. These organelles range in size from about 0.5-1.5 nm (H. Xu & Ren, 2015). The luminal pH of endolysosomes varies between about 4.5 to 6.0 (H. Xu & Ren, 2015). Endolysosomes use various membrane-resident channels and pumps to maintain their acidic luminal environment (Colacurcio & Nixon, 2016; Steinberg et al., 2010; Trivedi, Bartlett, & Pulinilkunnil, 2020). Endolysosomes contain various divalent cations such as Fe^{2+}, Zn^{2+}, Ca^{2+}, Mn^{2+}, and Cu^{2+} (H. Xu & Ren, 2015). Central to endolysosome function is its ability to maintain its luminal pH, and insults that lead to an increase in endolysosome pH often result in organellar and cellular dysfunction. Endolysosome deacidification induces the release of calcium and iron from these organelles (Christensen, Myers, & Swanson, 2002; Fernández et al., 2016).

Mitochondria

In 1890, Richard Altman identified a ubiquitous bacterium resembling structure in cells, which he termed "bioblast." Carl Benda coined these bioblasts as mitochondria which is Greek for "thread" "granules" (Ernster & Schatz, 1981; Pagliarini & Rutter, 2013). Structurally, mitochondria are organized into four main parts; 1) an outer mitochondrial membrane (OMM), 2) inner mitochondrial membrane (IMM), 3) intermembrane space (the space between OMM and IMM), and 4) matrix (space within IMM) (Ernster & Schatz, 1981). Moreover, the IMM

contain folds termed cristae, which function to increase the surface area of mitochondria and are sites of oxidative phosphorylation (Ernster & Schatz, 1981). Mitochondria function to produce energy for various processes throughout cells (Brand, 2005; Ernster & Schatz, 1981). Indeed, in our parlance mitochondria are known as the "powerhouse of the cell."

Within the mitochondrial matrix and on the IMM two biochemical processes occur which aid the production of energy in the form of adenosine triphosphate (ATP) (Brand, 2005). The tricyclic acid cycle (TCA), also known as the Krebs cycle, occurs within the mitochondrial matrix (Alabduladhem & Bordoni, 2021). The TCA is a series of eight enzymatic steps which consumes and produces citrate, amongst other molecules. As citrate becomes oxidized and other molecules are formed two reducing agents are formed, nicotinamide adenine dinucleotide hydride (NADH) and flavin adenine dinucleotide, hydroquinone form ($FADH_2$) (Alabduladhem & Bordoni, 2021). These reductants are used as electron donors to the electron transport chain (ETC). Oxidative phosphorylation is the process by which ATP is formed (Brand, 2005). The ETC is comprised of four complexes and an ATP synthase (Brand, 2005). NADH donates electrons to complex I which drives protons (H^+) from the mitochondrial matrix into the IMS. Similarly, $FADH_2$ donates electrons to complex II, which also leads to H^+ translocation to the IMS. As this process continues there is a buildup of H^+ within the IMS promoting a proton motive force which is an electrochemical gradient of H^+ that drives protons back into the mitochondrial matrix through the ATP synthase protein (Brand, 2005). As the ATP synthase protein coverts ADP to ATP, oxygen,

which enters the mitochondrial matrix, is used as a final electron acceptor forming H_2O (Brand, 2005). During oxidative phosphorylation, as electrons are being transferred to complex I, II, and III, mitochondria can produce ROS, which can lead to oxidative damage of lipid, DNA, and proteins (Kausar, Wang, & Cui, 2018; Quinlan, Perevoshchikova, Hey-Mogensen, Orr, & Brand, 2013). In addition, mitochondria play a large role in iron metabolism (D. R. Richardson et al., 2010). Indeed, the mitochondrial matrix is also the only site for heme synthesis, which is an important component of hemoglobin, and a major site for iron sulfur cluster formation (D. R. Richardson et al., 2010).

Iron Metabolism

Systemic Iron Regulation

Iron is an essential element that plays a major role in human physiology such as oxygen transport, energy production, DNA replication, cell proliferation, and immunity (Muckenthaler, Rivella, Hentze, & Galy, 2017; Wallace, 2016). Approximately 2 mg of iron is absorbed daily by enterocytes in the small intestine (Wallace, 2016). Humans derive iron from their diet. Iron in the diet can be found in the form of heme or non-heme iron (Wallace, 2016). Heme iron is transported into enterocytes via a heme transporter, potentially, heme carrier protein 1 or receptor-mediated endocytosis (Gulec, Anderson, & Collins, 2014). In order for iron to be taken into enterocytes it must be in its reduced oxidative state, ferrous iron (Fe^{2+}). Non-heme iron in our diet, e.g. meat and plants, is usually in its oxidative state, ferric iron (Fe^{3+}) (Gulec et al., 2014). Therefore, enterocytes have a membrane bound ferric reductase enzyme that is located on the apical brush

broader membrane that can reduce Fe^{3+} to Fe^{2+}. Once iron is reduced, it is transported by divalent metal transporter 1 (DMT1) across the apical brush broader of enterocytes. Intracellularly, ferrous iron has multiple fates. It can be taken up into the mitochondrial matrix where it is used to synthesize heme and iron-sulfur clusters (D. R. Richardson et al., 2010). Because Fe^{2+} has the ability to generate free radicals through Fenton chemistry (Figure 1), it is also stored within an iron storage protein ferritin (FTN) which is found in the cytosol and mitochondrial matrix. Fe^{2+} can be transported to FTN via a chaperone protein; poly-r(C) binding proteins (Shi, Bencze, Stemmler, & Philpott, 2008). Intracellular Fe^{2+} has a third fate, it can be exported out from cells and into the circulation. In order for Fe^{2+} to enter circulation it needs to pass through the basolateral membrane of intestinal enterocytes. There is only one known iron exporter, ferroportin (FPN) which resides on the basolateral membrane of enterocytes or the surface of other cells (Abboud & Haile, 2000; Donovan et al., 2005; Gulec et al., 2014). Ferroportin is negatively regulated by hepcidin, which is a hormone secreted by the liver (Donovan et al., 2005). Fe^{2+} released from enterocytes through FPN must be oxidized before it is transported; a copper-containing ferroxidase enzyme hephaestin is involved in this oxidizing process. When iron is in its oxidized form it can bind to the iron transport glycoprotein transferrin (TF), which has a high affinity for two Fe^{3+} ions. The binding of Fe^{3+} to transferrin prevents the formation of Fe^{3+} hydrolysis which produces insoluble ferric hydroxides (D. R. Richardson et al., 2010).

Figure 1.   The Fenton reaction was discovered by H.J.H. Fenton. He determined that oxidation of ferrous iron or the reduction of ferric iron in the presence of hydrogen peroxide catalyzes a reaction that produces hydroxy free radicals. Moreover, a reaction between two hydrogen peroxide molecules can catalyze the production of hydroxyl radicals. This image was obtained from https://www.chemistrylearner.com/fenton-reaction.html

Fenton Reaction

$$Fe^{2+} + H_2O_2 \longrightarrow Fe^{3+} + HO\cdot + OH^{-}$$

Ferrous   Hydrogen   Ferric   Hydroxyl   Hydroxyl
peroxide   radical

$$Fe^{3+} + H_2O_2 \longrightarrow Fe^{2+} + HOO\cdot + H^{+}$$

Hydroperoxyl   Proton

$$2\,H_2O_2 \longrightarrow HO\cdot + HOO\cdot + H_2O$$
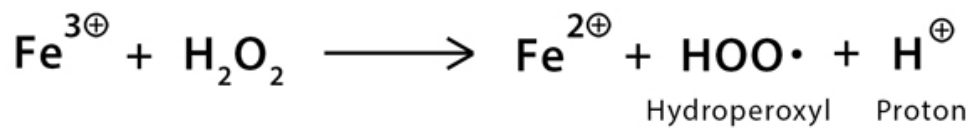
Cellular Iron Regulation

The diferric-transferrin (Fe_2-TF) complex is internalized into cells via receptor-mediated endocytosis by transferrin receptors (TFR). There are two forms of transferrin receptors, TFR1 and TFR2. TFR2 is primarily expressed in the liver and is unresponsive to intracellular iron levels, while TFR1 is ubiquitously expressed and responsive to intracellular iron levels (Kawabata et al., 2001). Moreover, TFR1 has a higher affinity for Fe_2-TF. In cells, once the Fe_2-TF/TFR1 complex is endocytosed into endosomes the iron dissociates from TF due to the low endolysosome pH (Dunn, Suryo Rahmanto, & Richardson, 2007; Ponka, 1997). The dissociated Fe^{3+} is then reduced to Fe^{2+} by the six-transmembrane epithelial antigen of prostate 3 (STEAP3), an endolysosome resident ferrireductase. After being reduced, Fe^{2+} can then be transported into the cytosol via endolysosome permeable channels such as divalent metal transporter 1 (DMT1) or transient receptor potential mucolipin 1 (TRPML1) (X. P. Dong et al., 2008; Gruenheid et al., 1999). The Fe^{2+} released from endolysosomes becomes part of the liable iron pool (LIP), which is defined as the collection of iron that can move between proteins and small molecules because it is not bound to proteins (Ackerman, Lee, & Chang, 2017). In contrast, the static iron pool is understood as iron bound or incorporated into certain proteins (Ackerman et al., 2017). For example, in order to prevent Fe^{2+} from undergoing Fenton chemistry, cells use the iron storage protein FTN. FTN is a 12- to 24-mer protein that has two subunits a heavy chain (FTH) and a light chain (FTL). FTH has ferroxidase activity allowing iron to be stored in its biologically inactive form. Ferritin can bind up to 4500 iron ions and serves as a major depot for iron (Muckenthaler et al.,

2017). When LIP levels are low, ferritin can be degraded via lysosomes and the iron can be released into the cytosol for cellular use (Kurz, Eaton, & Brunk, 2011). As described above, free iron can also be taken up mitochondria, where it can be incorporated into hemeproteins or iron sulfur clusters. As previously mentioned, mitochondria contain their own ferritin (Ftmt) (D. R. Richardson et al., 2010); one study showed that an overexpression of Ftmt decreased cytosolic iron levels, increased TFR1 levels, and increased mitochondrial iron loading. Thus, mitochondria act as cellular sinks for iron (Nie, Sheftel, Kim, & Ponka, 2005).

Brain Iron Metabolism

The brain, like other organs, requires iron for metabolic processes. The brain parenchyma is made up of astrocytes, which are the most abundant brain cell type and function to maintain brain homeostasis and structural support; neurons, which send electrochemical messages back and forth; oligodendrocytes, which myelinate neuronal axons; microglial cells, which provide phagocytosis; and pericytes, which aid in the formation of brain blood vessels and the maintenance of the BBB. Iron transport into the brain is largely mediated by the BBB, which protects the brain from iron overload (Mills, Dong, Wang, & Xu, 2010). Iron accumulation is observed in aging adults and is one of the known causes of neurodegenerative diseases (Ashraf, Clark, & So, 2018; Ke & Qian, 2007; Moos, Rosengren Nielsen, Skjorringe, & Morgan, 2007). Therefore, similar to peripheral tissues the cells of the CNS have developed extensive regulatory mechanisms to maintain iron levels.

The BBB is comprised of brain vascular endothelial cells (BVECs), which are joined by tight junctions (Daneman & Prat, 2015). BVECs have a luminal membrane and an abluminal membrane, which is enclosed by astrocyte end foot processes (Daneman & Prat, 2015). Ultimately, the BBB forms a physical barrier to the exchange of material between blood, brain tissue, and fluids (Daneman & Prat, 2015). TFR1 is localized on the luminal side of BVECs and mediates transferrin bound iron endocytosis into BVECs (Mills et al., 2010). There is also a non-transferrin-bound iron (NTBI) entry through vesicular and non-vesicular import mechanisms, one of which being through serum FTN and potential FTN receptors on BVECs (Mills et al., 2010) (Figure 2). However, it remains unclear whether that mode of transport is possible and additional work is required to characterize different types of NTBI entry into BVECs. In regards to transferrin bound iron, although still unclear, it has been suggested that channels such as TRPML1 and DMT1 might release endolysosome iron into the cytosol (Mills et al., 2010).

The end foot processes of astrocytes surround the BVECs also form connections with neurons (Daneman & Prat, 2015). Therefore, astrocytes play a pivotal role in regulating iron influx into the brain parenchyma from brain circulation (Mills et al., 2010). Uptake of iron into neurons is suggested to be through DMT1 or TFR1 (Ashraf et al., 2018; Dringen, Bishop, Koeppe, Dang, & Robinson, 2007; Qian, To, Tang, & Feng, 1999). Microglia phagocytose cells and in doing so release iron from ferritin or iron related proteins (Mills et al., 2010). Oligodendrocytes rely on T-cell immunoglobulin and mucin domain (Tim-2), a ferritin receptor, to take

Figure 2.   Iron transport across the blood brain barrier. A schematic
                depicting the transport of iron-bound transferrin across the blood
                brain barrier (BBB). On the luminal side of brain vascular
                endothelial cells (BVECs), transferrin (TF) bound ferric iron is
                taken up into endosomes by transferrin receptor (TF). Once
                within endosomes, ferric iron is released from transferrin where it
                can then be converted into ferrous iron via endolysosome
                resident ferrireductases. Iron can be released from endosomes
                into the cytosol via divalent metal transporter 1 (DMT1) or
                endosomes containing iron can undergo exocytosis and release
                ferric iron into the perivascular space. Iron that is released into
                the cytosol is released by iron exporter ferroportin (FPN) located
                on the abluminal membrane of BVECs. Once within the brain
                parenchyma ferrous iron is converted to ferric iron which can
                form complexes with citrate, ATP or ascorbate. Iron can be taken
                up by the various cells in the brain parenchyma such as
                astrocytes, oligodendrocytes, and neurons. This image is cited
                from (Mills et al., 2010).
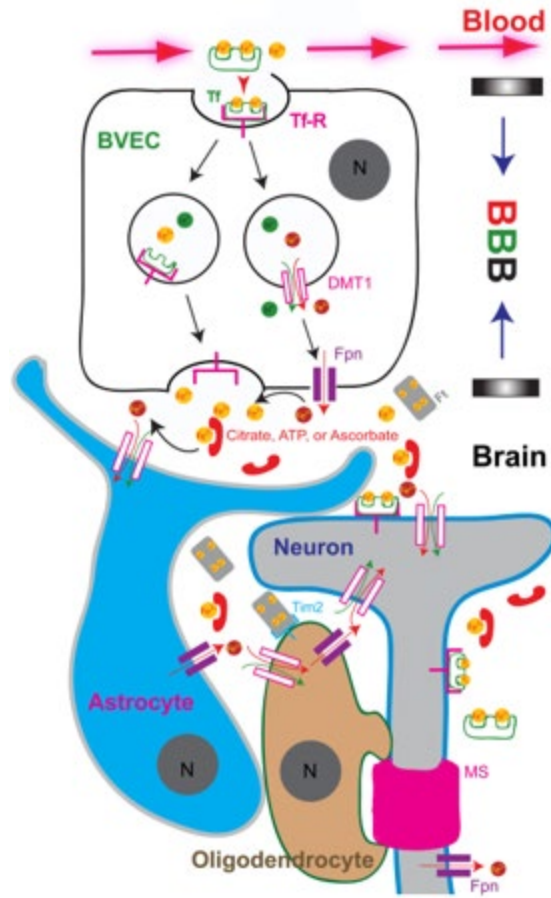
up NTBI (Mills et al., 2010). Iron export from brain parenchymal cells is the same as in peripheral tissues, it is mediated by ferroportin which works in concert with ceruloplasmin, a cooper-containing ferroxidase enzyme (Mills et al., 2010).

ROS Production and Oxidative Stress

Oxidative stress occurs when there is an imbalance between pro-oxidants and anti-oxidants within cells. There are nitrogen and oxygen derived pro-oxidants (Di Meo, Reed, Venditti, & Victor, 2016). In our studies, we focused primarily on oxygen derived pro-oxidants, which are highly reactive and are generally termed ROS (Kohen & Nyska, 2002). Superoxide radicals ($\cdot O_2^-$), hydrogen peroxide (H_2O_2), and hydroxyl radicals ($\cdot OH$) are commonly defined as ROS. Intracellularly, there are various locations where ROS is produced. A majority of ROS is produced in the mitochondria (Diebold & Chandel, 2016). For example, during oxidative phosphorylation as electrons are being passed along complexes I, II, and III $\cdot O_2^-$ is generated (Nickel, Kohlhaas, & Maack, 2014; Quinlan et al., 2013). Specifically, complex I and II generate $\cdot O_2^-$ in the mitochondrial matrix, while complex III produces $\cdot O_2^-$ in the matrix and IMS (Muller, Liu, & Van Remmen, 2004; Turrens, 2003). The superoxide produced in the IMS can be exported into the cytosol through the voltage-dependent anion channels (VDACs), which are located on the OMM. Within the mitochondrial matrix there is a superoxide dismutase 2 (SOD2) that quickly converts $\cdot O_2^-$ into H_2O_2, while cytosolic SOD1 converts $\cdot O_2$ released by complex III into H_2O_2 (Weisiger & Fridovich, 1973) (Figure 3). In the cytosol, Fe^{2+} can participate in the Fenton reaction ($Fe^{2+} + H_2O_2 \rightarrow Fe^{3+} + OH^- + OH\cdot$) and produce hydroxyl radicals (Eaton

19

& Qian, 2002). In order for the cells to maintain oxidative balance, the levels of

$\cdot O_2$ must be kept low and H_2O_2 levels should not accumulate (Diebold & Chandel,

2016). Therefore, cells have developed peroxide scavenging (peroxidase)

systems that reduce H_2O_2 into H_2O (Winterbourn, 2013). The two main peroxide

systems are thioredoxin/peroxiredoxin (TRX/PRX) and glutathione/glutathione

peroxidase (GSH/GPX), both of which use the oxidation of NADPH to NAD^+ to

reduce H_2O_2 into H_2O (Bindoli, Fukuto, & Forman, 2008). The physiological

consequences of ROS are many including cell death (L. J. Su et al., 2019; Q. Su

et al., 2018; Viviani, Corsini, Binaglia, Galli, & Marinovich, 2001). Oxidative stress

is implicated in various neurodegenerative diseases (Butler & Bahr, 2006; Kausar

et al., 2018; Louboutin & Strayer, 2014).

HIV-1 and Iron

In the context of HIV/AIDS, iron plays a critical role in HIV infections. Iron can

increase HIV-1 replication (Chang et al., 2015; Traore & Meyer, 2004). An

increase in hepcidin peptide leads to enhanced virus replication while increasing

ferroportin can inhibit virus replication (Kumari et al., 2016; Nekhai, Kumari, &

Dhawan, 2013; M. Xu et al., 2010). PLWH have elevated serum iron levels and

some researchers have suggested using iron chelators as an adjuvant therapy

(Chang et al., 2015; Nekhai et al., 2013). Interestingly, $CD4^+$ T cells infected with

HIV-1 and then treated with radiolabeled iron (^{59}Fe) demonstrate an increase in

^{59}Fe compared to uninfected cells (Chang et al., 2015).

Figure 3.   Mitochondrial production of reactive oxygen species. During oxidative phosphorylation superoxide radicals ($\cdot O_2$) are produced. As electrons pass through complex I and II superoxide is generated and remains in the mitochondrial matrix where it is converted to hydrogen peroxide (H_2O_2) by super oxide dismutase 2 (SOD2), while superoxide produced by electron transfer through complex III is released into the cytosol where it is converted into hydrogen peroxide by SOD1. Hydrogen peroxide in the presence of iron (II) or cooper participates in Fenton reaction and results in the production of hydroxyl radicals ($\cdot OH$) which can induce cellular damage. On the other hand, cells have peroxide systems such as thioredoxin/peroxiredoxin (TRX/PRX) and glutathione/glutathione peroxidase (GSH/GPX) system, which utilize the oxidation of NADPH to NAD^+ to reduce H_2O_2 to H_2O. This image is modified from (Diebold & Chandel, 2016).

Copyright clearance was obtained from the publisher, Elsevier, to reproduce figure.
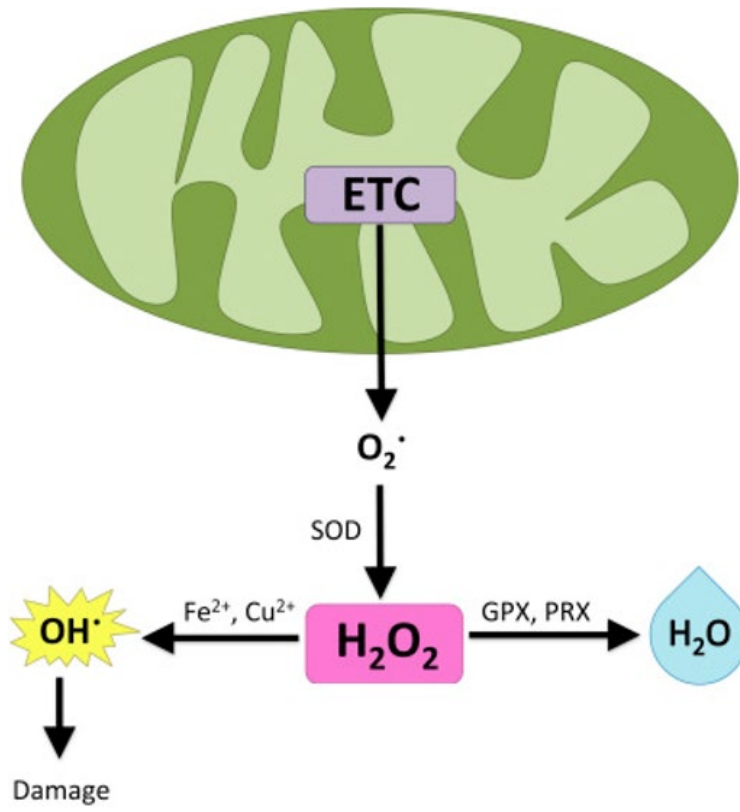
Moreover, the same study showed an elevation in TFR1 mRNA expression in HIV-1 infected cells, indicating a reduction in cytosolic iron levels (Chang et al., 2015). The authors of the study suggested that once the virus had infected CD4^{+} T-cells, it was attempting to create a "favorable environment for its own replication" (Chang et al., 2015). HIV-1 proteins Tat and gp120 can increase levels of ROS and can alter the morphology and functions of endolysosomes and mitochondria (Avdoshina et al., 2016; M. Bae et al., 2014; Datta, Miller, Afghah, Geiger, & Chen, 2019; Dawson, Dawson, Uhl, & Snyder, 1993; El-Amine et al., 2018; J. A. Fields et al., 2016; Foga, Nath, Hasinoff, & Geiger, 1997; Gelman et al., 2005; Hui, Chen, Haughey, & Geiger, 2012; Shah, Kumar, Simon, Singh, & Kumar, 2013). Moreover, oxidative stress is implicated in the pathogenesis of HAND (Louboutin & Strayer, 2014). Therefore, we set out in these studies to investigate the effects of HIV-1 gp120 on iron signaling and ROS production between endolysosomes and mitochondria.

Hypothesis

HIV-1 gp120 increases ROS production, and antioxidants, such as deferoxamine, blocks gp120's effect (Foga et al., 1997). Mitochondria are known to be major producers of ROS (Diebold & Chandel, 2016). However, the mechanisms underlying gp120-induced increases in ROS production remain unclear. Therefore, in Chapter 2, we tested the hypothesis that HIV-1 gp120-induced de-acidification of endolysosomes leads to an efflux of iron from

endolysosomes and an accumulation of iron in the cytosol and mitochondria, and subsequent increases in levels of cytosolic and mitochondrial ROS.

Iron is implicated in HIV-1 replication (Chang et al., 2015; Debebe et al., 2007), and gp120 promotes the production of ROS. It remains unclear how gp120 affects expression levels of iron related proteins. In Chapter 3, we tested the hypothesis that HIV-1 gp120 treatment decreases TFR1 and IRP2 and increases FTH and FPN protein levels.

Organellar stress responses in the endoplasmic reticulum and mitochondria are well characterized. These stress responses are initiated due to a stressor and promote the restoration of organellar function. However, lysosome stress and lysosome stress responses are ill-defined. Therefore, in Chapter 4, we used evidence for the work of others and us to define, prove the existence of, and provide criteria for lysosome stress responses.

CHAPTER 2

HIV-1 GP120 INDUCED ENDOLYSOSOME DE-ACIDIFICATION LEADS TO EFFLUX OF ENDOLYSOSOME IRON, AND INCREASES IN MITOCHONDRIAL IRON AND REACTIVE OXYGEN SPECIES

Lakpa KL[#], Halcrow PW[#], Khan N, Afghah Z, Miller N, Datta G, Chen X, Geiger JD.

Department of Biomedical Sciences
University of North Dakota School of Medicine and Health Sciences
Grand Forks, ND 58203, USA

# These authors contributed equally to this work

Abstract

The HIV-1 coat protein gp120 continues to be implicated in the pathogenesis of HIV-1 associated neurocognitive disorder (HAND); a condition known to affect ~50% of people living with HIV-1 (PLWH). Autopsy brain tissues of HAND individuals display morphological changes to mitochondria and endolysosomes, and HIV-1 gp120 causes mitochondrial dysfunction including increased levels of reactive oxygen species (ROS) and de-acidification of endolysosomes. Ferrous iron is linked directly to ROS production, ferrous iron is contained in and released from endolysosomes, and PLWH have elevated iron and ROS levels. Based on those findings, we tested the hypothesis that HIV-1 gp120-induced endolysosome de-acidification and subsequent iron efflux from endolysosomes is responsible for increased levels of ROS. In U87MG astrocytoma cells, HIV-1 gp120 de-acidified endolysosomes, reduced endolysosome iron levels, increased levels of cytosolic and mitochondrial iron, and increased levels of cytosolic and mitochondrial ROS. These effects were all attenuated significantly by the endolysosome-specific iron chelator deferoxamine, by inhibitors of endolysosome-resident two-pore channels and divalent metal transporter-1 (DMT-1), and by inhibitors of mitochondria-resident DMT-1 and mitochondrial permeability transition pores. These results suggest that oxidative stress commonly observed with HIV-1 gp120 is downstream of its ability to de-acidify endolysosomes, to increase the release of iron from endolysosomes, and to increase the uptake of iron into mitochondria. Thus, endolysosomes might represent early and upstream targets for therapeutic strategies against HAND.

26

Introduction

HIV-1 associated neurocognitive disorders (HAND) affects about 50% of people living with HIV-1 (PLWH) despite effective viral suppression achieved using antiretroviral therapies (ART) (McArthur et al., 2010). Clinically, HAND presents with deficits in cognition, memory, and motor function (Clifford & Ances, 2013); the severity varies from mild (asymptomatic) to severe (dementia) (Antinori et al., 2007). Pathologically, post-mortem brain samples exhibit decreased synaptodendritic arborization (Everall et al., 1999; Masliah et al., 1992; Masliah et al., 1997), Alzheimer's disease-like changes (Brew, Pemberton, Blennow, Wallin, & Hagberg, 2005), and morphological changes in subcellular organelles including endolysosomes (Gelman et al., 2005), endoplasmic reticulum (Lindl, Akay, Wang, White, & Jordan-Sciutto, 2007), and mitochondria (Avdoshina et al., 2016; J. Fields et al., 2013). Implicated in the pathogenesis of HAND are HIV-1 proteins (Kovalevich & Langford, 2012), reactive oxygen species (ROS) (Turchan et al., 2003) as well as ART drugs used to treat PLWH (Heaton et al., 2011). However, the full spectrum of underlying mechanisms of HAND remains unclear. Several soluble factors, including the HIV-1 proteins transactivator of transcription (Tat) and glycoprotein 120 (gp120) continue to be implicated in the pathogenesis of HAND (Kovalevich & Langford, 2012). Tat and gp120 are neurotoxic, decrease synaptodendritic arborization (J. Fields et al., 2013; Fitting et al., 2013; Toggas, Masliah, & Mucke, 1996), and disrupt intracellular levels of calcium and iron (Festa, Gutoskey, Graziano, Waterhouse, & Meucci, 2015; Haughey et al., 2001; Nath, Padua, & Geiger, 1995). Furthermore, Tat and

27

gp120 are capable of affecting the structure and function of subcellular organelles including endolysosomes and mitochondria (M. Bae et al., 2014; Datta et al., 2019; J. A. Fields et al., 2016; Hui, Chen, Haughey, et al., 2012).

Endosomes and lysosomes, collectively referred to here as endolysosomes, are dynamic organelles involved in the trafficking and degradation of intracellular cargo. Endolysosomes are acidic organelles that help regulate a wide variety of essential physiological functions including plasma membrane repair, cell homeostasis, energy metabolism, nutrient-dependent signal transduction, and immune responses (Ballabio & Bonifacino, 2020; Bird, Trapani, & Villadangos, 2009; Jaiswal, Andrews, & Simon, 2002; Mony, Benjamin, & O'Rourke, 2016; Settembre, Fraldi, Medina, & Ballabio, 2013). Additionally, endolysosomes contain readily releasable stores of biologically important cations including calcium and iron (Xiong & Zhu, 2016). De-acidification of endolysosomes, such as has been shown to occur with Tat and gp120 (M. Bae et al., 2014; Hui, Chen, Haughey, et al., 2012; Pietrella et al., 1998), releases calcium and iron (Christensen et al., 2002; Fernández et al., 2016) from endolysosomes and disrupts endolysosome membrane integrity (Hui et al., 2015). These actions of Tat and gp120 might affect mitochondrial function because calcium and iron overload in mitochondria can result in increased levels of ROS and cell death via apoptosis and ferroptosis (Brookes, Yoon, Robotham, Anders, & Sheu, 2004; Dixon et al., 2012; H. Huang et al., 2017).

PLWH often exhibit elevated serum iron levels (Chang et al., 2015), and iron has been implicated in HIV-1 progression and HAND pathogenesis (Chang et al., 2015; Nekhai et al., 2013; Patton et al., 2017). Extracellular ferric iron (Fe^{3+}) binds to the iron transport protein transferrin and is endocytosed into endosomes where it is reduced to ferrous iron (Fe^{2+}). Endolysosomes play an essential role in maintaining intracellular levels of iron; these acidic organelles are known to release iron when they are de-acidified and they contain a variety of cation channels through which iron can be released into the cytosol (X. P. Dong et al., 2008; Fernández et al., 2016; Kurz et al., 2011).

Through Fenton reactions (Eaton & Qian, 2002), ferrous iron in endolysosomes, cytoplasm, and mitochondria can generate ROS and can cause oxidative stress. Oxidative stress continues to be implicated in the pathogenesis of neurodegenerative diseases including HAND, and others and we have shown that Tat and gp120 both increase levels of ROS (Foga et al., 1997; S. H. Kim, Smith, Tan, Shytle, & Giunta, 2015; Viviani et al., 2001). Furthermore, HIV-1 gp120 can damage subcellular organelles, such as endolysosomes and mitochondria (Avdoshina et al., 2016; M. Bae et al., 2014; J. A. Fields et al., 2016; Viviani et al., 2001). However, prior to this study nothing was known about the extent to which gp120-induced release of iron from endolysosomes led to increased levels of ROS in the cytosol and in mitochondria. Therefore, we tested the hypothesis that HIV-1 gp120-induced de-acidification of endolysosomes leads to an efflux of iron from endolysosomes and an accumulation of iron in the

cytosol and mitochondria, and subsequent increases in levels of cytosolic and mitochondrial ROS.

Methods and Materials

Cell Cultures

Astrocytoma (U87MG) cells were cultured in 1x DMEM (Invitrogen) containing 10% fetal bovine serum and 1% penicillin/streptomycin (Invitrogen). U87MG cells were grown in T75 flasks and then sub-cultured in 35 mm^2 dishes (Mattek) or 12- and 24-well plates (Corning); cells were maintained in a 5% CO_2 incubator at 37°C. Cells were not used past their tenth passage.

Propidium Iodide Cell Death Assay

Cell death was measured by cellular uptake of propidium iodide (PI) staining (Sigma-Aldrich) (Crowley et al., 2016). U87MG cells were treated with gp120 (4 nM) in the absence or presence of deferoxamine (DFO; 100 µM) for 30 min or 24 h. Cells were washed once with pre-warmed 1x PBS then suspended in a PI (20 µg/mL) + PBS buffer for 30 min. Cells were analyzed using our Attune NxT flow cytometer. PI was excited by the blue (488 nm) excitation laser and light emission was determined using a BL2 (574/26 nm) filter. Mean fluorescent intensity, standard error of the mean, and the number (n) cells analyzed for PI were determined using Attune NxT software (ThermoFisher).

Endolysosome pH Measurements

As previously described (Hui, Chen, Haughey, et al., 2012), endolysosome pH was measured using a ratiometric indicator-dye LysoSensor Yellow/Blue DND-160; a dual excitation dye that measures pH independently of intracellular dye

concentration. U87MG cells were loaded with 5 to 10 µM DND-160 for 5 min at 37°C. Post-incubation, dye-containing media was removed, and fresh media was added to the cells just prior to imaging. Light emitted at 520 nm in response to excitation for 2 msec at 340/380 nm was measured every10 seconds using a filter-based imaging system (Zeiss Axiovert 200M, Germany). Ratios of light excited (340/380 nm) versus light emitted (520 nm) were converted to pH using a calibration curve as previously described (Hui et al., 2012). Using the formula pH = -log[H^+] we calculated percent reductions of intraluminal proton concentrations.

Endolysosome Morphology

Morphological features of plasma membranes, nucleus, and endolysosomes were determined by immunostaining. Lysosomes were stained with an anti-LAMP1 antibody and an Alexa 488 anti-rabbit secondary antibody. Plasma membranes were stained with an anti-beta1 sodium potassium ATPase antibody and an Alexa 594 anti-mouse antibody. Nuclei were stained with DAPI. Confocal scanning microscopy (Zeiss LSM800) was used to acquire z-stack images with a stack interval of 0.4 µm. Images were acquired and then reconstructed using Imaris (Oxford Instruments) imaging software (version 9.5).

Endolysosome Iron Measurements

FeRhoNox-1 (Goryo Chemical), which stains specifically for Fe^{2+} (Hirayama, 2018), was added at a final concentration of 30 µM; U87MG cells were seeded at a density of 8×10^3 cells on 35 mm^2 dishes and incubated at 37°C for 1 h. After washing cells twice with 1 x PBS, fresh PBS was added, and cells were imaged at an excitation wavelength of 537 nm and an emission wavelength of 569 nm

using our confocal scanning microscope (Zeiss, LSM800). Imaging parameters were kept the same throughout each set of experiments. Z-stack images were taken at a stack interval of 0.4 μm. Images were reconstructed using Imaris (Oxford Instruments) imaging software (version 9.5). The data were represented as mean fluorescence intensity (MFI).

Cytosolic Iron Measurements

Cytosolic iron levels were measured using PhenGreen™ SK diacetate (PGSK); a quenching probe for cytosolic iron (Petrat, Rauen, & de Groot, 1999). U87MG cells were seeded at a density of 2 to 3 x 10^4 cells on 35 mm^2 dishes and incubated with PGSK at a final concentration of 10 μM for 30 min at 37°C. Cells were washed three-times with 1 x PBS, collected, suspended and analyzed using our Attune NxT flow cytometer (ThermoFisher). PGSK was excited using the blue (488 nm) excitation laser and light was captured after passing through the BL1 (530/30 nm) emission filter. Mean fluorescent intensities, standard error of the mean, and the numbers (n) of cells analyzed for PGSK were determined using Attune NxT software (ThermoFisher).

Mitochondrial Iron Measurements

Mitochondrial iron levels were measured using rhodamine B-[2,2'-bipyridine-4-yl)-aminocarbonyl]benzyl ester (RDA) (Squarix). RDA is an Fe^{2+}-specific quenching dye that localizes within mitochondria; it excites at 562 nm and emits at 598 nm (Rauen et al., 2007). U87MG cells were seeded at a density of 2 to 3 x 10^4 cells on 35 mm^2 dishes and incubated with 200 nM RDA for 10 min at 37°C. Cells were washed once and resuspended with 1 x PBS. Z-stack images were

captured using confocal scanning microscopy (Zeiss LSM800); 11 to 23 slices

were used per z-stack image. Imaging parameters were kept the same

throughout each set of experiments. Images were taken before and 30 min after

the addition of HIV-1 gp120. In the deferoxamine (DFO) treatment group, cells

were incubated with DFO for 1 h followed by the removal of DFO-containing

media and the continuation of the above-described protocol. ImageJ software

was used to merge z-stack images, and to measure mean fluorescence intensity

(MFI) before (time zero) and after (time 30') the addition of HIV-1 gp120 or

vehicle. MFI per cell was determined by dividing MFI values at time zero by MFI

values at time 30' (ratio 0/30') and values were expressed as a percentage; the

values were normalized to control values obtained with heat-inactivated HIV-1

gp120 (gp120[i]).

ROS Measurements in Cytosol and Mitochondria

Cytosolic ROS levels were measured using 2,7-dichlorodihydrofluoroscein

diacetate (DCFDA), which when oxidized produces DCF; DCF excites at 495 nm

and emits at 529 nm. Mitochondrial ROS was measured using MitoSox Red

Superoxide Indicator, which excites at 510 nm and emits at 580 nm. U87MG

cells seeded at a density of 2 to 3 x 10^4 were incubated with 10 µM DCFDA or 5

µM MitoSox for 30 min at 37ºC in serum-free media. Cells were then washed

twice with 1 x PBS prior to being analyzed using our Attune NxT flow cytometer

(ThermoFisher). DCF-stained cells were excited by the blue (488 nm) excitation

laser and light was emitted through the BL1 (530/30 nm) emission filter. MitoSox

Red stained cells were excited by the blue (488 nm) excitation laser and light

was emitted by the BL2 (574/26 nm) emission filter. Mean fluorescence intensities, standard error of the mean, and the number (n) of cells analyzed for DCF and MitoSox Red were determined using Attune NxT software (ThemoFisher).

Reagents

Reagents were purchased from ThermoFisher Scientific unless noted otherwise; CISMBI (Sigma-Aldrich), TRO-19622 (TOCRIS) and Ned-19 (TOCRIS). HIV-1 gp120 IIIb was purchased from ABL Inc. and prepared aliquots were stored at -80°C to prevent freeze-thaw problems.

Statistics

All data were expressed as means and standard errors of the mean (SEM). Data analyses were completed using GraphPad Prism 8 software. Statistically significant differences between two groups was determined using a Student's t test. One-way ANOVA with Tukey's post-hoc tests were used to compare differences between multiple groups. $p < 0.05$ was designated to be statistically significant. All experiments were conducted a minimum of 3 independent times.

Results

HIV-1 gp120 and Baf A1 Decreased Endolysosome Numbers and Increased Endolysosome pH and Volumes

We determined the effect of HIV-1 gp120 (gp120) treatment on endolysosome pH. U87MG cells treated with 4 nM gp120 resulted in endolysosome de-acidification (Figure 4A); peak deacidification was observed by 30 min and pH units were significantly ($p < 0.0001$) increased by

Figure 4. HIV-1 gp120 and bafilomycin A1 increased endolysosome pH.
(A) Treatment of U87MG cells with 4 nM HIV-1 gp120 (gp120, closed squares) or 200 nM of the vacuolar ATPase inhibitor bafilomycin A1 (Baf A1, closed triangles) de-acidified endolysosomes; de-acidification by gp120 remained elevated for 30 min. The de-acidification effects of Baf A1 normalized about 12 min following its application. For gp120, peak de-acidification was observed by 30 min whereas for Baf A1 peak de-acidification was observed about 12 min following its application. **(B)** HIV-1 gp120 significantly ($p<0.0001$) increased endolysosome pH units and Baf A1 significantly ($p<0.0001$) increased endolysosome pH units. Data were represented as mean and SEM. N= 90, ****$p<0.0001$.

A.
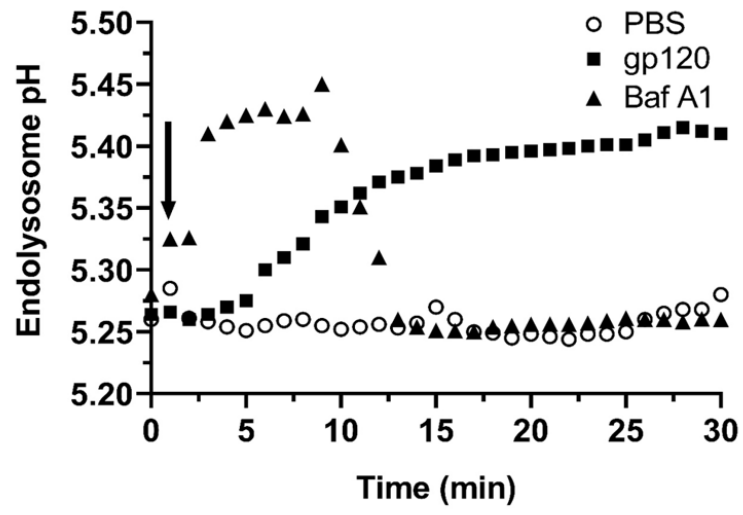
B.
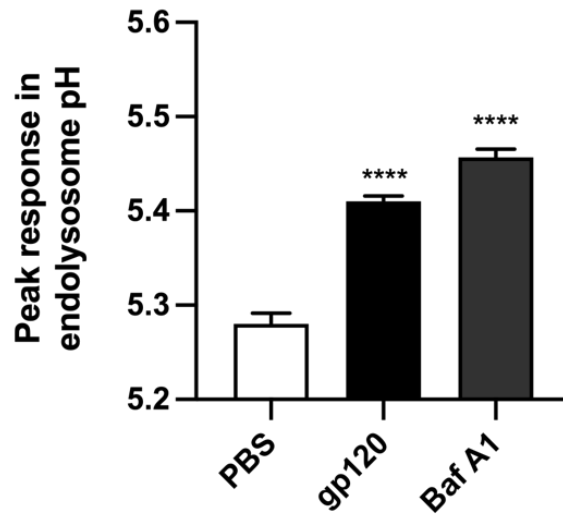
0.13 ± 0.01 pH units from control values of 5.28 ± 0.01 to values of 5.41 ± 0.01 (Figure 4B). Bafilomycin A1 (Baf A1), a vacuolar ATPase inhibitor that de-acidifies endolysosomes (Yoshimori, Yamamoto, Moriyama, Futai, & Tashiro, 1991), was used as a positive control and at a concentration of 200 nM it significantly (p<0.0001) increased endolysosome pH by 0.18 ± 0.01 pH units from control values of 5.28 ± 0.01 to 5.46 ± 0.01 (Figure 4B). These changes in pH corresponded to a 32% reduction in intraluminal proton concentration by Baf A1 and a 25% reduction by gp120. The endolysosome de-acidification by gp120 was observed after 5 min and remained elevated for 25 min while the effects of Baf A1 occurred immediately and normalized about 12 min following its application (Figure 4A).

Endolysosome de-acidification has been shown by others and us to change endolysosome morphology including numbers, sizes and positioning within cells (X. P. Dong et al., 2010; Fernández et al., 2016; Hui, Chen, Haughey, et al., 2012; D. E. Johnson, Ostrowski, Jaumouille, & Grinstein, 2016; Mauthe et al., 2018). Because gp120 de-acidified endolysosomes, we next determined the effects of gp120 on endolysosome numbers, sizes and cellular positioning. Qualitatively, endolysosomes exposed to heat-inactivated gp120 (gp120[i]) displayed a perinuclear distribution pattern, but when exposed to gp120 endolysosomes were enlarged and more dispersed towards plasma membranes (Figure 5A). Quantitatively, gp120 significantly (p<0.0001) decreased the number of LAMP1-positive vesicles per cell from 371 ± 19 to 256 ± 34 (Figure 2B), but nevertheless increased significantly (p<0.0001) the total

Figure 5.   HIV-1 gp120 and bafilomycin A1 decreased endolysosome numbers and increased endolysosome volumes.
(A) Representative Imaris 9.5 software (Oxford Instruments) reconstructed and confocal laser scanning microscopy (inset) images of U87MG cells treated for 30 min with 4 nM heat-inactivated gp120 (left panel, gp120^i) or HIV-1 gp120 (right panel, gp120). Lysosomes were stained with anti-LAMP1 antibody, plasma membranes were stained with anti-beta1 sodium potassium ATPase antibody (red), and nuclei were stained with anti-DAPI antibody. Endolysosomes exposed to gp120^i displayed a perinuclear distribution pattern but were enlarged and more dispersed towards plasma membranes when exposed to HIV-1 gp120, scale bar= 5 μm. **(B)** HIV-1 gp120 and the positive control bafilomycin A1 (Baf A1) both significantly ($p<0.0001$) decreased the number of LAMP1-positive vesicles per cell. **(C)** HIV-1 gp120 and the positive control Baf A1 both significantly ($p<0.0001$) increased the total volume of LAMP1-positive endolysosomes per cell. Data were represented as mean and SEM. N= 900, [****]$p<0.0001$.

A.

gp120[i]

LAMP1

5 um

gp120

LAMP1

5 um

B.

C.
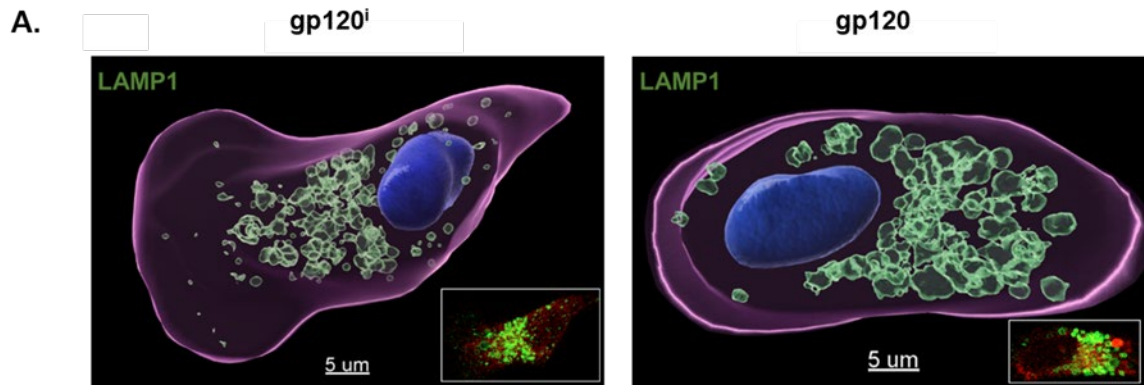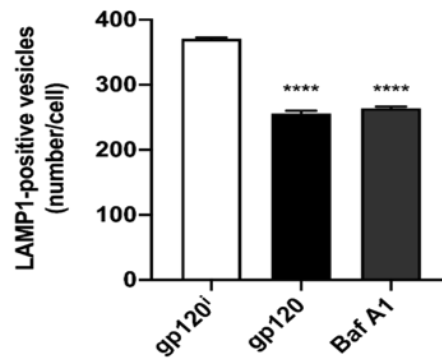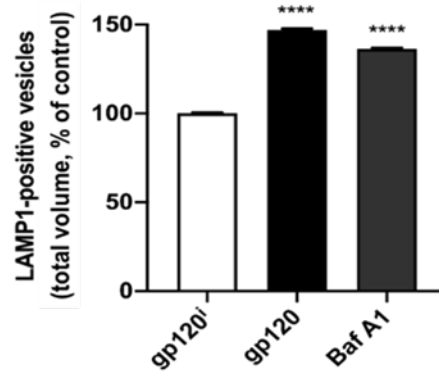
volume (μm^3) of LAMP1-positive vesicles by 47% (Figure 5C). Similarly, Baf A1

significantly (p<0.0001) decreased the number of LAMP1-positive vesicles from

371 ± 19 to 264 ± 19 (Figure 5B) and significantly (p<0.0001) increased the total

volume of LAMP1-positive vesicles by 36% (Figure 5C).

HIV-1 gp120-Induced Decreases in Levels of Endolysosome Iron were Blocked by an Inhibitor of TPC

De-acidification of endolysosomes can induce the release of divalent cations

from endolysosomes (Christensen et al., 2002; Fernández et al., 2016).

Because of this, we determined the extent to which gp120[i], gp120 and Baf A1

decreased levels of endolysosome Fe^{2+} and whether the inhibitor of

endolysosome associated two pore channels (TPC) trans-Ned-19 (Ned-19)

blocked these decreases because they are permeable to divalent cations such

as Fe^{2+} (Brailoiu et al., 2009; Calcraft et al., 2009; Fernández et al., 2016).

Qualitatively, treatment of U87MG cells for 30 min with 4 nM of gp120 but not

gp120[i] decreased FeRhoNox-1 fluorescence staining for Fe^{2+} (Figure 6A).

Quantitatively, gp120 significantly (p<0.01) decreased levels of endolysosome

iron by 41% (Figure 6B); the positive control Baf A1 significantly (p<0.0001)

decreased levels of endolysosome iron by 66% and this decrease was

significantly (p<0.01) greater than that produced by gp120 (Figure 6B). Next, we

investigated the extent to which the release of endolysosome Fe^{2+} induced by

gp120 involved endolysosome-resident TPCs. As expected, we observed a

robust co-localization between FeRhoNox-1 and LAMP1 staining regardless of

the treatments applied (Figure 6C-F). Qualitatively, HIV-1 gp120 decreased

Figure 6.   HIV-1 gp120 decreased levels of endolysosome Fe^{2+} and these decreases were blocked by an inhibitor of two pore channels. **(A)** Representative confocal laser confocal microscopy images of U87MG cells treated for 30 min with either heat-inactivated gp120 (left panel, gp120[i]) or 4 nM HIV-1 gp120 (right panel, gp120). Treatment of U87MG cells for 30 min with 4 nM gp120 but not gp120[i] decreased FeRhoNox-1 fluorescence staining for Fe^{2+}, scale bar= 5 µm **(B)** Levels of endolysosome Fe^{2+} as indicated by mean fluorescence units (MFI) for FeRhoNox-1 staining were significantly decreased by gp120 and by Baf A1 ($p<0.0001$); the decrease produced by Baf A1 was significantly ($p<0.01$) greater than that produced by HIV-1 gp120. **(C–F)** Representative confocal laser scanning microscopy images of U87MG cells treated for 30 min with (C) gp120[i], (D) 10 µM Ned-19 (E) 4 nM gp120 or (F) 10 µM Ned-19 added 30 min prior to the addition of gp120. Cells were labelled with FeRhoNox-1 (red) for endolysosome stores of Fe^{2+} (left panels), Cell-Light LAMP1-GFP BacMam 2.0 for endolysosomes (middle panels), and merged FeRhoNox-1 and LAMP1 images (right panels); scale bar = 5 µm. **(G)** MFI values for FeRhoNox-1 staining were significantly ($p<0.01$) decreased by gp120 and these decreases were significantly ($p<0.01$) blocked by 10 µM Ned-19. Data were represented as mean and SEM. N = 900, **$p<0.01$, **$p<0.0001$.

41

A.

B.

C. gp120^i

D. Ned-19

E. gp120

F. Ned-19+gp120

G.
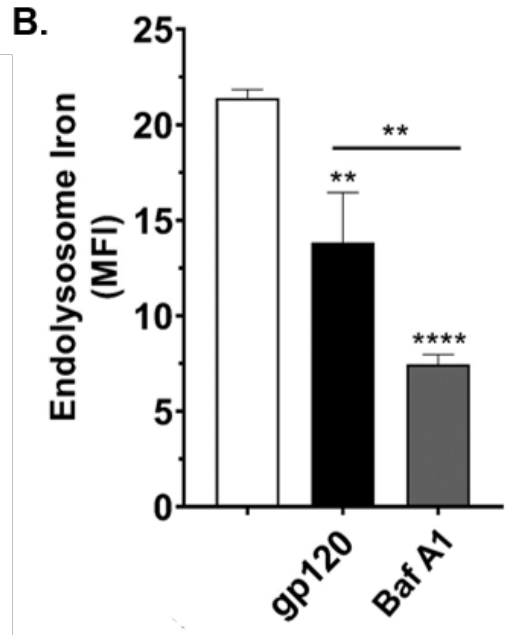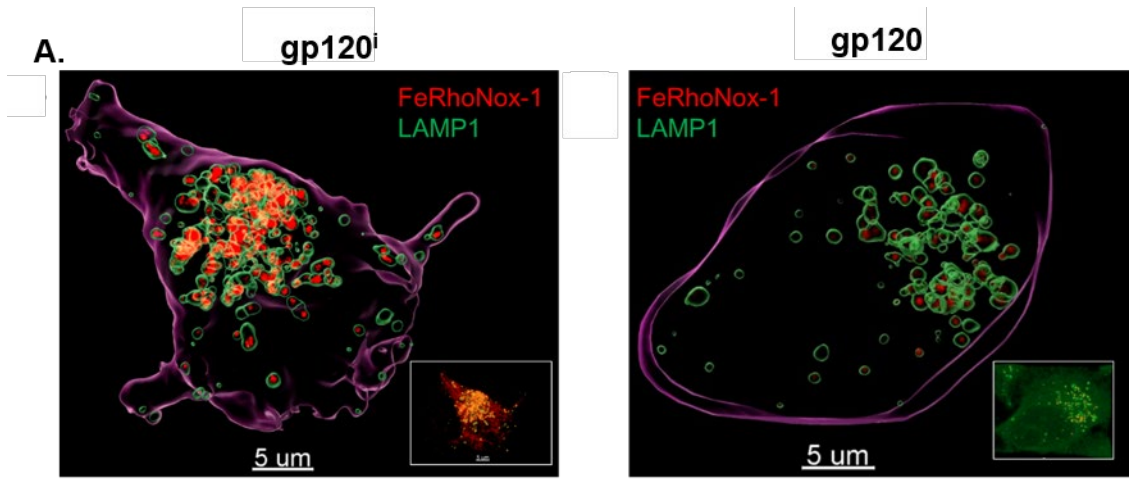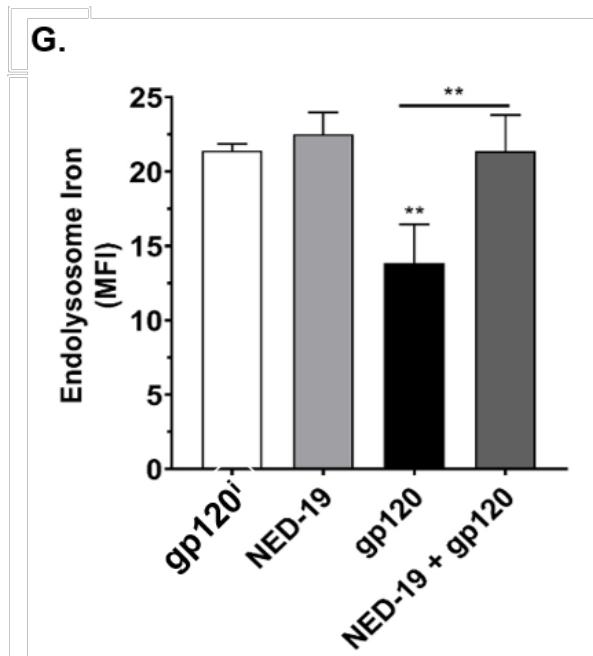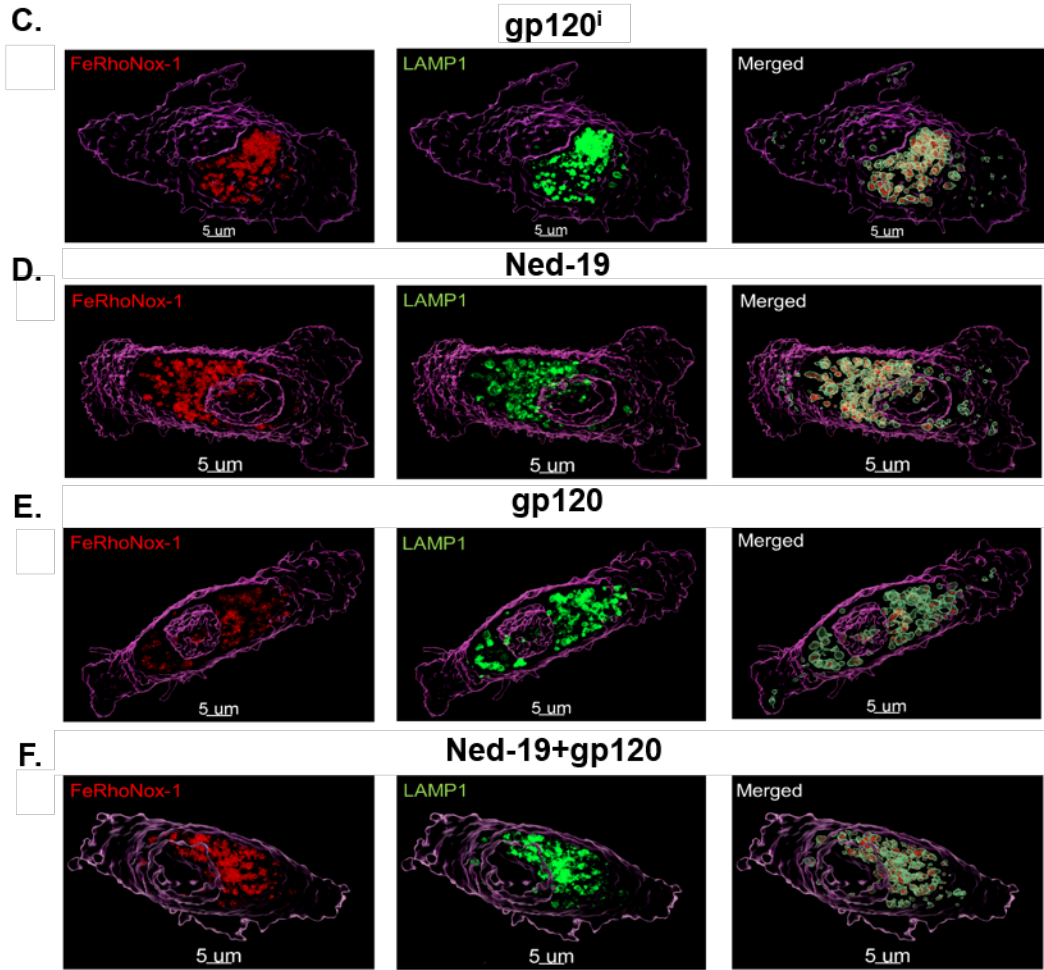
FeRhoNox-1 staining in endolysosomes and these decreases were blocked by

the Ned-19 (Figure 6 E-F). Compared to control treatments with gp120[i], 4 nM

gp120 decreased significantly (p<0.01) levels of endolysosome iron (Figure 6G)

and caused marked changes in endolysosome morphology (Figure 6A); these

effects of gp120 were significantly (p<0.01) blocked by pretreatment of cells with

Ned-19 (Figure 6G).

Deferoxamine, and Inhibitors of Two Pore Channels and Divalent Metal Transporter 1, Reduced HIV-1 gp120-Induced Increases in Cytosolic Iron and ROS Levels, and Deferoxamine Reduced Basal Levels of Cytosolic ROS

Having found that gp120 caused an increased release of Fe^{2+} from

endolysosomes, we next sought to determine the extent to which and

mechanisms by which gp120 affected levels of cytosolic Fe^{2+} and levels of

cytosolic reactive oxygen species (ROS). Cytosolic Fe^{2+} levels were measured

with the quenching metal indicator PhenGreen SK™ (PGSK) (Petrat et al., 1999).

4 nM HIV-1 gp120 significantly (p<0.0001) increased levels of cytosolic Fe^{2+} by

about 40% (Figure 7A). Pre-treatment with 100 µM deferoxamine (DFO), a

specific chelator of endolysosome Fe^{2+}, significantly (p<0.0001) blocked

gp120-induced increases in cytosolic Fe^{2+} (Figure 7A). Because levels of ROS

are increased by Fe^{2+} through Fenton-reaction chemistry, we determined the

extent to which endolysosome iron released by gp120 affected cytosolic ROS

levels. 4 nM gp120-induced a significantly (p<0.0001) increased cytosolic ROS

levels by about 66% (Figure 7B). By itself, 100 µM DFO significantly (p<0.0001)

inhibited cytosolic levels of ROS and DFO significantly (p<0.0001) blocked

gp120-induced increases in cytosolic ROS (Figure 7B).

Figure 7. DFO, Ned-19 and CISMBI blocked HIV-1 gp120-induced increases in levels of cytosolic iron and ROS. **(A)** Levels of cytosolic Fe^{2+} were measured using the "turn-off" quenching dye PhenGreen SK™ (PGSK). Data were transformed to the reciprocal of mean fluorescence intensity (1/MFI) to illustrate more clearly the ability of HIV-1 gp120 (gp120) to increase levels of cytosolic Fe^{2+}. Levels of cytosolic Fe^{2+} were significantly ($p<0.0001$) increased by 30 min treatment with 4 nM gp120. Pre-treatment of cells for 1 h with 100 µM deferoxamine (DFO), an endolysosome-specific Fe^{2+} chelator, significantly ($p<0.0001$) blocked gp120-induced increases in levels of cytosolic Fe^{2+}. Levels of cytosolic Fe^{2+} were not significantly affected by vehicle control (PBS). **(B)** Levels of cytosolic ROS using 2,7-dichlorodihydrofluoroscein (DCF) were significantly ($p<0.0001$) increased by 30 min treatments of 4 nM gp120. Pre-treatment of cells for 1 h with 100 µM DFO significantly ($p<0.0001$) decreased basal levels of cytosolic ROS and significantly ($p<0.0001$) blocked gp120-induced increases in cytosolic ROS. **(C)** Pre-treatment of cells with 10 µM Ned-19, an inhibitor of endolysosome associated two pore channels, significantly ($p<0.05$) blocked gp120-induced increases in levels of cytosolic ROS. **(D)** Pre-treatment of cells with 100 µM CISMBI, an inhibitor of divalent metal transporter 1, significantly ($p<0.01$) blocked HIV-1 gp120-induced increases in levels of cytosolic ROS. Levels of DCF fluorescence were measured as mean fluorescence intensity (MFI). Data were represented as mean and SEM. N =10,000, *$p<0.05$; **$p<0.01$; ****$p<0.0001$.

A.

B.

C.

D.
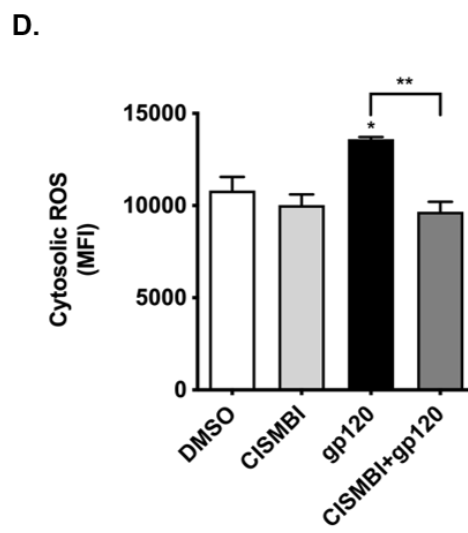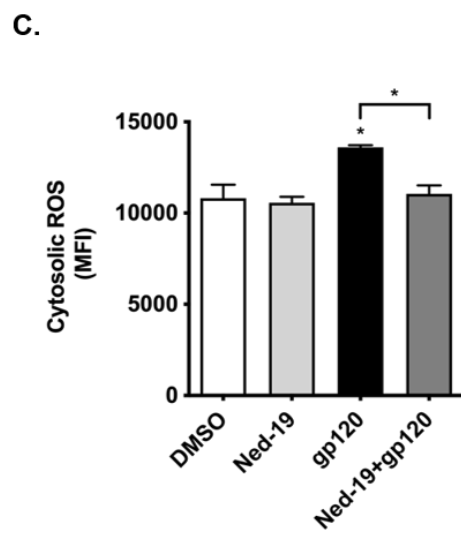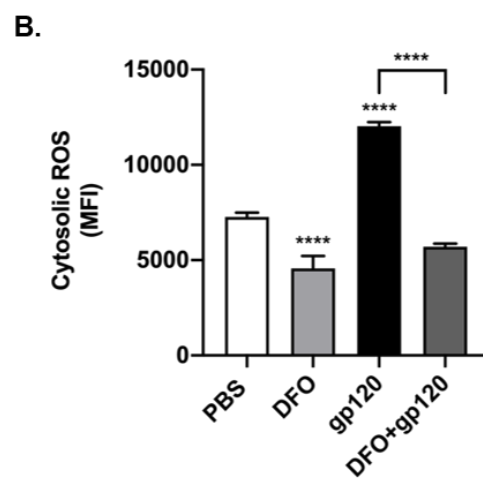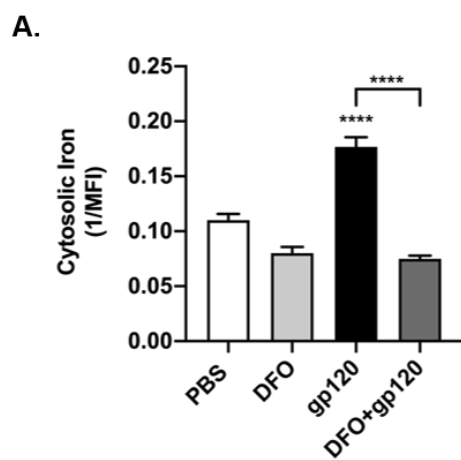
Based on these findings as well as findings described above, we further investigated the effects of blocking gp120-induced endolysosome iron release through TPC on cytosolic ROS levels. Pre-treatment of cells for 30 min with 10 μM of Ned-19 significantly ($p<0.05$) blocked gp120-induced increases in ROS (Figure 4C). Because Fe^{2+} in endolysosomes can also be released through divalent metal transporter 1 (DMT1), we next determined the extent to which the DMT1 competitive inhibitor 2-(3-carbamimidoylsulfanylmethyl-benzyl)-isothiourea (CISMBI) (Montalbetti, Simonin, Dalghi, Kovacs, & Hediger, 2014) affected gp120-induced increases in cytosolic ROS and found that CISMBI significantly ($p<0.01$) blocked gp120-induced increases in ROS (Figure 7D).

Deferoxamine, and Inhibition of Two Pore Channel, Mitochondrial Permeability Transition Pore Opening, and Divalent Metal Transporter 1 Blocked HIV-1 gp120-Induced Increases in Mitochondrial Iron and ROS

Mitochondria uptake cytosolic Fe^{2+} and next we determined the extent to which gp120-induced release of endolysosome Fe^{2+} resulted in increased levels of Fe^{2+} in mitochondria using the "turn-off" quenching dye RDA. Qualitatively, increased levels of mitochondrial Fe^{2+} were observed in cells treated with gp120, but not with gp120[i], DFO, or DFO added 1 h prior to gp120 (Figure 8A). Quantitatively, 4 nM gp120 significantly ($p<0.0001$) increased levels of mitochondrial Fe^{2+} (decreased RDA MFI) by, on average, about 28% (Figure 8B). Pre-treatment of cells with 100 μM DFO prior to the addition of gp120 significantly ($p<0.0001$) blocked gp120-induced increases in mitochondrial Fe^{2+} (Figure 8B).

Mechanistically, we next determined the extent to which inhibitors of mitochondrial permeability transition pore (mPTP) opening, DMT1, and

Figure 8.   Effects of DFO on HIV-1 gp120-induced increases in mitochondrial Fe^{2+} levels. **(A)** Mitochondrial iron levels were measured using the quenching dye rhodamine B-[(2,2'-bipyridine-4-yl)-aminocarbonyl]benzyl ester (RDA) by confocal laser scanning microscopy. Images are shown of control cells taken prior to (upper panels) or 30 min following (lower panels) the addition of heat inactivated HIV-1 gp120 (gp120[i]), 100 µM deferoxamine (DFO), 4 nM HIV-1 gp120 (gp120), or 4 nM gp120 added 1 h after 100 µM DFO (DFO+gp120). Qualitatively, gp120 decreased the fluorescence intensity of RDA staining and DFO blocked the gp120-induced decreases in RDA fluorescence. **(B)** U87MG cells treated with 4 nM gp120 significantly ($p<0.0001$) increased levels of mitochondrial iron while 1 h pre-treatment with 100 µM DFO significantly ($p<0.0001$) blocked gp120-induced increases in mitochondrial Fe^{2+} levels. Data were represented as mean and SEM. N ≥ 25, ****$p<0.0001$.

A.

B.
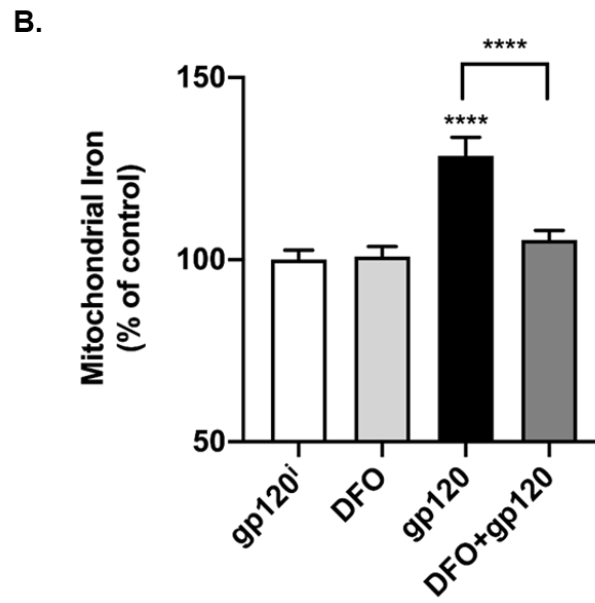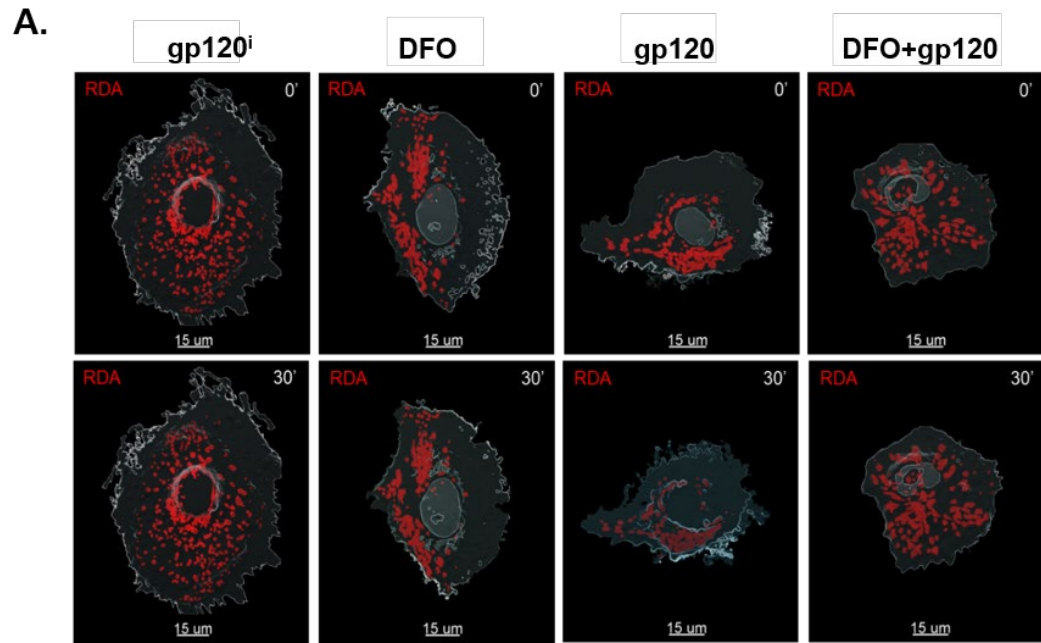
endolysosome TPCs could block gp120-induced increases in levels of mitochondrial Fe^{2+}. Qualitatively, increased levels of mitochondrial iron were observed in cells treated with gp120; these increases were blocked by the mPTP inhibitor TRO-19622 (TRO), the DMT-1 inhibitor CISMBI, and the TPC inhibitor Ned-19 (Figure 9A). Quantitatively, 4 µM gp120 significantly ($p<0.0001$) increased levels of mitochondrial iron (Figure 9B) and these increases were blocked by pre-treating cells for 30 min with 3 µM of TRO ($p<0.0001$), 100 µM of CISMBI ($p<0.001$), or 10 µM of Ned-19 (Figure 9B).

Because levels of ROS are increased by Fe^{2+} through Fenton-reaction chemistry, we determined next the extent to which endolysosome iron released by gp120 affected mitochondrial ROS levels. 4 nM gp120 significantly ($p<0.0001$) increased, by about 89%, levels of mitochondrial ROS (Figure 10A). 100 µM DFO alone did not affect levels of mitochondrial ROS, but did significantly ($p<0.001$) block gp120-induced increases in mitochondrial ROS (Figure 10A). Pretreatment of cells for 30 min with 10 µM Ned-19, 3 µM TRO and 100 µM CISMBI each significantly ($p<0.0001$) reduced HIV-1 gp120-induced increases in mitochondrial ROS (Figure 10B-D).

Figure 9.   Ned-19, TRO, and CISMBI blocked HIV-1 gp120-induced increases in mitochondrial Fe^{2+} levels. **(A)** Mitochondrial iron levels were measured using the quenching dye RDA by confocal laser scanning microscopy. Mitochondrial iron levels of control cells taken prior to (upper panels) or 30 min following (lower panels) the addition of heat-inactivated HIV-1 gp120 (gp120[i]), 4 nM HIV-1 gp120 (gp120), for 30 min with either 3 µM TRO-, an inhibitor of mitochondrial permeability transition pore (mPTP) opening; 100 µM CISMBI, an inhibitor of divalent metal transporter 1; or 10 µM Ned-19, an inhibitor of endolysosome associated two pore channels, prior to addition with 4 nM gp120. Qualitatively, gp120 decreased the fluorescence intensity of RDA, while TRO, CISMBI and Ned-19 each blocked gp120-induced decrease in RDA fluorescence. **(B)** Quantitatively, pre-treatment of cells with 3 µM TRO ($p<0.0001$), 100 µM CISMBI ($p<0.001$), or 10 µM Ned-19 ($p<0.0001$) blocked gp120-induced increases in mitochondrial Fe^{2+} levels. Data were represented as mean and SEM. N ≥ 25, ***$p<0.001$, ****$p<0.0001$

A.

| gp120i | gp120 | TRO+gp120 | CISMBI+gp120 | Ned-19+gp120 |
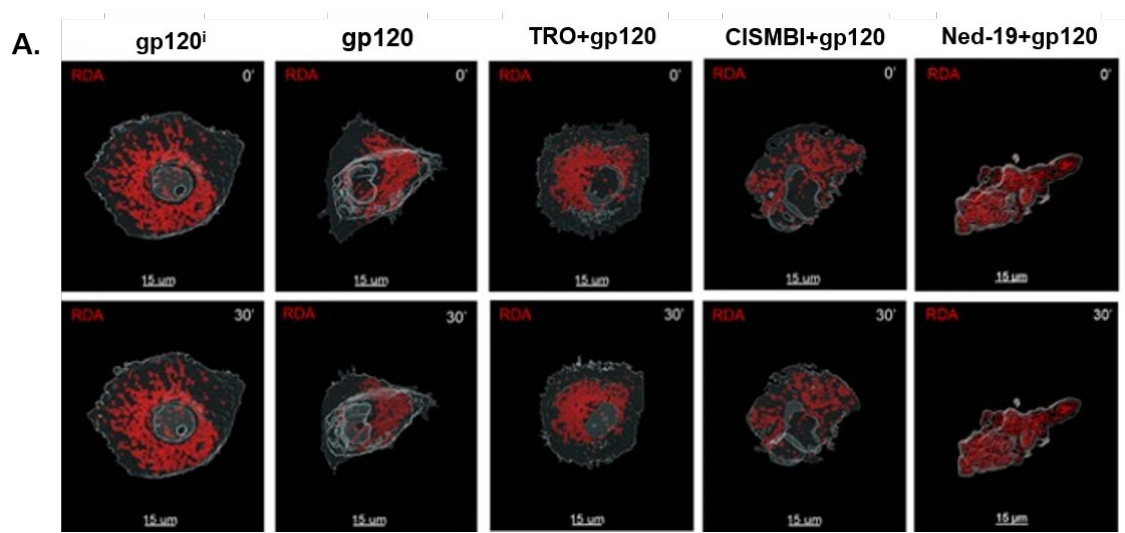
B.
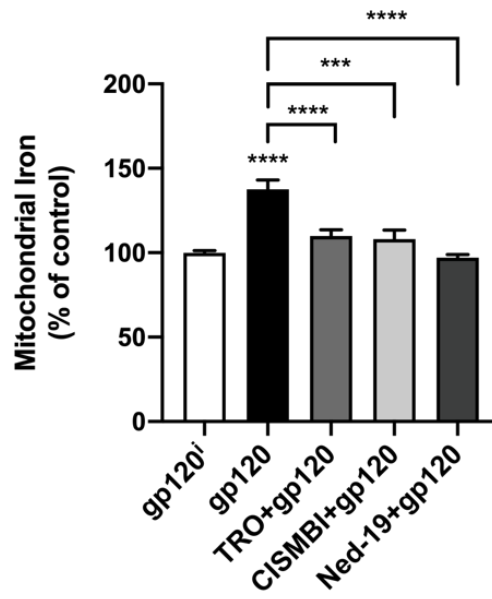
Figure 10.   DFO, CISMBI, and TRO blocked HIV-1 gp120-induced increases in mitochondrial ROS levels. **(A)** MitoSox Red was used as a measure of mitochondrial ROS and superoxide radicals. Mean fluorescence intensity (MFI) was significantly ($p<0.0001$) increased by 30 min treatment of U87MG cells with 4 nM gp120. Pre-treatment of cells for 1 h with 100 µM DFO significantly ($p<0.0001$) reduced gp120-induced increases in mitochondrial ROS. **(B)** HIV-1 gp120-induced increases in mitochondrial ROS were significantly ($p<0.0001$) inhibited by pre-treating cells for 30 min with 10 µM Ned-19. **(C)** HIV-1 gp120-induced increases in mitochondrial ROS were significantly ($p<0.0001$) inhibited by pre-treating cells for 30 min with 3 µM TRO. **(D)** HIV-1 gp120-induced increases in mitochondrial ROS were significantly ($p<0.0001$) inhibited by pre-treating cells for 30 min with 100 µM CISMBI. Data were represented as mean and SEM. N ≥ 25, ****$p<0.0001$.
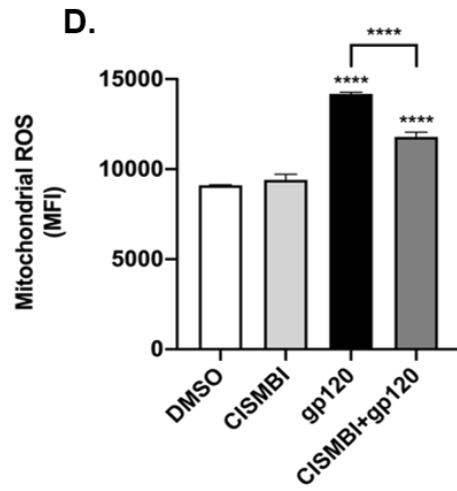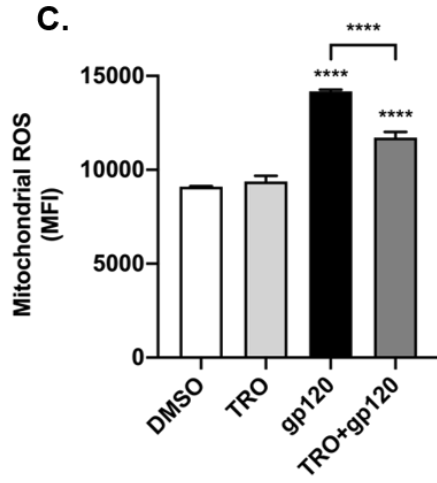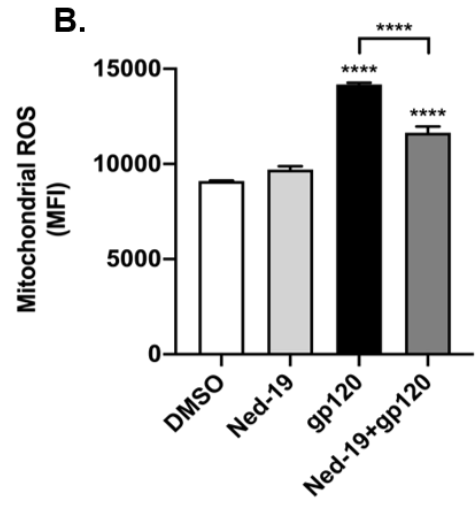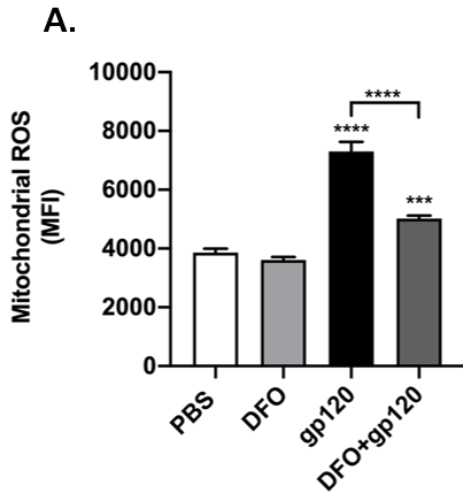
Lack of Effect of Vehicle, DFO and HIV-1 gp120 on Cell Viability

The main focus of the studies reported here was to determine the effects of gp120 on intracellular levels of Fe^{2+} and links between Fe^{2+} and ROS; not gp120-induced cell death. Accordingly, we determined under our experimental conditions whether gp120 decreased cell viability (Dawson et al., 1993; Nath et al., 2000; Yang, Yao, Lu, Wang, & Buch, 2010). Using propidium iodide (PI) uptake as a measure of cell death (Crowley et al., 2016), no statistically significant changes in the MFI of PI were observed between control and 4 nM gp120 treatments for 30 min (Figure 11A) or 24 h (Figure 11B). We also found that treatments with 100 µM DFO for 30 min (Figure 11A) or 24 h (Figure 11B) did not affect cell viability in the absence or presence of 4 nM gp120.

Discussion

Over the past three decades, the development and use of effective antiretroviral therapeutics has transformed HIV-1/AIDS into a chronic therapeutically managed disease (Arts & Hazuda, 2012). Associated with HIV-1/AIDS in the ART-era is a high prevalence of a spectrum of cognitive, motor and behavioral symptoms ranging in intensity from mild (asymptomatic) to severe (dementia) (McArthur et al., 2010). Collectively, these symptoms are referred to as HIV-1 associated neurocognitive disorders (HAND) (Antinori et al., 2007; Clifford & Ances, 2013) and underlying its pathology are findings of increased levels of oxidative stress, subcellular organelle dysfunction, synaptodendritic damage, and

Figure 11.   Deferoxamine and HIV-1 gp120 did not affect cell viability.
(A) U87MG cells treated for 30 min with DMSO vehicle (0.1%),
4 nM HIV-1 gp120 (gp120), or 100 µM DFO treatment 1 h prior
to 4 nM gp120 did not significantly affect cell viability as
determined by propidium iodide (PI) uptake. **(B)** U87MG cells
treated for 24 h with DMSO vehicle (0.1%), 4 nM HIV-1 gp120, in
the absence or presence of 100 µM DFO did not significantly
affect cell viability as determined by PI uptake. PI fluorescence
was measured as mean fluorescence intensity (MFI). Data were
represented as mean and SEM. N=10,000.

A. 30 min

B. 24 h
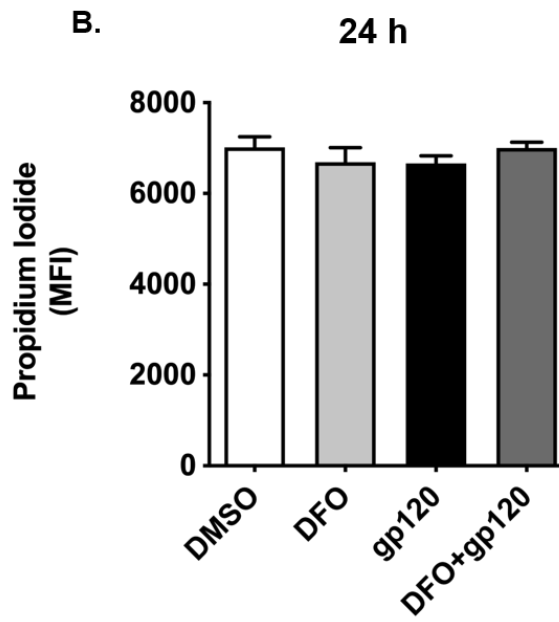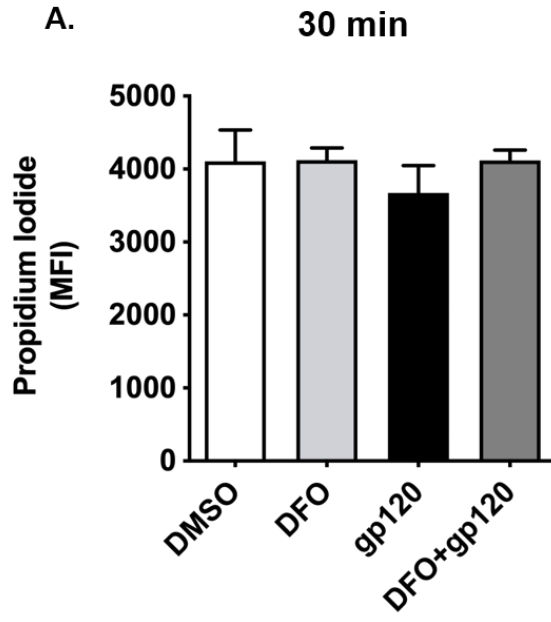
neuroinflammation (Avdoshina et al., 2016; Everall et al., 1999; J. A. Fields et al., 2016; Gelman et al., 2005; Kovalevich & Langford, 2012; Sanchez & Kaul, 2017; Saylor et al., 2016; Scutari et al., 2017). Implicated in the pathogenesis of HAND are soluble factors including the HIV-1 proteins Tat and gp120 as well as ART treatments themselves (Sanchez & Kaul, 2017; Scutari et al., 2017). Accordingly, additional investigative work is required to understand better the mechanisms underlying HAND pathogenesis with the goal of identifying effective therapeutic interventions.

Here, we showed that HIV-1 gp120 de-acidified endolysosomes, increased the release of ferrous iron out of endolysosomes, and that this released iron accumulated in the cytosol and mitochondria where it increased levels of ROS. Furthermore, we showed the involvement of two pore channels, divalent metal transporter 1, and mitochondrial permeability transport pore opening in these effects. By inhibiting iron release from endolysosomes and/or iron uptake into mitochondria it was possible to block HIV-1 gp120-induced effects on iron homeostasis and ROS production. Together these results suggest that HIV-1 gp120-induced changes to mitochondria might be downstream of endolysosome effects and that therapeutic strategies against HAND might be directed against these upstream targets (Figure 12).

Previously, we reported that HIV-1 gp120 de-acidified neuronal endolysosomes and that this de-acidification was reversed by the TRPML1 agonist ML-SA1 (M. Bae et al., 2014). Others too have reported, this time using human monocytes, that HIV-1 gp120 impaired endolysosome acidification (Pietrella et al., 1998).

Figure 12.   HIV-1 gp120-induced release of Fe^{2+} from endolysosomes results in increased levels of Fe^{2+} and ROS in cytosol and mitochondria. HIV-1 gp120 increases endolysosome pH, which then induces an efflux of ferrous iron (Fe^{2+}) through endolysosome-resident cation channels including divalent metal transporter (DMT1) and two pore channels (TPC). Ferrous iron released from endolysosomes can accumulate in the cytosol and can be taken into mitochondria via DMT1 or mitochondrial permeability transition pore (mPTP) opening. Fe^{2+} can catalyze Fenton reactions and the generation of reactive oxygen species (ROS). Mitochondrial ROS may signal back to endolysosomes to further exacerbate endolysosome dysfunction and the release of Fe^{2+}. HIV-1 gp120-mediated increases in cytosolic and mitochondrial ROS can be attenuated with inhibitors of DMT1 (CISMBI), TPC (Ned-19), and mPTP (TRO) channels.
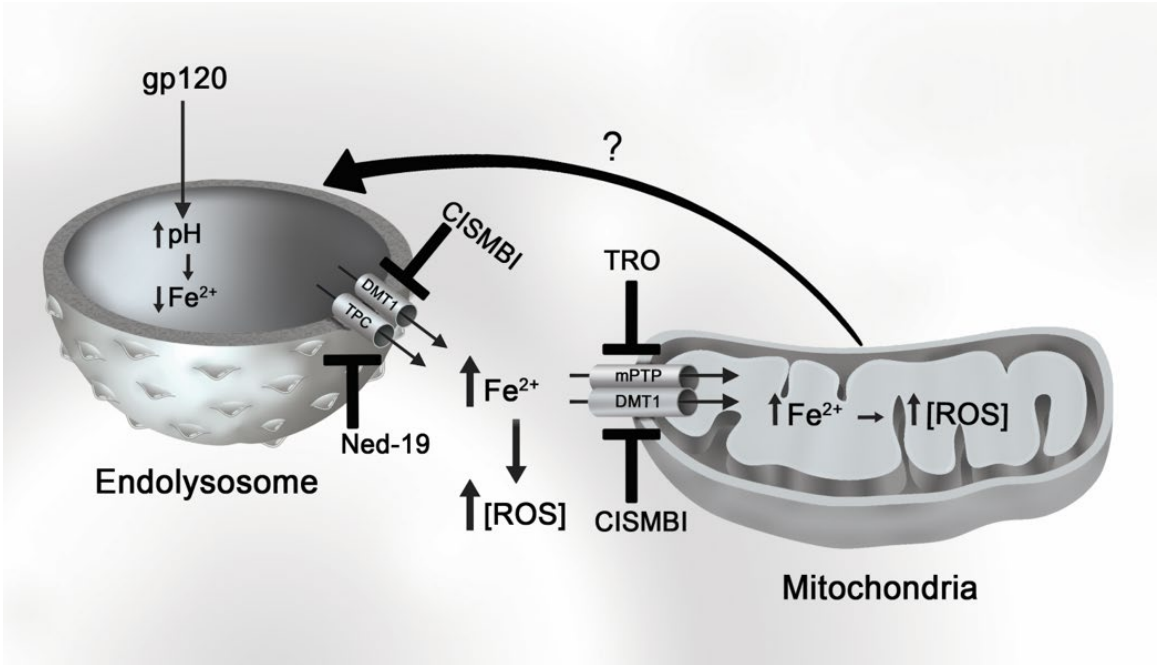
Here, we confirmed and extended these studies by showing in U87MG

astrocytoma cells that HIV-1 gp120 de-acidified endolysosome pH to an extent

similar to the vacuolar ATPase inhibitor Baf A1; a known endolysosome de-

acidifier (Yoshimori et al., 1991). Linked to endolysosome de-acidification are

changes to endolysosome morphology including increased endolysosome

volumes, decreased numbers of endolysosomes, and re-positioning of

endolysosomes in cells (Datta et al., 2019; Fernández et al., 2016; Myers,

Prendergast, Holman, Kuntz, & LaRusso, 1991; Ohkuma & Poole, 1981).

Accordingly, we determined the effects of HIV-1 gp120 on endolysosome

volumes and numbers and found that HIV-1 gp120, similar to Baf A1, increased

endolysosome volumes and decreased endolysosome numbers.

Endolysosome positioning inside of cells is influenced by multiple factors

including nutrient status, motor proteins, as well as cytosolic and intra-lysosomal

pH (Heuser, 1989; D. E. Johnson et al., 2016; Korolchuk et al., 2011; Parton et

al., 1991; Pu, Guardia, Keren-Kaplan, & Bonifacino, 2016). Previously, we

reported that HIV-1 gp120 promoted the movement of endolysosomes away from

the nucleus and towards plasma membranes as well as increased endolysosome

exocytosis (Datta et al., 2019) and here using U87MG cells we found similarly

that HIV-1 gp120 and the positive control Baf A1 both caused movement of

endolysosomes towards the periphery of cells and away from their normal more

perinuclear localization. Our results that de-acidified endolysosomes localize

towards the periphery of the cell while more acidic endolysosomes are positioned

in a more juxtanuclear manner support findings from multiple laboratories (Heuser, 1989; D. E. Johnson et al., 2016; Parton et al., 1991).

Endolysosomes contain multiple mechanisms capable of regulating H^+ levels as well as levels of various divalent cations including calcium, iron, copper and zinc (Abouhamed et al., 2006; X. P. Dong et al., 2008; Fernández et al., 2016). Endolysosome de-acidification is known to induce the release of these cations through various channels and transporters (Christensen et al., 2002; Fernández et al., 2016). Here we focused largely on two-pore channels (TPC) because of findings that they are endolysosome-resident and when activated by their endogenous agonist nicotinic adenine dinucleotide phosphate (NAADP) they release into the cytosol both calcium (Calcraft et al., 2009) and iron (Fernández et al., 2016). We found that HIV-1 gp120 significantly decreased levels of Fe^{2+} in endolysosomes and that HIV-1 gp120 significantly increased levels of Fe^{2+} in cytosol and mitochondria. Those findings suggest that HIV-1 gp120-induced release of ferrous iron from endolysosome stores was sufficient to increase levels in the cytosol and in mitochondria. This suggestion was supported further by findings that pre-treatment with deferoxamine, an endocytosed cell-impermeable iron chelator that specifically chelates iron in endolysosomes (Cable & Lloyd, 1999; Lloyd, Cable, & Rice-Evans, 1991), blocked the HIV-1 gp120-induced increases in the cytosol and mitochondria. Further, inhibiting mPTP opening and DMT-1 both blocked HIV-1 gp120-induced increases in mitochondrial iron. Because DMT-1 are localized on mitochondria and endolysosome membranes (Abouhamed et al., 2006; Wolff, Garrick, Zhao,

Garrick, & Thevenod, 2014; Wolff et al., 2018), our results with the DMT-1 inhibitor, CISMBI might have been the result of inhibiting endolysosome iron release and/or blocking mitochondrial iron uptake.

Although, our results suggest that HIV-1 gp120 disrupts endolysosome-mitochondrial iron signaling, it is not yet clear how iron is transferred between the two organelles. One possibility is a "kiss-and-run" mechanism where endolysosomes dock with and transfer iron to mitochondria (Das, Nag, Mason, & Barroso, 2016; Hamdi et al., 2016). Alternatively, endolysosome de-acidification might increase the iron translocation between endolysosomes and mitochondria and thereby contribute to oxidative stress (Uchiyama et al., 2008). Regardless, HIV-1 gp120-induced endolysosome iron efflux appears to be an upstream regulator of cytosolic and mitochondrial iron homeostasis.

A well-known biological consequence of elevated cytosolic and mitochondrial iron is the production of ROS through Fenton-based chemical reactions. We used assays to determine effects of HIV-1 gp120 on levels of intracellular hydroxyl radicals ($\cdot OH$), hydrogen peroxide (H_2O_2), and superoxide radicals ($\cdot O_2-$) as well as mitochondrial $\cdot O_2-$ (Dikalov & Harrison, 2014). Our findings of HIV-1 gp120-induced increases in mitochondrial-generated superoxide and cytosolic ROS are consistent with previous findings that gp120 increased levels of intracellular ROS (Datta et al., 2019; Lopez et al., 2017; Russo et al., 2005; Shah et al., 2013). Our findings that pre-treatment with DFO reduced significantly HIV-1 gp120-induced increases in ROS strongly suggest the involvement of endolysosome iron in these effects. However, we cannot rule out the possibility that other cations might

also be involved as well as the possible involvement of endolysosome-independent mechanisms. Although another study showed that endolysosome de-acidification led to increased ROS in mitochondria independent of endolysosome iron release (Yambire et al., 2019), it is possible that their experimental paradigm of persistent de-acidification resulted in endolysosome iron depletion as well as sequestration of cytosolic iron by iron storage proteins.

Elevated levels of oxidative stress can result in many biological events up to and including cell death. Under the conditions used here, we did not find any significant increase in levels of cell death with 30 min or 24 h treatments with HIV-1 gp120. However, others have noted ≤10% cell death in U87MG and SHSY5Y cells treated for 24 h with HIV-1 gp120 (Lopez et al., 2017; Russo et al., 2005). In contrast, 7–10-day HIV-1 gp120 treatments of U87MG cells increased cell viability and cell proliferation (Valentín-Guillama et al., 2018). Furthermore, HIV-1 gp120-induced increases in ROS promoted U87MG cell proliferation through the activation of glycolysis and the induction of protectant GRP78 (Lopez et al., 2017; Valentín-Guillama et al., 2018). Cancer cells have elevated ROS and antioxidant levels compared to non-cancer cells (Liou & Storz, 2010; Schieber & Chandel, 2014) and further studies are warranted in other types of cells to determine mechanisms underlying HIV-1 gp120-induced effects on cell proliferation, antioxidant levels, and cell viability.

Overall, our studies suggest that HIV-1 gp120 can induce a lysosomal stress response that includes the release of endolysosome stores of ferrous iron. Further, this release of iron from endolysosomes results in increased levels of

iron in cytosol and mitochondria that as well as increased oxidative stress. Thus, crosstalk between endolysosomes and mitochondria might participate in the pathogenesis of HAND and endolysosome iron might be targeted as an early and upstream target for therapeutic interventions against HAND.

CHAPTER 3

**EFFECTS OF HIV-1 GP120 ON IRON-RELATED
PROTEINS IN U87MG CELLS**

Introduction

Iron is a fundamental element for sustaining life. It is an integral component of

heme and non-heme iron proteins and plays a role in oxygen transport, electron

transfer, DNA synthesis and nitrogen fixation (Anderson, Shen, Eisenstein, &

Leibold, 2012). Iron is primarily found in one of two oxidative states; ferric (Fe^{3+})

and ferrous (Fe^{2+}). On the one hand, Fe^{2+} is biologically active and can undergo

Fenton chemistry (Fe (II) + $H_2O_2 \rightarrow$ Fe (III) + OH^- + OH·), which leads to oxidative

stress and even cell death (Eaton & Qian, 2002). On the other hand, Fe^{3+} is

biologically unavailable. Because of the necessity and toxicity of iron, organisms

have developed systemic and cellular regulatory mechanisms to control the

transport, uptake, storage, and export of iron (Anderson et al., 2012).

Systemically, in humans, Fe^{3+} is transported through circulation by a plasma

glycoprotein, transferrin (TF) (MacKenzie, Iwasaki, & Tsuji, 2008). Transferrin

receptor 1 (TFR1) is a transmembrane homodimer protein expressed on the

surface of cells and is involved in receptor-mediated endocytosis of iron bound

TF (Ponka & Lok, 1999). Two molecules of Fe^{3+} bind to one molecule of TF. The

diferric-transferrin complex binds to TFR1 and is endocytosed. Once the

diferric- TF-TFR1 complex is within endosomes, the iron is released from TF

due to the acidic luminal environment of endolysosomes; TF remains bound to TFR1 (Ponka & Lok, 1999). Then, TF-TFR1 is recycled back to the plasma membrane and TF is released from its receptor into the extracellular space (Ponka & Lok, 1999).

Fe^{3+} within endosomes is reduced to Fe^{2+} via endosome-resident ferrireductase six-transmembrane epithelial antigen of prostate 3 (STEAP3). Fe^{2+} can be released through various channels and transporters including endosome-resident divalent metal transporter 1 (DMT-1) or other iron permeable channels such as transient receptor potential mucolipin 1 (TRPML1) (X. P. Dong et al., 2008; MacKenzie et al., 2008). The iron released into the cytosol becomes part of the intracellular liable iron pool (LIP) where it can be stored, incorporated in metalloproteins and metalloenzymes, or act as a catalyst for the production of reactive oxygen species (ROS) (Lv & Shang, 2018).

Intracellularly, cells contain different iron-related proteins that help regulate the LIP including iron sensors, iron regulatory proteins 1 and 2 (IRP1/2), the iron storage protein ferritin (FTN); and the iron exporter ferroportin (FPN). IRP1 and IRP2 regulate iron-related proteins at the post-transcriptional level via the iron responsive element/iron responsive protein (IRE/IRP) system (Anderson et al., 2012; Wallace, 2016). IRPs are cytosolic proteins that bind to the 5'- or 3'-untranslated regions (UTR) of iron uptake (TFR1, DMT-1), storage (FTN), and export (FPN) mRNAs (Anderson et al., 2012).

When levels of iron in the cytosol are low, IRPs bind to the 5'-UTR of FTN and FPN leading to their transcriptional repression, while IRPs bind to the 3'-UTR of TFR1 and DMT-1 leading to the stabilization of their mRNAs and translation (Anderson et al., 2012; W. Wang, Di, D'Agostino, Torti, & Torti, 2007). Conversely, when cytosolic iron levels are high, IRP2 undergoes proteasomal degradation, while IRP1 binds to iron-sulfur (4Fe-4S) clusters (Anderson et al., 2012; W. Wang et al., 2007). This leads to the translational activation of iron storage and export proteins, while the mRNA transcripts of iron uptake proteins are degraded by RNases (reviewed by (Anderson et al., 2012; Wallander, Leibold, & Eisenstein, 2006)).

As previously described, ferritin is an iron storage protein (Torti & Torti, 2002). Ferritin is comprised of two subunits, a light (FTL) and heavy chain (FTH) that form a 12- or 24-mer hollow sphere which can bind up to 4500 molecules of Fe^{3+} (Crichton, Wilmet, Legssyer, & Ward, 2002; Torti & Torti, 2002). The heavy chain subunit of ferritin contains a ferroxidase center which oxidizes Fe^{2+} to Fe^{3+} (Lv & Shang, 2018). Thus, ferritin is used by cells to store excess cytosolic iron in its biologically inactive state and protect cells from oxidative stress (Torti & Torti, 2002). When cells are in demand of Fe^{2+}, ferritin is mobilized into lysosomes where it is degraded and releases Fe^{3+} into the lysosomal lumen, which can then be released as Fe^{2+} from lysosomes (Konijn et al., 1999).

Ferroportin is an exporter of iron that enables iron release from cells into circulation (MacKenzie et al., 2008). Fe^{3+} is released by FPN and conversion to Fe^{2+} is catalyzed by plasma membrane resident ceruloplasmin, a cooper-

containing ferroxidase (MacKenzie et al., 2008; Wallace, 2016). Ferroportin is post-translationally regulated by hepcidin, a hormone released by the liver, which induces the internalization and lysosomal degradation of ferroportin (MacKenzie et al., 2008).

Experimentally, deferoxamine (DFO) and ferric ammonium citrate (FAC) are used to modulate iron related protein levels *in vitro* and *in vivo* (Hoepken, Korten, Robinson, & Dringen, 2004; L. B. Li et al., 2019; Varghese, James, Vaulont, McKie, & Jacob, 2018). DFO is used to reduce cytosolic iron levels, while FAC is used to increase cytosolic iron levels. DFO is a cell impermeable iron chelator, which localizes in endolysosomes (Cable & Lloyd, 1999; Lloyd et al., 1991). FAC is an extracellular iron supplement and is dissolvable as iron salt ferric citrate (H. Wang et al., 2018). The mechanisms of FAC internalization are not fully elucidated however FAC appears to enter cells via a TF-TFR1 independent pathway (L. B. Li et al., 2019; D. R. Richardson & Ponka, 1995; Trinder, Batey, Morgan, & Baker, 1990).

Of interest, PLWH have elevated levels of serum iron and saturated TF (Chang et al., 2015). Furthermore, HIV-1 reduces intracellular iron levels, which is indicated by an increase in TFR1 mRNA levels in CD4^{+} cells and an increase in uptake of radiolabeled iron (Chang et al., 2015). In HAND, increased levels of iron seem to be associated with declined cognitive status (Kallianpur et al., 2019). Although the underlying mechanisms of HAND pathogenesis are unclear, oxidative stress and HIV-1 proteins appear to play a role (Kovalevich & Langford, 2012). Others and we have shown that HIV-1 gp120 can promote ROS

production (Datta et al., 2019; Lopez et al., 2017; Russo et al., 2005; Shah et al., 2013). HIV-1 gp120 also leads to low levels of cell death (Lopez et al., 2017; Russo et al., 2005; Valentín-Guillama et al., 2018). HIV-1 gp120 transgenic mice do not survive as long as wild-type mice and have a high incidence of glioma tumors (Valentín-Guillama et al., 2018).

Cancer cells have elevated levels of ROS and antioxidants compared to non-cancer (Liou & Storz, 2010; Schieber & Chandel, 2014). Because HIV-1 gp120 does not produce cell death in cancer cells (Lopez et al., 2017; Valentín-Guillama et al., 2018) but does increase levels of ROS, we investigated the effects of HIV-1 gp120 on iron related proteins in U87MG cells. It is plausible that U87MG cells may upregulate iron-related proteins to prevent cell death. The role of HIV-1 gp120 on expression levels of iron related protein levels has yet to be explored. Therefore, in this study we determined the effects of long-term HIV-1 gp120 treatment on iron-related proteins. Specifically, we hypothesized that 24 h HIV-1 gp120 treatment would decrease TFR1 and IRP2 and increase FTH and FPN protein levels in U87MG cells.

Materials and Methods

Cell Culture

Astrocytoma (U87MG) cells were cultured in 1x DMEM (Invitrogen) containing 10% fetal bovine serum (R&D systems) and 1% penicillin/streptomycin (Invitrogen). U87MG cells were grown in T75 and T125 flasks (Invitrogen) and then sub-cultured in 35 mm^2 dishes (MatTek), 6-, 12-, 24-well plates (Corning), or

100 mm dishes (Corning); cells were maintained in a 5% CO_2 incubator (NuAire) at 37°C. Cells were not used past their tenth passage.

Cell Surface Immunofluorescence Staining

Cells were seeded at 5 x 10^5 cells in 6 well plates and allowed to attach overnight. The next day, cells were treated with gp120, DFO, gp120[i], or FAC for 24 h. After treatment, cells were harvested in PBS and centrifuged at 1500 x g for 2 min. Post-centrifugation, cells were fixed with 4% PFA for 5 min. Then, cells were washed twice with 1x PBS and blocked with 0.01% FBS in PBS for 1 h on ice. Cells were centrifuged at 1500 x g for 2 min and blocking buffer was removed and cell pellets were washed twice with PBS. After the washing step, cells were incubated with Alexa Fluor (AF) 647 anti-transferrin receptor antibody (Abcam, ab187777), AF647 anti-ferroportin antibody (R&D systems; FAB9924R), or AF647 anti-IgG1 isotype control antibody (Abcam, ab239459). Then, cells were centrifuged as described above, and washed twice with PBS, and finally resuspended in PBS. AF647-labeled cells were excited by red (637 nm) excitation laser and light emission was determined using RL1 (670/14 nm) filter. Mean fluorescence intensity (MFI), standard error of the mean (SEM), and n were determined using Attune NxT software (ThermoFisher).

Western Blot

U87MG cells were seeded at a density of 1.5 x 10^5 cells in 100 mm^2 dishes. After incubation with control or treatments, cells were harvested and lysed in triple detergent lysis buffer (10 mM NaCl, 50 mM Tris, 0.5% sodium deoxychloate, 10 mM sodium pyrophosphate, 0.1% SDS, 5 mM EDTA, 1 mM DTT) plus

phosphatase and protease inhibitor cocktail (PIC; ThermoFisher, 78443) and

were mixed three times with 10 min rest between each mixing. Then, cell lysates

were centrifuged at 14,000 x g for 10 min at 4 °C, supernatants were collected,

and protein concentrations were determined by Bradford protein assay (Bio-

Rad). Samples were prepared using 4x Laemmli buffer (Bio-Rad). Proteins (5-

15 µg) were loaded into and separated by SDS-PAGE (4-20% precast gels, Bio-

Rad) and transferred unto PVDF membranes via iBlot2 Dry Blotting

System (ThermoFisher; IB21001). Total protein staining (LI-COR, 926-1101) was

used to normalize protein samples. Then, membranes were stained with anti-

ferritin antibody (Cell Signaling Technology, #3998S) or anti-transferrin receptor

antibody (Cell Signaling Technology, #13113S). After primary antibody

incubation, membranes were incubated with IRDye goat anti-rabbit secondary

antibody (Licor, 925-32211). Then, blots were imaged using the Odyssey Fc

Imaging System (LI-COR). Image Studio software (LI-COR) was used to quantify

results; quantification of results was performed by densitometry and the results

were analyzed as total integrated densitometric volume values (au). Treatment

groups were normalized to control groups.

Data Analysis

All data were expressed as mean and SEM. Data analyses were completed

using GraphPad Prism 9 software. Statistically significant differences between

two groups was determined using a Student's t-test. One-way ANOVA with

Tukey's post-hoc tests and two-way ANOVA with Tukey's post-hoc tests were

used to compare differences between multiple groups with one or two factors, respectively.

Chemicals

Deferoxamine (DFO) and ferric ammonium citrate (FAC) were purchased from Millipore Sigma (St. Louis, MO, USA). DMSO, PBS, and DMEM were purchased from ThermoFisher Scientific (Waltham, MA, USA). HIV-1 gp120 was purchased from ABL Inc. (Rockville, MD, USA). All of the drugs were prepared and stored as aliquots at -20°C, and HIV-1 gp120 was aliquoted and stored at -80°C until used. The stock solutions of all chemicals were diluted in H_2O, DMSO, or PBS to reach the final working concentrations applied to cells. The final concentration of DMSO soluble chemicals or other vehicles, water or PBS, were kept ≤0.1%.

Results

Effects of Deferoxamine on Transferrin Receptor 1 Protein Levels

We first determined how U87MG cells responded to iron supplementation or iron chelation. We hypothesized that DFO would increase expression levels of TFR1 protein in a concentration- and time-dependent manner. We treated cells for 6 h, 12 h, or 24 h with H_2O vehicle control (Ctrl) or DFO at 30 µM, 100 µM, or 300 µM. Then, whole cell lysates were used to determine changes in TFR1 protein levels by Western blotting. 24 h DFO treatment at 30 µM ($p<0.01$), 100 µM ($p<0.01$), and 300 µM ($p<0.01$) induced a 74%, 59%, and 72% increase, respectively, in TFR1 levels compared to vehicle control (Figure 13A). 24 h DFO treatment at 30 µM, 100 µM, and 300 µM significantly ($p<0.0001$) increased transferrin receptor protein levels compared to 6 h DFO treatment at 30 µM and

Figure 13.   24 h DFO treatment at 30 µM, 100 µM, and 300 µM increased transferrin receptor 1 (TFR1) protein levels. Ordinary two-way ANOVA analysis determined that both time and DFO concentrations have effects on expression levels of TFR1 protein. Furthermore, there is a significant interaction between time and DFO concentrations. **(A)** U87MG cells were treated for 6 h, 12 h, or 24 h with H_2O vehicle control (Ctrl), 30 µM, 100 µM, or 300 µM deferoxamine (DFO). 24 h DFO treatment at 30 µM ($p<0.001$), 100 µM ($p<0.01$), and 300 µM ($p<0.001$) significantly increased protein levels of transferrin receptor 1 (TFR1). (Refer to Table 1 for statistical comparisons) **(B)** 100 µM DFO treatment significantly increased TFR1 levels at 6 h ($p<0.01$) and 24 h ($p<0.0001$) time points but not at 12 h compared to vehicle control. 12 h DFO treatment significantly reduced transferrin receptor protein levels compared to 6 h ($p<0.05$) and 24 h ($p<0.001$) DFO treatment. Data represented as mean and SEM. N= three independent experiments run in duplicate, *$p<0.05$, **$p<0.01$, ***$p<0.001$, ****$p<0.0001$.
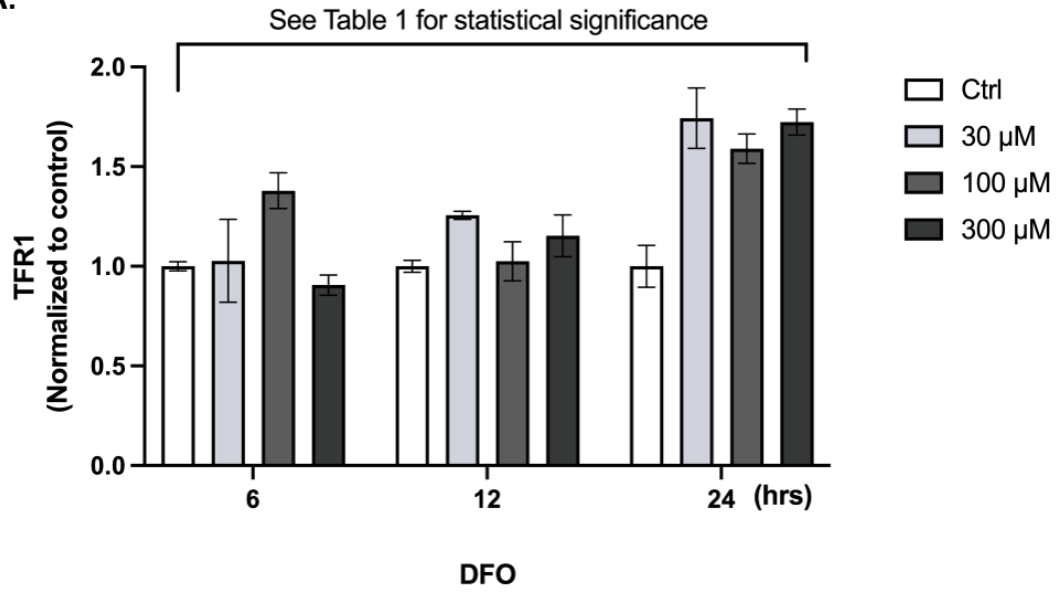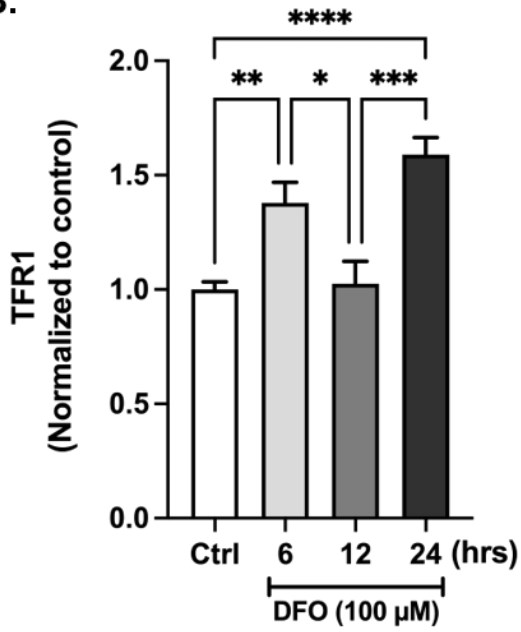
300 µM and 12 h DFO treatment at 30 µM, 100 µM, and 300 µM (Figure 13A;

Table 1 and 2). Next, we compared the time point at which 100 µM DFO

increases transferrin receptor protein (Figure 13B). U87MG cells treated for 6 h

with DFO induced a 38% increase ($p<0.001$) in TFR1 compared to vehicle

control. 12 h DFO treatment did not significantly affect in TFR1 levels compared

to controls but 12 h DFO treatment induced a 35% decrease ($p<0.01$) in TFR1

levels compared to 6 h DFO treatment. 24 h DFO treatment led to a 59%

increase ($p<0.0001$) in TFR1 compared to controls and a 55% increase

($p<0.001$) compared to 12 h DFO treatment.

Table 1. Ordinary two-way ANOVA results for figure 13A, with an alpha level set at 0.05. Sum of squares (SS), degrees of freedom (DF), mean squares (MS).

Source of Variation	% of total variation	P value	Significant?	
Interaction	22.41	0.0007	Yes	
Time	34.55	<0.0001	Yes	
Concentration	16.78	0.0004	Yes	
ANOVA table	SS	DF	F (DFn, DFd)	P value
Interaction	1.231	6	F (6, 36) = 5.122	P=0.0007
Time	1.898	2	F (2, 36) = 23.68	P<0.0001
Concentration	0.9220	3	F (3, 36) = 7.671	P=0.0004
Residual	1.442	36		

Table 2. Ordinary two-way ANOVA with Tukey's multiple comparisons for Figure 13A. Only statistically significant comparisons are shown.
*p<0.05, **p<0.01, ***p<0.001, ****p<0.0001

Tukey's multiple comparisons test	Summary
6 h Treatment	
Ctrl vs. 24 h:30 µM	***
Ctrl vs. 24 h:100 µM	**
Ctrl vs. 24 h:300 µM	***
30 µM vs. 24 h:30 µM	***
30 µM vs. 24 h:100 µM	*
30 µM vs. 24 h:300 µM	**
300 µM vs. 24 h:30 µM	****
300 µM vs. 24 h:100 µM	**
300 µM vs. 24 h:300 µM	****
12 h Treatment	
Ctrl vs. 24 h:30 µM	***
Ctrl vs. 24 h:100 µM	**
Ctrl vs. 24 h:300 µM	***
100 µM vs. 24 h:30 µM	***
100 µM vs. 24 h:100 µM	*
100 µM vs. 24 h:300 µM	***
300 µM vs. 24 h:30 µM	**
300 µM vs. 24 h:300 µM	*
24 h Treatment	
Ctrl vs. 24 h:30 µM	***
Ctrl vs. 24 h:100 µM	**
Ctrl vs. 24 h:300 µM	***

DFO Increased, while FAC Decreased Cell Surface Expression Levels of Transferrin Receptor Protein 1

Next, we determined the effects of 24 h DFO and FAC treatment on cell surface expression levels of TFR1. U87MG cells were treated for 24 h with H_2O vehicle control (Ctrl), 100 µM DFO, or 100 µM FAC and then cells were stained with AF647-conjugated anti-transferrin receptor 1 antibody. Mean fluorescence intensity (MFI) of cell surface TFR1 was measured by flow cytometry. DFO treatment significantly ($p < 0.0001$) increased the MFI for surface TFR1 from control values of $14,825 \pm 13$ to $23,458 \pm 70$ (Figure 14). FAC treatment significantly ($p < 0.0001$) decreased surface TFR1 MFI from control levels of $14,825 \pm 13$ to $12,811 \pm 20$ (Figure 14).

FAC Decreased Transferrin Receptor Protein 1 Expression Levels

We next measured the effects 24 h 100 µM FAC treatment on total protein levels of TFR1. U87MG cells were treated for 24 h with H_2O vehicle (Ctrl) or 100 µM FAC and whole cell lysates were used to determine changes in TFR1 protein by Western blotting. 24 h FAC treatment induced a 63% decrease ($p < 0.01$) in TFR1 expression levels compared to vehicle control (Figure 15).

Effects of Ferric Ammonium Citrate on Ferritin Heavy Chain Protein Levels

We next determined the time- and concentration-dependence of FAC-induced increases in FTH protein levels. We treated cells for 6 h, 12 h, or 24 h with H_2O vehicle control (Ctrl) or FAC at 30 µM, 100 µM, or 300 µM. Then whole cell lysates were used to determine changes in FTH protein levels by Western blotting. 6 h FAC treatment at 30 µM ($p < 0.05$), 100 µM ($p < 0.01$), and 300 µM ($p < 0.01$) induced a 148%, 140%, and 195% increase in FTH protein,

Figure 14.   DFO increased and FAC decreased cell surface expression levels of transferrin receptor 1. U87MG cells were treated for 24 h with H_2O vehicle control (Ctrl), 100 µM deferoxamine (DFO), or 100 µM ferric ammonium citrate (FAC). Levels of cell surface TFR1 were determined by immunofluorescence staining of U87MG cells with AF647-conjugated anti-transferrin receptor antibody and fluorescence was measured by flow cytometry. DFO significantly ($p < 0.0001$) increased TFR1 MFI compared to vehicle control, while FAC significantly ($p < 0.0001$) decreased TFR1 MFI. AF647 fluorescence was measured as mean fluorescence intensity (MFI). Data represented as mean and SEM. N=921, ****$p < 0.0001$.
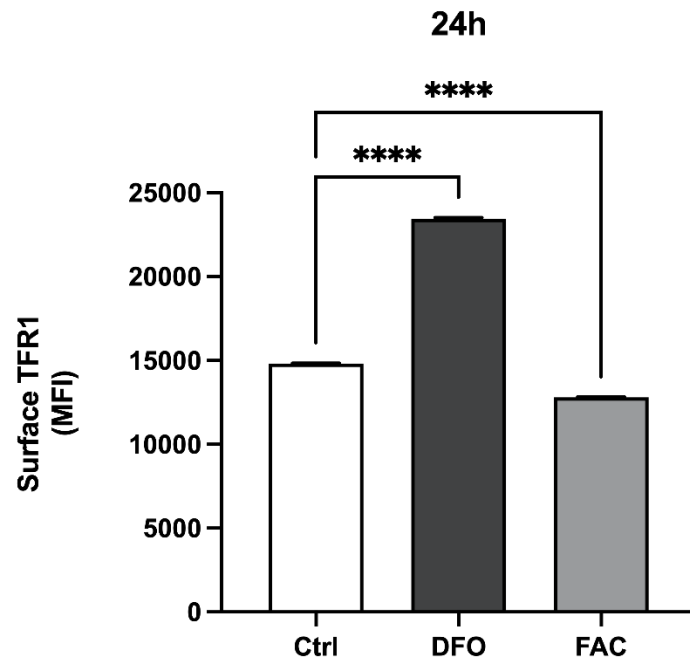
Figure 15.   FAC decreased whole cell expression levels of transferrin receptor 1 protein. U87MG cells were treated for 24 h with H_2O vehicle control (Ctrl) or 100 µM ferric ammonium citrate (FAC). FAC treatment significantly ($p<0.01$) decreased whole cell levels of transferrin receptor 1 (TFR1) protein. Data is represented as mean and SEM. N= three independent experiments run in duplicate.

24h
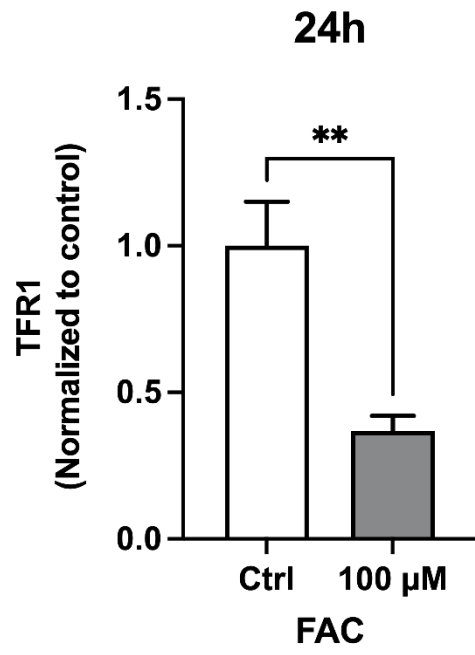
respectively, compared to vehicle control. 12 h FAC treatment at 30 µM (p<0.01), 100 µM (p<0.001), and 300 µM (p<0.0001) induced a 203%, 237%, and 331% increase in FTH protein, respectively, compared to vehicle control. 24 h FAC treatment at 30 µM (p<0.0001), 100 µM (p<0.0001), and 300 µM (p<0.0001) induced a 521%, 763%, and 1040% increase in FTH protein, respectively, compared to vehicle control. 24 h 30 µM treatment induced a 150% increase (p<0.0001) in FTH protein compared to 6 h FAC 30 µM treatment and a 105% increase (p<0.0001) in FTH protein compared to 12 h FAC 30 µM treatment. 24 h FAC treatment at 100 µM induced a 260% increase (p<0.0001) in FTH protein compared to 6 h FAC treatment at 100 µM and a 156% increase (p<0.0001) compared to 12 h FAC 100 µM treatment. 24 h FAC treatment at 300 µM induced a 285% (p<0.0001) increase in FTH protein compared to 6 h FAC 300 µM treatment and a 164% (p<0.0001) increase compared to 12 h FAC 300 µM treatment (Figure 16A; Table 3 and 4).

Figure 16.   Ferric ammonium citrate increased ferritin heavy chain protein levels in a time- and concentration-dependent manner. Ordinary two-way ANOVA analysis determined that both time and FAC concentrations have effects on expression levels of FTH protein. Furthermore, there is a significant interaction between time and FAC concentrations. **(A)** U87MG cells were treated for 6 h, 12 h, and 24 h with H_2O vehicle control (Ctrl), and 30 µM, 100 µM, or 300 µM ferric ammonium citrate (FAC). 6 h FAC treatment significantly increased ferritin heavy chain (FTH) protein levels at 30 µM ($p < 0.05$), 100 µM ($p < 0.01$), and 300 µM ($p < 0.01$). 12 h FAC treatment significantly increased FTH protein levels at 30 µM ($p < 0.01$), 100 µM ($p < 0.001$), 300 µM ($p < 0.0001$). 24 h FAC treatment significantly increased FTH protein levels at 30 µM ($p < 0.0001$), 100 µM ($p < 0.0001$), 300 µM ($p < 0.0001$). (Refer to Table 2 for statistically significant comparisons). **(B)** FTH protein was significantly increased with 100 µM FAC treatment at 6 h ($p < 0.01$), 12 h ($p < 0.0001$), and 24 h ($p < 0.0001$) compared to vehicle control. 24 h FAC treatment induced a significant increase in FTH protein compared to FAC treatment at 6 h ($p < 0.0001$) and 12 h ($p < 0.0001$). Data represented as mean and SEM. N= three independent experiments run in duplicate, **$p < 0.01$, ****$p < 0.0001$.

A.

B.
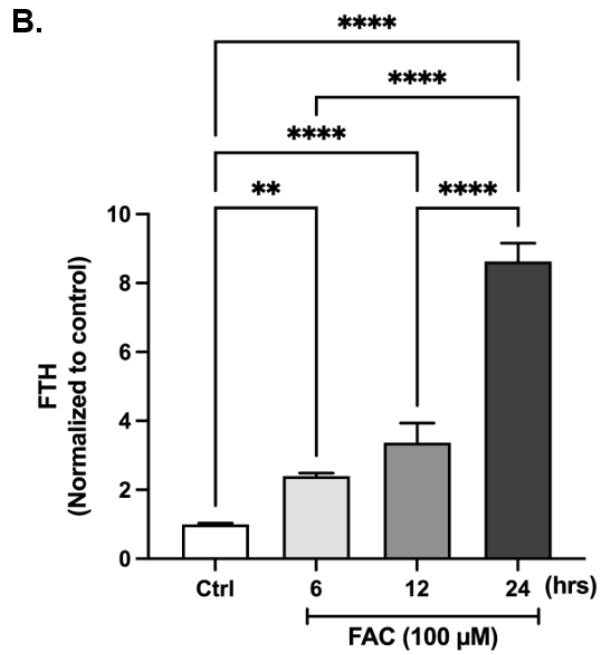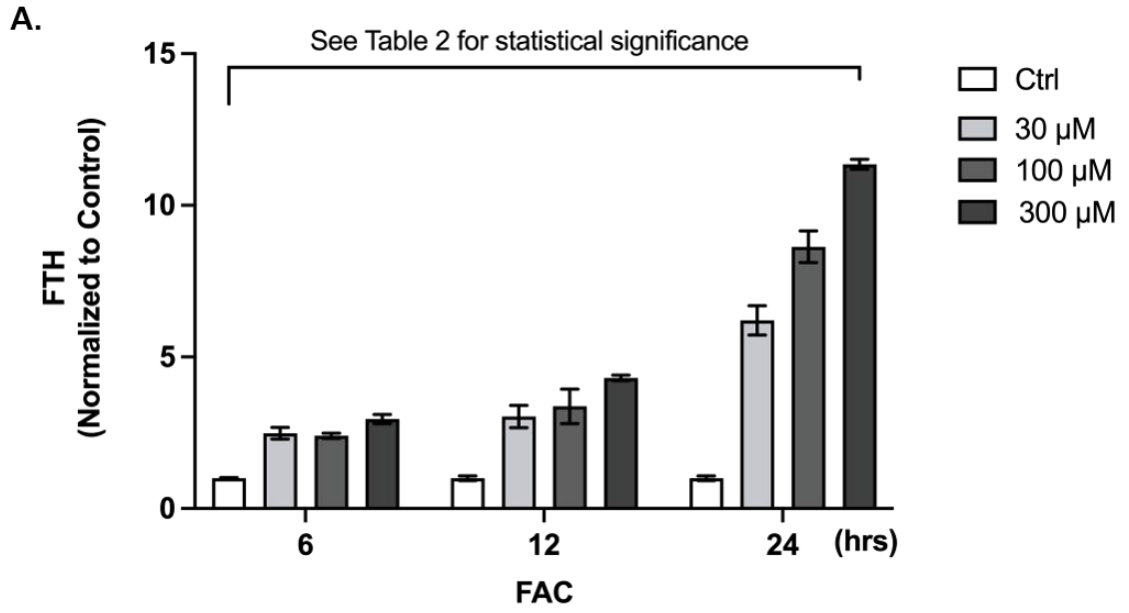
Table 3. Ordinary two-way ANOVA results for figure 16A, with an alpha level set at 0.05. Sum of squares (SS), degrees of freedom (DF), mean squares (MS).

Source of Variation	% of total variation	P value	P value summary	Significant?	
Interaction	19.08	<0.0001	****	Yes	
Row Factor	41.31	<0.0001	****	Yes	
Column Factor	36.87	<0.0001	****	Yes	
ANOVA table	SS	DF	MS	F (DFn, DFd)	P value
Interaction	90.13	6	15.02	F (6, 36) = 41.91	P<0.0001
Row Factor	195.1	2	97.56	F (2, 36) = 272.2	P<0.0001
Column Factor	174.1	3	58.05	F (3, 36) = 161.9	P<0.0001
Residual	12.90	36	0.3585		

Table 4. Ordinary two-way ANOVA with Tukey's multiple comparisons for Figure 16A. Only statistically significant comparisons are shown. *p<0.05, **p<0.01, ***p<0.001, ****p<0.0001

Tukey's multiple comparisons test	Summary
6 h Treatment	
Ctrl vs. 6:30 µM	*
Ctrl vs. 6:300 µM	**
Ctrl vs. 12:30 µM	**
Ctrl vs. 12:100 µM	***
Ctrl vs. 12:300 µM	****
Ctrl vs. 24:30 µM	****
Ctrl vs. 24:100 µM	****
Ctrl vs. 24:300 µM	****
30 µM vs. 12:Ctrl	*
30 µM vs. 12:300 µM	**
30 µM vs. 24:Ctrl	*
30 µM vs. 24:30 µM	****
30 µM vs. 24:100 µM	****
30 µM vs. 24:300 µM	****
100 µM vs. 12:300 µM	**
100 µM vs. 24:30 µM	****
100 µM vs. 24:100 µM	****
100 µM vs. 24:300 µM	****
300 µM vs. 12:Ctrl	**
300 µM vs. 24:Ctrl	**
300 µM vs. 24:30 µM	****
300 µM vs. 24:100 µM	****
300 µM vs. 24:300 µM	****
12 h Treatment	
Ctrl vs. 12:30 µM	**
Ctrl vs. 12:100 µM	***
Ctrl vs. 12:300 µM	****
Ctrl vs. 24:30 µM	****
Ctrl vs. 24:100 µM	****
Ctrl vs. 24:300 µM	****
30 µM vs. 24:Ctrl	**
30 µM vs. 24:30 µM	****
30 µM vs. 24:100 µM	****
30 µM vs. 24:300 µM	****
100 µM vs. 24:Ctrl	***
100 µM vs. 24:30 µM	****
100 µM vs. 24:100 µM	****
100 µM vs. 24:300 µM	****
300 µM vs. 24:Ctrl	****
300 µM vs. 24:30 µM	**
300 µM vs. 24:100 µM	****
300 µM vs. 24:300 µM	****
24 h Treatment	
Ctrl vs. 24:30 µM	****
Ctrl vs. 24:100 µM	****
Ctrl vs. 24:300 µM	****
30 µM vs. 24:100 µM	****
30 µM vs. 24:300 µM	****
100 µM vs. 24:300 µM	****

Next, we determined the optimal time point at which 100 µM FAC increased

levels of FTH protein. U87MG cells, were treated for 6, 12, and 24 h with H_2O

vehicle control (Ctrl) or 100 µM FAC. 6 h ($p<0.01$), 12 h ($p<0.0001$), and 24 h

($p<0.0001$) FAC treatment induced significantly increased FTH levels by 140%,

237%, and 763% respectively. Increased levels of FTH with 24 h FAC treatment

were significantly (260%) higher ($p<0.0001$) than 6 h FAC treatments and

significantly (156%) higher ($p<0.0001$) than 12 h FAC treatments (Figure 16B).

Deferoxamine Decreased Ferritin Heavy Chain Protein Levels

Next, we determined the effects of DFO on protein levels of FTH. U87MG cells

were treated with H_2O vehicle control (Ctrl) or 100 µM DFO. 24 h DFO treatment

significantly decreased ($p<0.01$) FTH levels compared to vehicle control

(Figure 17).

Ferric Ammonium Citrate Decreased Iron Regulatory Protein 2 Protein Levels

Here we measured the effect of DFO and FAC on IRP2 protein levels. U87MG

cells were treated for 24 h with H_2O vehicle control (Ctrl), 100 µM FAC, or

100 µM DFO. FAC treatment significantly decreased (85%) ($p<0.0001$) IRP2

protein levels compared to vehicle controls. DFO treatment did not significantly

affect IRP2 protein levels (Figure 18).

HIV-1 gp120 did not Alter Levels of Total and Surface Transferrin Receptor Protein

Next, we determined concentration-dependent effects of HIV-1 gp120 on total

TFR1 protein levels. U87MG cells were treated for 24 h with heat-inactivated

gp120 (gp120[i]) or HIV-1 gp120 at concentrations: 0.044, 0.444, 1.33, and 4 nM.

Figure 17.   24 h DFO treatment decreased ferritin heavy chain protein levels. U87MG cells were treated for 24 h with H_2O vehicle control (Ctrl) or 100 µM DFO. DFO treatment significantly (p<0.01) decreased ferritin heavy chain (FTH) levels. Data represented as mean and SEM. N= three independent experiments run in duplicate, **p<0.01

24h
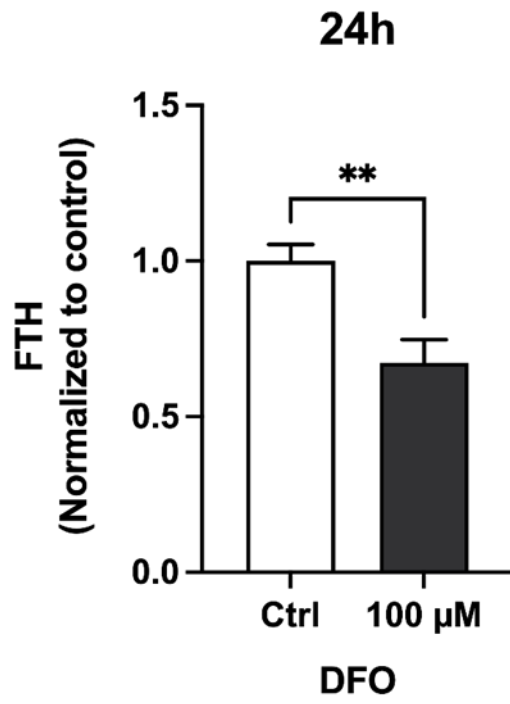
Figure 18.   FAC decreased iron regulatory protein 2 (IRP2) protein levels.
              U87MG cells were treated for 24 h with H_2O vehicle control
              (Ctrl), 100 µM FAC or 100 µM DFO. FAC significantly ($p < 0.0001$)
              decreased iron related protein 2 (IRP2) protein levels. Data
              represented as mean and SEM. N= three independent
              experiments run in duplicate, ****$p < 0.0001$.

24h
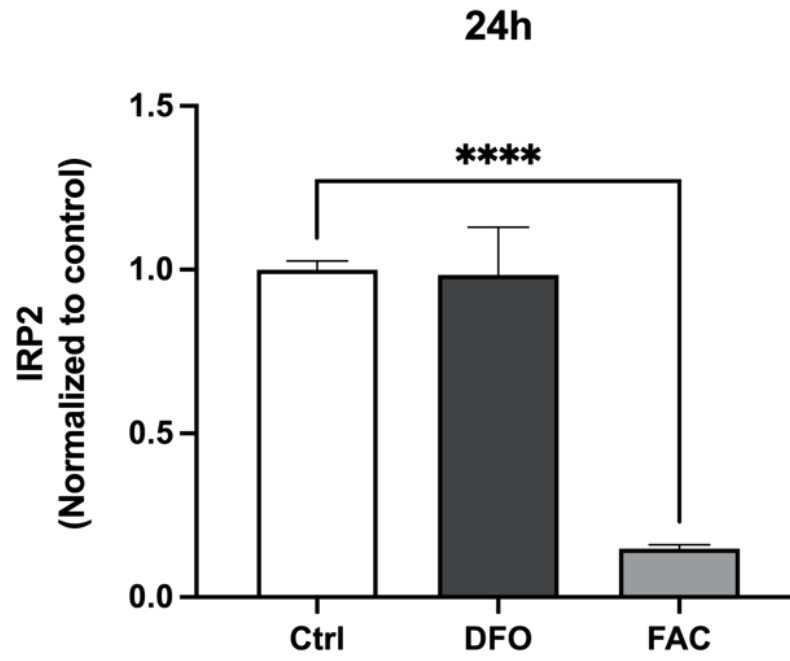
A significant ($p < 0.05$) decrease in FTH protein levels was only observed with 1.33 nM gp120; a 23% decrease (Figure 19). Next, we determined the concentration at which HIV-1 gp120 affects surface expression levels of TFR1 levels. As described above, U87MG cells were treated for 24 h with gp120[i] or gp120 at 0.044, 0.444, 1.33, or 4 nM. Then cells were stained with AF647-conjugated anti-transferrin receptor 1 antibody and MFI of AF647-positive cells in each group was measured by flow cytometry. HIV-1 gp120 did not significantly change cell surface expression levels of transferrin receptor (Figure 20).

HIV-1 gp120 did not Affect Protein Levels of Ferritin Heavy Chain and Iron Regulatory Protein 2

We next investigated HIV-1 gp120 concentration-dependent changes in FTH protein levels. U87MG cells were treated for 24 h with gp120[i] or with gp120 at varying concentrations as described above. We did not observe any statistically significant changes in FTH protein (Figure 21). Likewise, when we measured levels of IRP2 after 24 h treatment with gp120[i] or gp120 we did not observe a change in IRP2 levels compared to controls (Figure 22).

HIV-1 gp120 and FAC Increased Cell Surface Expression Levels of Ferroportin

Based on our findings that 24 h HIV-1 gp120 treatment did not affect IRP2 or FTH, we hypothesized that HIV-1 gp120 induces an increase in surface levels of ferroportin (FPN), a plasma membrane resident iron export channel. U87MG cells were treated for 24 h with gp120[i]; FAC, which acted as a positive control (G. Y. Zhao, Di, Wang, Zhang, & Xu, 2014); or 4 nM HIV-1 gp120. Then cells were

Figure 19.   HIV-1 gp120 decreased total cellular levels of transferrin receptor 1 protein. U87MG cells were treated for 24 h with heat-inactivated gp120 (gp120[i]) or HIV-1 gp120 at varying concentrations: 0.044, 0.444, 1.33, and 4 nM. Transferrin receptor (TFR1) protein levels were significantly ($p<0.05$) reduced with 1.33 nM HIV-1 gp120, while treatments with 0.044, 0.444 and 4 nM did not induce a significant decrease in TFR1 protein. Data represented as mean and SEM. N= four independent experiments run in duplicate, *$p<0.05$.

24h
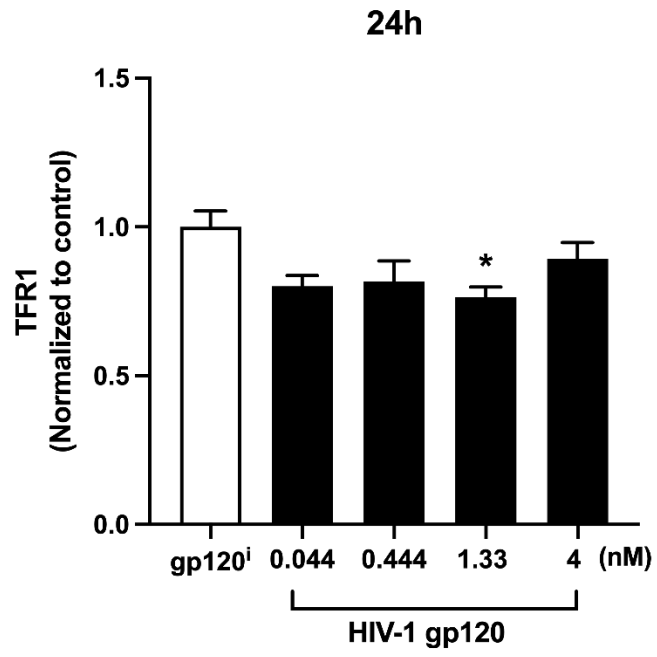
Figure 20.   HIV-1 gp120 treatment did not significantly affect surface levels
of transferrin receptor 1. U87MG cells were treated for 24 h with
heat-inactivated gp120 (gp120[i]) or with HIV-1 gp120 at varying
concentrations: 0.044, 0.444, 1.33, or 4 nM HIV-1 gp120. There
was no significant change in surface transferrin receptor 1
(TFR1) expression levels at any concentration tested. Levels of
surface TFR1 were determined by immunofluorescent staining of
U87MG cells with AF647-conjugated anti-transferrin receptor
antibody and AF647 mean fluorescence intensity (MFI) was
measured by flow cytometry. Data represented as mean and
SEM. N=1500.

24h
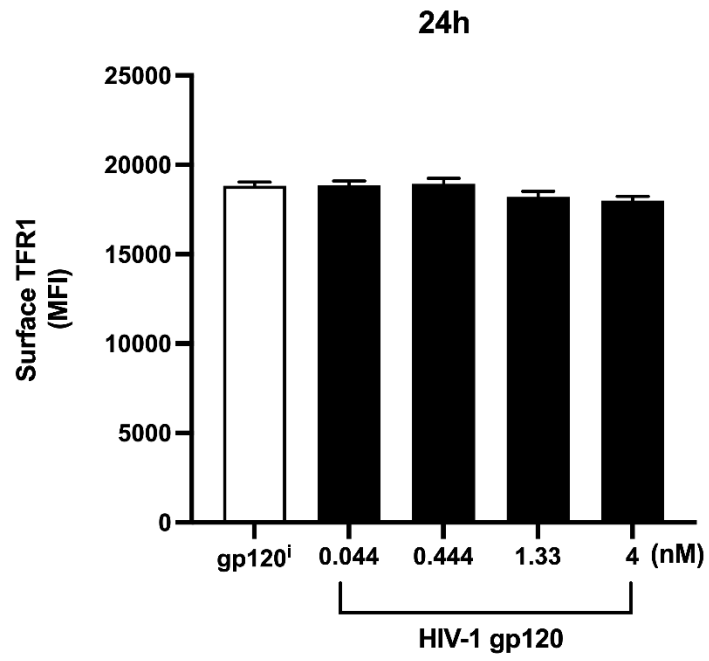
Figure 21.   HIV-1 gp120 did not alter total cellular levels of ferritin heavy chain protein. U87MG cells were treated for 24 h with heat-inactivated gp120 (gp120^i) or HIV-1 gp120 at varying concentrations: 0.044, 0.444, 1.33, or 4 nM. HIV-1 gp120 did not induce a significant increase in ferritin heavy chain (FTH) protein at any concentration. Data represented as mean and SEM. N= four independent experiments run in duplicate.

24h

FTH
(Normalized to control)

gp120^i   0.044   0.444   1.33   4   (nM)
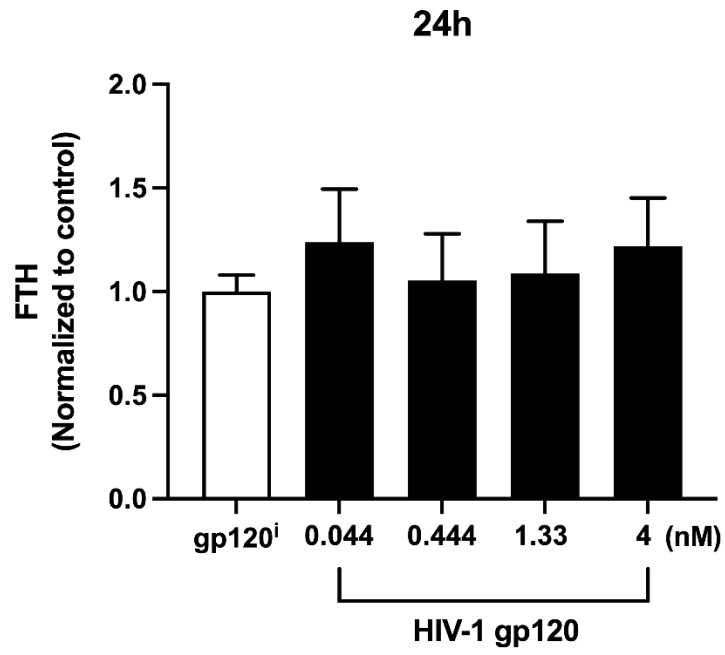
HIV-1 gp120

Figure 22.   HIV-1 gp120 did not significantly affect iron regulatory protein 2 protein levels. U87MG cells were treated for 24 h with heat-inactivated gp120 (gp120^i), 0.044, 0.444, 1.33, or 4 nM HIV-1 gp120. There was no significant change in iron regulatory protein 2 (IRP2) with HIV-1 gp120 treatment. Data represented as mean and SEM. N=three independent experiments run in duplicate.

24h
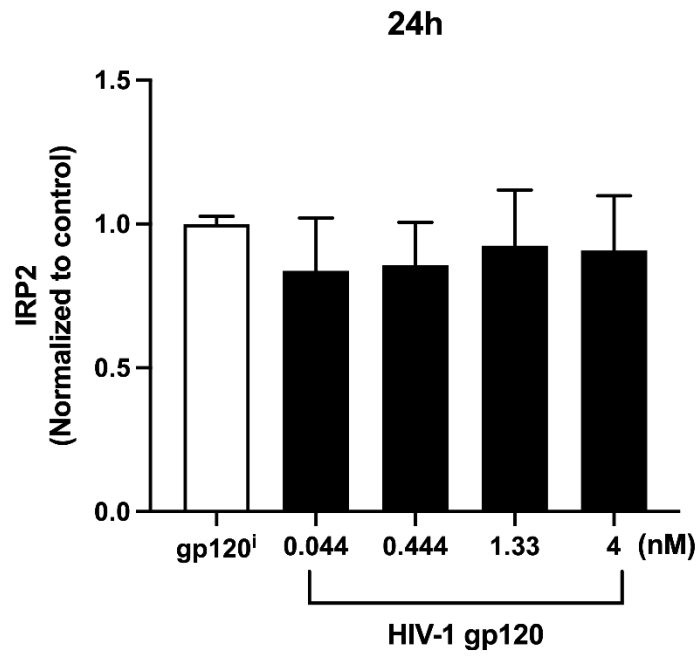
stained with AF647-conjugated anti-ferroportin antibody and MFI of AF647-

positive cells were measured by flow cytometry. HIV-1 gp120 significantly

(p<0.0001) increased surface FPN levels with an increase of MFI from control

values of 490 ± 9.4 to 581 ± 9.4. Similarly, FAC treatment significantly (p<0.0001)

increased surface FPN levels with an increase of MFI from control values of

490 ± 9.4 to 554 ± 9.7 (Figure 23).

Figure 23.   HIV-1 gp120 and FAC increased surface ferroportin levels.
U87MG cells were treated for 24 h with heat-inactivated gp120
(gp120^i), 4 nM HIV-1 gp120 (gp120), or 100 µM FAC.
U87MG cell surface levels of ferroportin (FPN) were significantly
increased by gp120 (p<0.0001) and FAC (p<0.0001) treatment.
Levels of surface FPN were determined by immunofluorescent
staining of U87MG cells with AF647-conjugated anti-FPN
antibody and AF647-positive cells mean fluorescence intensity
(MFI) was measured by flow cytometry. Data represented as
mean and SEM. N=2400, ****p<0.0001.

24h
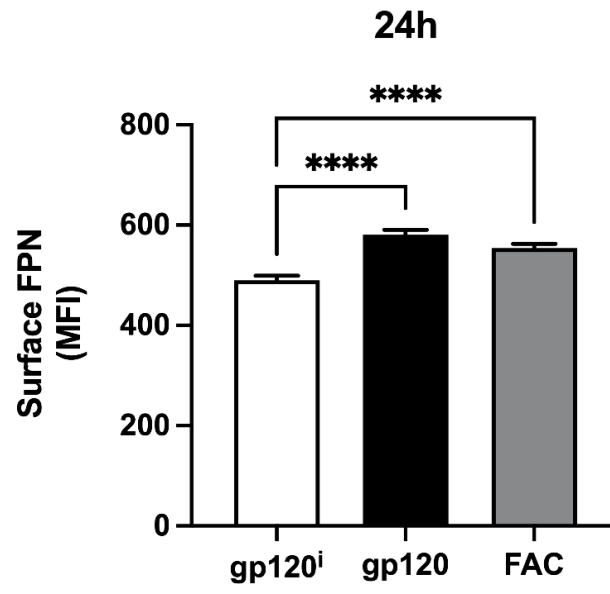
Discussion

Increases and decreases in levels of the intracellular labile iron pool (LIP) can affect expression levels of iron related proteins. Because gp120 was found to release iron from endolysosomes and increase iron levels in the cytosol, we tested the extent to which deferoxamine (DFO), ferric ammonium citrate (FAC) and HIV-1 gp120 affect iron-related protein expression levels. In our first set of experiments we investigated time- and concentration-dependent effects of DFO on transferrin receptor 1 (TFR1) protein levels in U87MG cells. We hypothesized that DFO would increase TFR1 protein levels over time in a concentration-dependent manner.

DFO is a hydrophilic cell impermeable iron chelator that localizes in endolysosomes (Bridges & Cudkowicz, 1984; Cable & Lloyd, 1999; Lloyd et al., 1991). We treated U87MG cells at 3 different time points with 3 different concentrations of DFO. U87MG cells were treated for 6 h, 12 h, and 24 h with 30 µM, 100 µM, or 300 µM DFO. We observed a concentration-dependent and significant increase at 24 h in TFR1 protein levels, the increases we observed at 24 h was consistent with findings reported by others (Bridges & Cudkowicz, 1984; Hoepken et al., 2004).

Next, we determined the time point at which 100 µM DFO treatment increased TFR1 protein levels. We observed significant increase at 6 h and 24 h but not 12 h. It remains unclear to us as to why there was a reduction in TFR1 protein at 12 h. However, because we did observe a concentration- and time-dependent increase in TFR1 at 30 µM and 300 µM the results from 12 h incubation with

100 µM DFO treatment group were likely due to experimental error. DFO can induce time-dependent increases of surface expression levels of TFR1 protein (Bridges & Cudkowicz, 1984; Hoepken et al., 2004). Accordingly, we next determined levels of surface TFR1 after treatment with 100 µM DFO. Surface expression levels of TFR1 increased by approximately 2-fold in the DFO treatment group; a finding previously reported (Bridges & Cudkowicz, 1984).

TFR1 protein levels are reciprocally regulated by cytosolic LIP. An increase in LIP leads to a decrease in TRF1 protein (Hoepken et al., 2004; Ponka & Lok, 1999). Thus, we measured the levels of total and surface TFR1 after 24 h treatment with 100 µM FAC. As expected, when cells were treated with 100 µM FAC, total and surface TFR1 expression levels were decreased. These findings are consistent with findings previously reported by others (Hoepken et al., 2004; Ponka & Lok, 1999) .

Extracellular iron supplementation with FAC increases the intracellular LIP (Hoepken et al., 2004; D. Richardson & Baker, 1992; Trinder et al., 1990). An increase in intracellular iron increases FTH protein (Hoepken et al., 2004; Nash et al., 2019). Accordingly, we next tested the hypothesis that FAC treatment would increase FTH protein in a time- and concentration-dependent manner. Time-dependent increases in FTH expression levels were observed starting at 6 h and these increases were still found with incubations up to 24 h; concentration-dependent increases began at 12 h. There was a robust concentration-dependent increase in FTH protein with 24 h treatments. When we investigated the time point at which 100 µM FAC increased FTH, we found that beginning at

6 h FAC increased FTH. Conversely, 24 h treatment with DFO lead to a reduction in FTH protein levels; these findings were consistent with findings reported by others (Hoepken et al., 2004).

Iron regulatory protein 2 (IRP2) is a cytosolic RNA-binding protein that acts as a cytosolic iron sensor (Meyron-Holtz et al., 2004). When cytosolic iron levels are elevated, IRP2 is degraded via proteasomal degradation (Iwai et al., 1998). However, when cytosolic iron levels are low IRP2 translocates to the nucleus where it stabilizes mRNA of iron uptake proteins such as TFR1 (Meyron-Holtz et al., 2004; Ponka & Lok, 1999). U87MG cells were treated for 24 h with either 100 µM FAC or DFO. As expected, FAC treatment decreased IRP2 levels. However, 100 µM DFO treatment did not significantly affect IRP2 protein levels. This finding is inconsistent with the findings of others that DFO significantly increased IRP2 protein levels in MDA-MB-231 triple-negative breast cancer cells (C. Chen, Liu, Duan, Cheng, & Xu, 2019). Our findings need to be confirmed using the cell-permeable iron chelators such as deferiprone or 2'-2'-bipyridine. Another alternative explanation for the lack of effect of DFO on IRP2 protein levels could be that a higher concentration or a longer treatment period is necessary. Nevertheless, these results suggest to us that at 24 h when our U87MG cells are challenged with either iron supplementation or chelation they properly response by increasing or decreasing the protein levels of TFR1 and FTH, while changes in IRP2 protein is only observed in the presence of elevated cytosolic iron.

We next investigated the possible effects of 24 h HIV-1 gp120 treatment on iron related protein expression levels. We determined concentrations at which HIV-1 gp120 affected total and surface levels of TFR1, and total levels of FTH and IRP2. Experimentally, effects of HIV-1 gp120 have been observed at concentrations ranging from picomolar to nanomolar (M. Bae et al., 2014; Datta et al., 2019; Foga et al., 1997; Vesce, Bezzi, Rossi, Meldolesi, & Volterra, 1997). Accordingly, we treated U87MG cells with HIV-1 gp120 at varying concentrations ranging from 0.044 to 4 nM. We did not observe significant changes in surface TFR1 levels at any concentration of HIV-1 gp120 tested except for a significant decrease in TFR1 total protein levels at 1.33 nM gp120.

Next, we determine the effects of gp120 on FTH and IRP2 protein expression levels. We did not observe a change in FTH or IRP2 protein levels at any concentration of HIV-1 gp120 tested. Others have reported that HIV-1 gp120 increased FTH protein in primary rat cultured neurons (Festa et al., 2015). Because HIV-1 gp120 might induce iron efflux out of the cell in order to maintain the intracellular LIP, we next measured expression levels of plasma membrane resident iron exporter, FPN. Treatment with HIV-1 gp120 resulted in significant increases in surface expression levels of ferroportin and these results were comparable to those observed for the positive control FAC. These results suggested to us that U87MG cells upregulate surface levels of ferroportin and export iron out of the cells in order to maintain cytosolic iron levels. These findings might explain the lack of effect of 24 h HIV-1 gp120 treatment on FTN, IRP2, and TFR1 protein levels.

This study demonstrates that U87MG cells respond as expected to iron supplementation and iron chelation. Therefore, the lack of effect that HIV-1 gp120 treatment had on total and surface protein levels of TFR1, and total protein levels of FTN, and IRP2 was not due to an unresponsive system. What these findings reveal is that 24 h HIV-1 gp120 treatment of U87MG cells induces an increase of surface expression levels of FPN which we interpreted as a way for the cells to maintain LIP. However, in order confirm whether HIV-1 gp120 increases cytosolic iron levels we need to measure those levels. Moreover, other questions remain one of which being, what are the effects of 24 h HIV-1 gp120 treatment on endolysosome iron stores? Lastly, since cancer cells have elevated iron levels and ROS levels, and HIV-1 gp120 does not induce cell death in U87MG but promotes cell proliferation (Liou & Storz, 2010; Lopez et al., 2017; Schieber & Chandel, 2014; Valentín-Guillama et al., 2018), it is possible that U87MG cells may be an inadequate cell model to conduct these studies; primary human astrocytes may be a more appropriate cell model to continue this work.

CHAPTER 4

LYSOSOMAL STRESS RESPONSE (LSR):
PHYSIOLOGICAL IMPORTANCE AND PATHOLOGICAL RELEVANCE

Koffi L. Lakpa, Nabab Khan, Zahra Afghah, Xuesong Chen
and Jonathan D. Geiger

Department of Biomedical Sciences
University of North Dakota School of Medicine and Health Sciences
Grand Forks, ND 58203, USA

Abstract

Extensive work has characterized endoplasmic reticulum (ER) and mitochondrial stress responses. In contrast, very little has been published about stress responses in lysosomes; subcellular acidic organelles that are physiologically important and are of pathological relevance. The greater lysosomal system is dynamic and is comprised of endosomes, lysosomes, multivesicular bodies, autophagosomes, and autophagolysosomes. They are important regulators of cellular physiology, they represent about 5% of the total cellular volume, they are heterogeneous in their sizes and distribution patterns, they are electron dense, and their subcellular positioning within cells varies in response to stimuli, insults and pH. These organelles are also integral to the pathogenesis of lysosomal storage diseases and it is increasingly recognized that lysosomes play important roles in the pathogenesis of such diverse conditions as neurodegenerative disorders and cancer. The purpose of this review is to focus attention on lysosomal stress responses (LSR), compare LSR with better characterized stress responses in ER and mitochondria, and form a framework for future characterizations of LSR. Here, we present the concept of LSR such that the definition of LSR can be modified as new knowledge is added and specific therapeutics are developed.

Introduction

Lysosomes were described in 1955 by Christian de Duve and since that time it has become increasingly obvious that these acidic organelles are physiologically important as well as pathologically relevant (de Duve, 2005). Decades ago, lysosomes were simply thought to be cellular waste bins and endpoints of cellular degradation events. Now, however, increasingly appreciated are the many cellular functions homeostatically regulated by lysosomes (Pu et al., 2016; Settembre et al., 2013; H. Xu & Ren, 2015). They represent about 5% of the total cellular volume, they are heterogeneous in their sizes and distribution patterns, they are electron dense, and their subcellular positioning in the cytoplasm varies in response to stimuli, insults and pH (Holtzman, 1989; Pu et al., 2016; Wartosch, Bright, & Luzio, 2015).

Lysosomes are integral to the greater lysosomal system, which is also comprised of endosomes, multivesicular bodies (MVB), autophagosomes, and autophagolysosomes (Huotari & Helenius, 2011). The importance and the dynamic nature of endosomes and lysosomes, henceforth referred to as endolysosomes, continues to be recognized in many ways including the awarding of Nobel Prizes for the discovery of lysosomes themselves, for receptor-mediated endocytosis, and for autophagy. These organelles are also integral to the pathogenesis of lysosomal storage diseases (LSD) and it is increasingly recognized that lysosomes play important roles in the pathogenesis of a variety of diseases including neurodegenerative disorders and cancer. However, when considered in the same vein as other subcellular organelles it

could be argued that lysosomes do not receive the same degree of recognition as do other intracellular organelles. While endoplasmic reticulum (ER) and mitochondria have well known and clearly described stress responses (Huotari & Helenius, 2011; Martinus et al., 1996; Oakes & Papa, 2015; Valera-Alberni & Canto, 2018; Q. Zhao et al., 2002), lysosomal stress responses (LSR) are ill-defined and have been referred to in the literature only sparingly.

The purpose of this review is to focus attention on LSR and initiate a framework for its existence, its characterization, its physiological importance, and its pathological relevance. First, we provide an overview of lysosome biogenesis, function and dysfunction. Second, we discuss ER and mitochondrial stress responses in order to provide a context for LSR. Third, we discuss the characterization of LSR as well as briefly review evidence of LSR in ER and mitochondrial stress responses. Ultimately, a better understanding of stress responses in lysosomes may enhance our understanding of cellular physiology and disease pathogenesis and promote the discovery of new treatments for diseases.

Overview of Lysosome Biogenesis, Function and Dysfunction

Lysosome Biogenesis

Lysosome biogenesis includes the formation of lysosomes through the maturation of endocytic vesicles as well as the delivery of newly synthesized lysosomal enzymes and membrane proteins from the trans-Golgi network (Kornfeld & Mellman, 1989; Saftig & Klumperman, 2009). The maturation process of endosomes has been extensively reviewed elsewhere (Huotari &

Helenius, 2011; Kornfeld & Mellman, 1989; Luzio, Hackmann, Dieckmann, & Griffiths, 2014; Saftig & Klumperman, 2009), but to provide context we briefly outline this process here. When extracellular cargo is endocytosed, it is trafficked into early endosomes and from there it is either recycled back to the plasma membrane or alternatively it is degraded in lysosomes (Huotari & Helenius, 2011; Saftig & Klumperman, 2009). Cargo that is destined for degradation stays contained in endosomes as they mature from early endosomes to late endosomes, and during this maturation endosomes undergo changes in size and morphology, become more acidic, traffic perinuclearly, and form intraluminal vesicles (ILVs); late endosomes containing ILVs are termed MVBs (Huotari & Helenius, 2011). MVBs can fuse with existing MVBs or late endosomes to form late endosomes. Late endosomes can fuse with existing lysosomes to form endolysosomes where degradation of cargo takes place. After fusion, endolysosomes are converted into lysosomes where acidic hydrolases and lysosomal membrane proteins are stored (Huotari & Helenius, 2011).

The biosynthesis and delivery of lysosomal enzymes and membrane proteins are critical for the development and proper functioning of lysosomes. It is well understood that most newly synthesized lysosomal proteins are post-translationally modified in the Golgi complex (Braulke & Bonifacino, 2009; Kornfeld & Mellman, 1989; Luzio et al., 2014; Saftig & Klumperman, 2009). Lysosomal hydrolases are inserted into the ER lumen where they receive signal sequence cleavage and core glycosylation followed by trafficking to the cis-Golgi network (CGN). In the CGN, lysosomal enzymes are unmasked revealing a

114

mannose-6-phosphate (M6P) signal (Kornfeld & Mellman, 1989). Once these proteins reach the trans-Golgi network (TGN), they are recognized by M6P receptors (M6PR) (Kornfeld & Mellman, 1989; Saftig & Klumperman, 2009). The binding of M6P tagged proteins to M6PR leads to receptor-dependent vesicle transport of these proteins to endolysosomes via transport vesicles derived from the TGN. When lysosomal proteins reach their destination in the acidic environment of endolysosomes there is a dissociation between M6PRs and M6P-tagged proteins; M6PRs are recycled back to the TGN (Kornfeld & Mellman, 1989; Saftig & Klumperman, 2009).

Lysosome biogenesis (Figure 24) is coordinated by transcription factor EB (TFEB) (Sardiello et al., 2009). TFEB is a member of the microphthalmia-transcription factor E (MiT/TFE) family of proteins, which are involved in responding and adapting to intracellular stresses (La Spina et al., 2020; Rehli, Den Elzen, Cassady, Ostrowski, & Hume, 1999; Steingrimsson, Copeland, & Jenkins, 2004). The subcellular localization of TFEB is modified by kinases and phosphatases; phosphorylated TFEB targets the cytosol and de-phosphorylated TFEB targets the nucleus. The serine/threonine kinase mammalian target of rapamycin complex 1 (mTORC1) phosphorylates TFEB on serine residues 211 and 122, which results in binding by 14-3-3 proteins. Other serine/threonine kinases such as mitogen-activated protein kinases 1 (MAPK1), protein kinase B (Akt), glycogen synthase kinase 3ß (GSK3ß), and mitogen-activated protein kinase kinase kinase kinase 3 phosphorylate TFEB at Ser142, Ser467,

Figure 24.	Involvement of mTOR-TFEB in mediating lysosomal stress responses (LSR). Under unstressed conditions, mammalian target of rapamycin complex 1 (mTORC1) is localized on lysosome membranes and phosphorylates transcription factor EB (TFEB), which is a master regulator of lysosome biogenesis. Phosphorylated TFEB is bound by 14-3-3 protein promoting the sequestration of TFEB in the cytoplasm. Under stressful conditions, which can be caused by any drug, pathogen, or material that enters the endolysosome system (termed LSR inducers), lysosomes undergo lysosomal stress responses (labeled 1-9). We posit that during LSR, stressed lysosomes can use various signals, one of which being mTOR-TFEB signaling pathway to promote lysosome biogenesis. When lysosomes are stressed, mTORC1 is released from lysosome membranes, calcium is released through calcium permeable channels (depicted by blue cylinder) into the cytosol where it activates the cytosolic phosphatase calcineurin. Activated calcineurin dephosphorylates TFEB allowing it to translocate into the nucleus where it binds at the coordinated lysosomal expression and regulation (CLEAR) element of lysosome biogenesis genes. Subsequently, there is an increase of lysosome-related genes that lead to the possible restoration of stressed lysosomes. Thus, LSR may use lysosome biogenesis as one of the pathways to restore lysosome function.

1. ↑ pH
2. ↑ size
3. Membrane permeabilization
4. Cationic efflux
5. Repositioning
6. Misfolded protein
7. LDL accumulation
8. Redox catastrophe
9. Bioenergetic crisis

Lysosome (stressed)

LSR inducers

mTORC1

14-3-3

P TFEB

Lysosome (normal)

mTORC1

↑ Lysosome Biogenesis Genes

TFEB

CLEAR

Nucleus

P TFEB

TFEB

Ca²⁺

Ca²⁺

Calcineurin
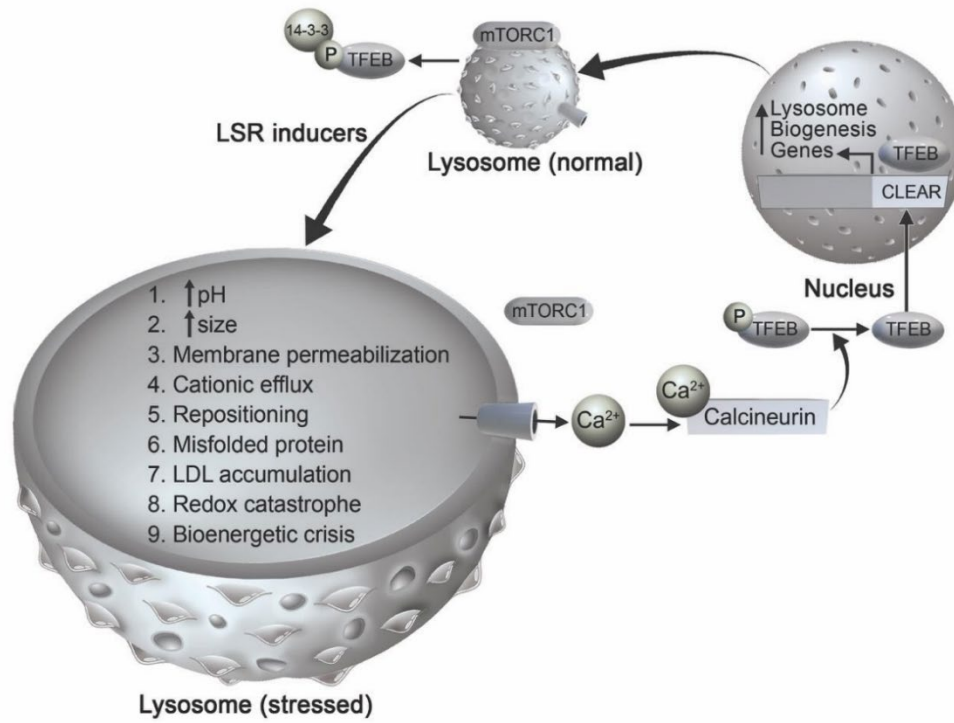
Ser134/138, and Ser3, respectively (Hsu et al., 2018; Y. Li, M. Xu, et al., 2016; Palmieri et al., 2017; Settembre et al., 2011). Phosphorylation of TFEB results in its cytosolic sequestration and an inhibition of its ability to upregulate lysosome related genes (Roczniak-Ferguson et al., 2012; Vega-Rubin-de-Celis, Pena-Llopis, Konda, & Brugarolas, 2017). Genes that encode for lysosome function contain a coordinated lysosomal expression and regulation (CLEAR) binding element in their promoter region. TFEB is dephosphorylated by the phosphatases calcineurin and protein phosphatase 2 (D. Chen et al., 2018; Martina & Puertollano, 2018; Medina et al., 2015). Dephosphorylated TFEB translocates to the nucleus where it binds to CLEAR elements and promotes an increase of lysosomal-, autophagy-, and mitochondrial-gene expression (Sardiello et al., 2009; Settembre et al., 2011). Recently, a mechanistic study revealed how TFEB activity is regulated. STIP1 homology and u-box containing protein 1 (STUB1) increases TFEB activity by clearing ubiquitinated and phosphorylated TFEB for proteasomal degradation (Sha, Rao, Settembre, Ballabio, & Eissa, 2017); mTORC1 phosphorylates TFEB which is proposed to form heterodimers with non-phosphorylated TFEB thus sequestering TFEB to the cytosol and preventing the promotion of lysosome biogenesis (Sha et al., 2017).

Lysosome Function

Lysosomes are single membrane acidic organelles that function to degrade intracellular cargo (Holtzman, 1989). These organelles are heterogeneous in size (range 0.5 to 1.5 nm), have intraluminal pH values ranging from 4.5 to 6.0, and contain over 60 different acidic hydrolase enzymes (H. Xu & Ren, 2015). The

intraluminal pH of lysosomes is maintained by membrane-resident ion channels

and vacuolar-ATPases (Colacurcio & Nixon, 2016; Huotari & Helenius, 2011;

Mindell, 2012; Steinberg et al., 2010).

The acidic lumen of lysosomes provides an environment that is conducive for

optimal activity levels of resident hydrolase enzymes which catalyze the

degradation of cargo that is received via endocytic or autophagic pathways

(Kornfeld & Mellman, 1989). Lysosomes also contain readily releasable stores of

biologically important divalent cations including iron and calcium (Lakpa,

Halcrow, Chen, & Geiger, 2020; H. Xu & Ren, 2015). Intracellularly, the

positioning of endolysosomes is dynamic and their positioning in the cytoplasm

changes markedly according to many factors including cell type and intraluminal

pH; highly acidic endolysosomes are perinuclearly positioned while de-acidified

endolysosomes are re-positioned more towards the periphery of cells near

plasma membranes (D. E. Johnson et al., 2016; Pu et al., 2016).

As mentioned above, lysosomes can receive cargo from endocytic or autophagic

pathways. Once cargo enters the endolysosomal system it has two fates, it can

either be trafficked toward lysosomes to be degraded or it can be recycled to the

plasma membrane. Along the maturation path of endosomes to lysosomes,

intraluminal vesicles begin to form in endosomes thus creating MVBs (van Niel,

D'Angelo, & Raposo, 2018). Cargo within MVBs can be trafficked toward the

plasma membrane to release contents into the extracellular space; these

secreted ILVs are termed exosomes; a type of extracellular vesicles. The release

of exosomes can potentially serve as intercellular signals, therapeutic delivery-

vesicles, and biomarkers for various pathologies (Fais et al., 2016; Lener et al., 2015; Maia, Caja, Strano Moraes, Couto, & Costa-Silva, 2018; Torrano et al., 2016).

Autophagy is the means by which cytoplasmic material is degraded. There are different forms of autophagy such as macro-autophagy (which will be referred to as autophagy), micro-autophagy (selective autophagy), and chaperone-mediated autophagy (Galluzzi et al., 2017; Ravikumar et al., 2010). Intracellular cargo is engulfed by double membrane vesicles called autophagosomes; autophagosome formation, elongation, and maturation have been reviewed elsewhere (Ravikumar et al., 2010). Important to the clearance of damaged proteins and dysfunctional organelles via autophagy is the fusion of autophagosomes with lysosomes forming autolysosomes (Ravikumar et al., 2010; Galluzzi et al., 2017; Yim and Mizushima, 2020). In post-mitotic cells, such as neurons, the autophagic-lysosome system is important for the maintenance of neuronal health (Kuijpers, Azarnia Tehran, Haucke, & Soykan, 2020).

Apart from their degradative roles, lysosomes also participate in intracellular nutrient sensing (Perera & Zoncu, 2016; Settembre et al., 2013; H. Xu & Ren, 2015). Lysosomes use mTOR and TFEB to sense and regulate intracellular nutrient conditions, and the roles of mTOR and TFEB in lysosome nutrient sensing and cellular function were reviewed extensively elsewhere (Perera & Zoncu, 2016; Rabanal-Ruiz & Korolchuk, 2018; Settembre et al., 2013). mTOR is part of a larger protein complex that interacts with lysosome membranes and senses cytosolic nutrient levels (Rabanal-Ruiz & Korolchuk, 2018). During high

nutrient conditions, mTOR is recruited to lysosome membranes where it is activated and initiates downstream effectors that promote cell growth and proliferation. Conversely, during low nutrient conditions mTOR is inactive, disassociates from lysosome membranes, and is no longer able to phosphorylate TFEB; dephosphorylated TFEB promotes the production of lysosome genes (Napolitano & Ballabio, 2016; Rabanal-Ruiz & Korolchuk, 2018; Sardiello et al., 2009).

Lysosome Dysfunction

Central to lysosome dysfunction appears to be an increase in intraluminal pH - lysosome deacidification. Lysosome de-acidification causes many changes to the biology of cells including endolysosome positioning in the cytoplasm, endolysosome sizes and volumes, intraluminal and cytosolic levels of divalent cations, expression levels and activity levels of acid hydrolases, and the aggregation of various proteins. And, as we will expand on later, these changes are also central to the concept of LSR.

The intracellular distribution (positioning) of endolysosomes in the cytoplasm is affected by endolysosome de-acidification; an increase in endolysosome pH causes redistribution of lysosomes away from the nucleus and more toward plasma membranes (Heuser, 1989; D. E. Johnson et al., 2016; Parton et al., 1991). The cytosolic pH which is influenced by H$^+$ ions originating from endolysosomes also affects endolysosome positioning (Gottschling & Nystrom, 2017); cytosolic acidification promotes the localization of lysosomes towards plasma membranes and cytosolic alkalinization leads to perinuclear localization

of lysosomes (Halcrow et al., 2019; Heuser, 1989; Parton et al., 1991). Although the biological significance of the pH-dependent re-positioning of endolysosomes in cells is unclear, some have shown that the location of endolysosomes dictates their pH and not that their pH dictates the location (D. E. Johnson et al., 2016). Microtubules and motor proteins also contribute to the translocation and clustering of endolysosomes (Cabukusta & Neefjes, 2018; Matteoni & Kreis, 1987).

Morphologically, endolysosome de-acidification leads to increased endolysosome size and an accumulation of undigested intracellular cargo (Myers et al., 1991; Ohkuma & Poole, 1981; Yoshimori et al., 1991). Endolysosome de-acidification also leads to impaired fusion between autophagosomes and lysosomes, and such changes have been implicated in cell death (Doherty & Baehrecke, 2018; Mauthe et al., 2018).

Endolysosomes contain readily releasable stores of biologically important divalent cations including calcium, iron, copper and zinc. De-acidification of endolysosomes induces the efflux of calcium and iron (Christensen et al., 2002; Fernández et al., 2016; Hui et al., 2015; Kiselyov et al., 2011; Kurz et al., 2011; J. H. Lee et al., 2015; H. Xu & Ren, 2015) such that accumulations are measurable in cytosol, mitochondria, and ER. As a result of decreased levels of cations in endolysosomes, downstream events can occur including ER stress as well as mitochondrial redox catastrophe and bioenergetic crisis (Baixauli et al., 2015; Lv & Shang, 2018; Martina, Diab, Brady, & Puertollano, 2016; Nakashima et al., 2019; Uchiyama et al., 2008; F. Wang, Gomez-Sintes, & Boya, 2018).

Lysosome Dysfunction in Neurodegenerative Diseases

Dysfunctional lysosomes have been implicated in several neurodegenerative disorders including lysosomal storage diseases (LSD), Alzheimer's disease (AD), Parkinson's disease (PD), and Huntington's disease (HD) (Audano, Schneider, & Mitro, 2018; Bonam, Wang, & Muller, 2019; Martini-Stoica, Xu, Ballabio, & Zheng, 2016; Nguyen, Wong, Ysselstein, Severino, & Krainc, 2019; Wallings, Humble, Ward, & Wade-Martins, 2019). Neurological complications are observed in people living with LSD, which are characterized by intra-lysosomal aggregation of substrates due to mutations in lysosome hydrolases (Platt, 2018). The inhibition of autophagosome-lysosome fusion and/or the accumulation of autophagosomes in LSDs could be a potential mechanism underlying the neuropathogenesis of LSDs (Cao et al., 2006; Fukuda et al., 2006; Koike et al., 2005; Tanaka et al., 2000). Further observed in LSD are impaired autophagy of damage mitochondria (mitophagy), increased production of reactive oxygen species, and bioenergetic crisis.

Amyloid plaques and hyperphosphorylated tau are hallmarks of AD and in AD there is lysosome dysfunction and an impairment of autophagic flux. Endolysosomes are the sites where amyloidogenic processing of amyloid precursor protein occurs; the result is accumulation of amyloid beta (Aß) proteins Aß40 and Aß42 (Oikawa & Walter, 2019). Neurofibrillary tangles are made from hyperphosphorylated tau protein and lysosomal enzymes (cathepsin B, D, and E) generate and digest both Aß and tau (Siman et al., 1993). Lysosome dysfunction leads to an accumulation of Aß42 in neurons, inhibition of lysosomal cathepsins

B and E, increases expression of cathepsin D, increases lysosomal pH, impairs autophagy, and changes permeability of lysosomal membranes (Bi et al., 2000; Cataldo et al., 1995; Cataldo, Paskevich, Kominami, & Nixon, 1991; Wolfe et al., 2013). Furthermore, defective autophagy and mitophagy are present in AD (Reddy & Oliver, 2019).

The hallmark of PD are Lewy bodies which are made up of alpha-synuclein aggregates in neurons. Genetic mutations in GBA1 (encoding for lysosomal hydrolase glucocerebrosidase), which is the most common genetic factor of PD is linked to Lewy body formation (Wallings et al., 2019). Extracellular alpha-synuclein can be internalized into endolysosomes via clathrin-mediated endocytosis leading to changes in lysosome morphology, decreased cathepsin D activity, increased lysosome pH, and impaired fusion with autophagosomes (Hoffmann et al., 2019; Winslow et al., 2010).

HD is a rare autosomal-dominant neurodegenerative disease that is caused by a mutation in the HTT gene leading to HTT mutants (mHTT) prone to aggregation. mHTT localizes in lysosomes, impairs autophagy, inhibits trafficking of non-mutant HTT to lysosomes, and changes cathepsin activity (del Toro et al., 2009; Q. Liang, Ouyang, Schneider, & Zhang, 2011; Ratovitski, Chighladze, Waldron, Hirschhorn, & Ross, 2011; Ravikumar, Duden, & Rubinsztein, 2002; Ravikumar et al., 2004; Rubinsztein, 2006; Trajkovic, Jeong, & Krainc, 2017; Wallings et al., 2019). Interestingly, one study shows that mHTT induces perinuclear localization of lysosomes, reduces lysosome mobility, and promotes premature fusion of lysosomes with autophagosomes (Erie, Sacino, Houle, Lu, & Wei, 2015).

Impairment of the autophagic-lysosomal pathway can also promote the release of toxic intracellular protein aggregates in exosomes; such observations have been made for AD, PD, and HD (Danzer et al., 2012; Guix, 2020; Miranda et al., 2018; Perez-Gonzalez, Gauthier, Kumar, & Levy, 2012; Sardar Sinha et al., 2018; Trajkovic et al., 2017). An increase in the release of undigested substrates and stored material also occurs in LSDs (Tancini et al., 2019).

ER and Mitochondrial Stress Responses

Stress is a holistic concept that affects organisms at every conceivable level; minor stressors can promote resilience while major stressors can induce cell death (Figure 25). Cellular stressors include, but are not limited to, hypoxia, heat shock, nutrient depletion, and genetic defects (Deus, Yambire, Oliveira, & Raimundo, 2020). Thus, organelles have developed stress responses to counter the potential detrimental effects of stress. It happens with ER, it happens with mitochondria, and, as we will later describe, it happens with lysosomes where stress responses attempt to maintain and/or restore organellar function. In order to contextualize the concept of LSR, we will first discuss ER and mitochondria stress responses.

ER Stress Response

ER helps to maintain calcium homeostasis and lipid metabolism and are sites for synthesis and proper folding of secretory and transmembrane proteins. Molecular chaperones in ER bind newly synthesized proteins and facilitate the acquisition of three-dimensional structures. Proteins are then delivered to Golgi apparatus where they undergo post-translational modifications. In the case of misfolded

Figure 25.   Flow diagram depicting responses and outcomes resulting from lysosomal stress. High levels of lysosomal stress (major) can lead to transcriptional/translational changes including increases in lysosome biogenesis. Lower levels of lysosomal stress (minor) can lead to selective autophagy and/or lysophagy. In either case, outcomes can include cell life or death.
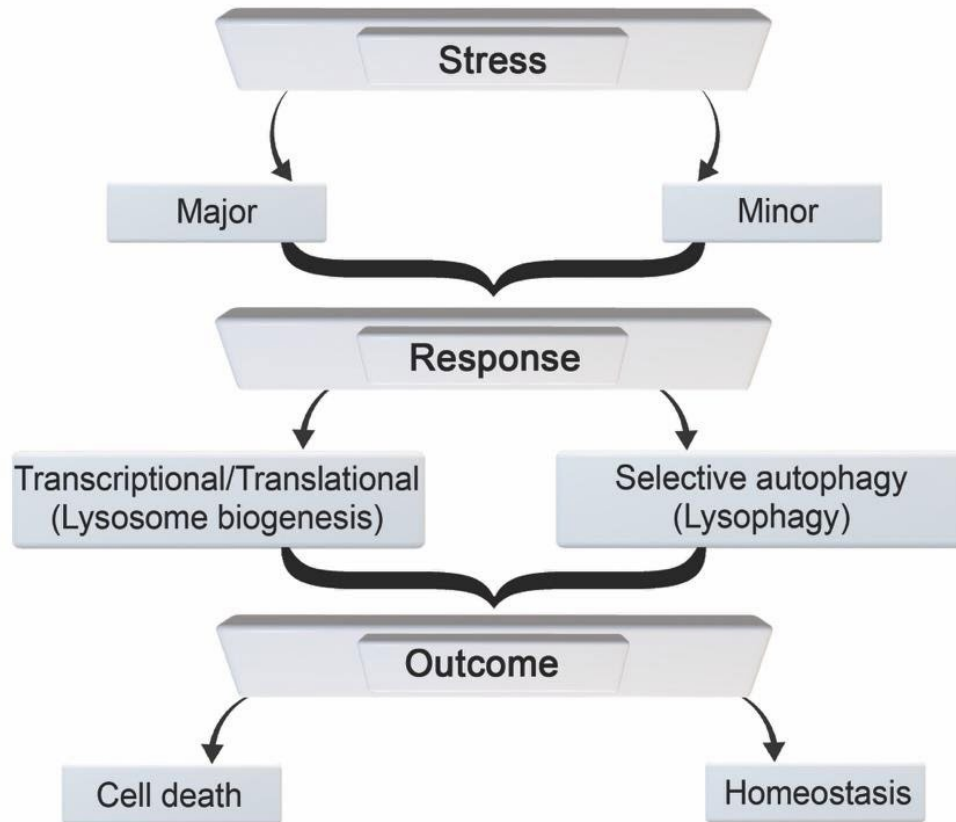
proteins, proteins are released from ER into the cytosol where they are targeted for proteasomal degradation; ER associated degradation (ERAD) (Ruggiano, Foresti, & Carvalho, 2014). When levels of misfolded proteins exceed ERAD capacity, ER stress is triggered and accumulation of misfolded and/or unfolded proteins occurs in the lumen of ER (Bravo et al., 2013; Mori, 2015). In response to ER stress, the unfolded protein response (UPR) is activated, and this results in halting the translation of and increasing gene expression of ER folding proteins (Bravo et al., 2013; Kohno, Normington, Sambrook, Gething, & Mori, 1993; Mori, 2015; Partaledis & Berlin, 1993). UPR was first discovered in 1988 for glucose deprivation initiating the accumulation of misfolded proteins within the ER lumen, which then leads to a subsequent transcriptional response to increase ER-resident molecular chaperones (Kozutsumi, Segal, Normington, Gething, & Sambrook, 1988; Mori, 2015).

ER uses three resident transmembrane proteins as sensors of ER stress and initiators of the UPR signaling pathways; inositol requiring protein 1 alpha (IRE1), activating transcription factor 6 (ATF6), and protein kinase RNA-like ER kinase (PERK) (Hetz, 2012; Sasaki & Yoshida, 2015). IRE1 senses ER stress luminally, is activated via oligomerization and phosphorylation of its cytosolic domain, and once activated splices immature X box protein 1 (XBP1) mRNA into mature XBP1 mRNA. After protein translation, XBP1 is translocated into the nucleuswhere it acts as a transcription factor to promote the expression of ERAD genes (A. H. Lee, Iwakoshi, & Glimcher, 2003; Yoshida et al., 2003). PERK is an ER transmembrane protein (Harding, Zhang, Bertolotti, Zeng, & Ron, 2000;

Harding, Zhang, & Ron, 1999) and similar to IRE1, PERK is activated by

oligomerization and phosphorylation when it senses ER stress luminally

(Harding, Novoa, et al., 2000; Harding, Zhang, et al., 2000). Once activated,

PERK phosphorylates eukaryotic translational initiation factor 2 alpha (eIF2),

which reduces protein translation and increases translation of activating

transcription factor 4 (ATF4); ATF4 is a transcription factor that increases gene

expression of anti-oxidation and pro-apoptotic genes (Harding, Novoa, et al.,

2000; Harding et al., 2003). The ER transmembrane protein ATF6 senses ER

stress and once translocated to Golgi apparatus, it is cleaved by proteases

(Shen, Chen, Hendershot, & Prywes, 2002). Then, the cytosolic domain of ATF6

is translocated to the nucleus to increase the expression of ER chaperone genes

(J. Ye et al., 2000).

Mitochondrial Stress Response

Mitochondria produce energy in the form of adenosine triphosphate (ATP) via

oxidative phosphorylation, serve as sinks for cations such as calcium and iron,

and help maintain redox balance. Although mitochondria contain their own

genome, the majority of mitochondrial proteins are nuclear-encoded and those

proteins are translated in the cytoplasm (Sasaki & Yoshida, 2015). Unfolded

proteins are transported from the cytoplasm into mitochondria via heat shock

protein 70 (HSP70); a molecular chaperone (Ryan & Hoogenraad, 2007). Once

translocated into the inner membrane space of mitochondria, the proper folding

of proteins is assisted by mitochondrial HSP70 (mtHSP70) and mtHSP60 (Endo,

Yamano, & Kawano, 2011; Sasaki & Yoshida, 2015).

Mitochondrial stress is characterized by redox catastrophe and bioenergetic

crisis caused by dysfunctional oxidative phosphorylation, increased levels of

ROS, and/or accumulation of misfolded proteins (Hill, Sataranatarajan, & Van

Remmen, 2018). Mitochondrial UPR (UPR_MT) was first described in 2004 (Yoneda

et al., 2004); it helps restore mitochondrial function (M. L. Huang et al., 2019;

Manoli et al., 2007; Martinus et al., 1996; Q. Zhao et al., 2002) via transcriptional

signaling pathways (Sasaki & Yoshida, 2015) and removing the mitochondrial

genome or mutating matrix proteins (Martinus et al., 1996; Q. Zhao et al., 2002).

Lysosome Stress Response (LSR)

Lysosome Stress

The term "lysosomal stress" appears to have been first mentioned in 1968 in the

context of a freeze-thaw method used to rupture lysosomes (Persellin, 1969).

However, it appeared to take another 50 years before "lysosome stress" was

described as "any disturbance in lysosomal membrane integrity, enzyme

function, or internal pH that leads to cell damage or even diseases" (Lin et al.,

2016). We posit that in addition to membrane integrity, enzyme function and pH,

more recent reports from others and us strongly suggests that additional criteria

be added including size, efflux of cations, organelle repositioning within cells,

protein aggregation, LDL cholesterol accumulation, and increases in reactive

oxygen species (M. Bae et al., 2014; Gowrishankar et al., 2015; He et al., 2018;

Hui, Chen, & Geiger, 2012; Hui, Chen, Haughey, et al., 2012; L. Li et al., 2019;

Lin et al., 2016; Pan, Alamri, & Valapala, 2019; Papadopoulos et al., 2017;

Yogalingam et al., 2017). These criteria are consistent with findings from the

study of LSDs; mutations in lysosomal acid hydrolases lead to aggregation of substrates, elevated luminal pH, altered morphology and subcellular distribution patterns, and lowered luminal concentrations of biologically important metal ions (Ballabio & Gieselmann, 2009; Fossale et al., 2004; Holopainen, Saarikoski, Kinnunen, & Jarvela, 2001; S. Lee, Sato, & Nixon, 2011; Lloyd-Evans et al., 2008; Marques & Saftig, 2019; Platt, 2018; Raben, Roberts, & Plotz, 2007; Sun, 2018; Yanagawa et al., 2007; Zigdon et al., 2017).

Characterization of Lysosome Stress Response (LSR)

In this section we provide a framework for characterizing LSR. The greater lysosomal system is complex and so too is the nomenclature used to describe lysosome function, dysfunction and stress. Although there is likely overlap between the concepts of lysosome stress, LSR and lysosome dysfunction, there are also differences. Lysosome dysfunction is the progressive accumulation of undegraded substrates within lysosomes (Settembre & Ballabio, 2014) and we posit that lysosome stress is a state that lysosomes enter into due to internal or external stimuli; the lysosome responses to those stimuli characterize LSR. Currently, we propose nine criteria with which to characterize LSR; (1) increased intralysosomal pH, (2) increased lysosome size, (3) membrane permeabilization, (4) cationic efflux, (5) repositioning intracellularly, (6) misfolded protein aggregation, (7) LDL cholesterol accumulation, (8) redox catastrophe, and (9) bioenergetic crisis (see Figure 26). Principal among these 9 criteria might be lysosome de-acidification because lysosome de-acidification can trigger each of the other 8 criteria involved in LSR. LSR might be distinct from lysosome

Figure 26.   Lysosome stress response characteristics and examples of stimuli that cause LSR. Lysosomal stress responses can be characterized by (1) increased lysosome pH, (2) increased lysosome size, (3) lysosomal membrane permeabilization, (4) cationic efflux, (5) intracellular repositioning, (6) intraluminal protein aggregation, (7) intraluminal accumulation of LDL cholesterol, (8) redox catastrophe, and (9) bioenergetic crisis. Endogenous and exogenous stimuli such as the HIV-1 proteins Tat and gp120, drugs of abuse including methamphetamine and opioids, nanoparticles, LDL cholesterol, and chloroquine (CQ) and hydroxychloroquine (HCQ) can induce lysosome stress.

Lysosome stress response (LSR)

HIV-1 proteins (Tat, gp120)

LDL cholesterol

Drugs of abuse (METH, opioids)

Nanoparticles

CQ & HCQ

1. Increased intralysosomal pH
2. Increased lysosome size
3. Membrane permeabilization
4. Cationic efflux
5. Repositioning intracellularly
6. Misfolded protein aggregation
7. LDL cholesterol accumulation
8. Redox catastrophe
9. Bioenergetic crisis
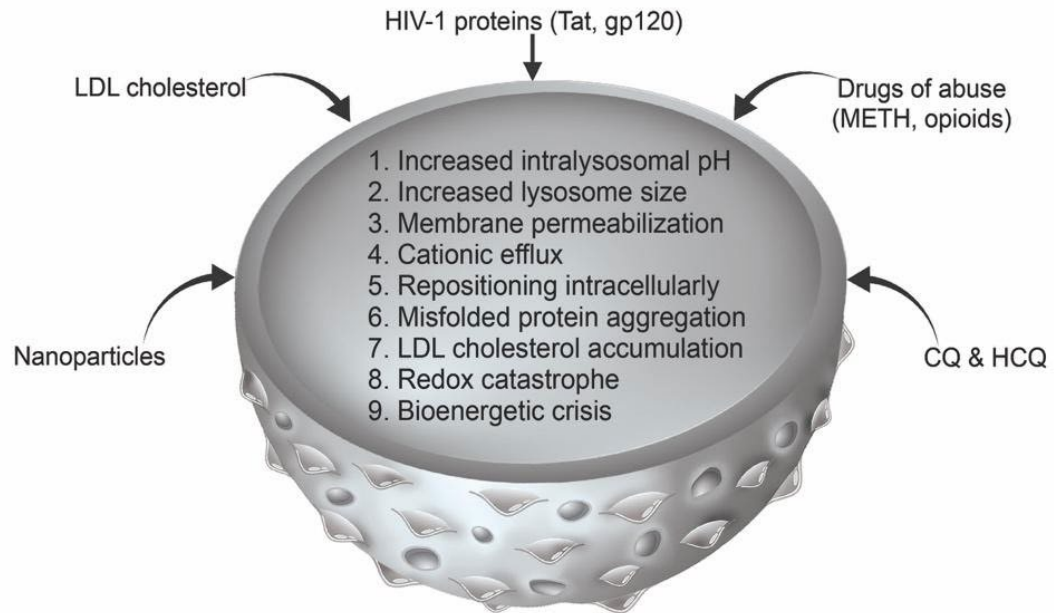
dysfunction because LSR is the means by which lysosomes attempt to adapt to environmental cues. The concept of LSR is built on the foundation of lysosome adaptation, which is the ability of lysosomes to respond to metabolic changes (Settembre & Ballabio, 2014). Here, we are broadening the idea of lysosome adaptation; LSR is lysosomal adaptation to stimuli such as pathogens, drugs, molecules or other material that could affect the greater endolysosome system. LSR utilizes selective autophagy and transcriptional response machinery in an attempt to restore lysosome function. Thus, the term – LSR.

For both ER and mitochondrial stress, selective autophagy works to remove damaged organelles (Chino & Mizushima, 2020; Galluzzi et al., 2017; Kubli & Gustafsson, 2012; J. R. Liang et al., 2020). When lysosomes are damaged, they are cleared through selective autophagy; lysophagy (Galluzzi et al., 2017; Yu, Chen, & Tooze, 2018). Lysophagy detects and clears membrane-permeabilized endolysosomes (Papadopoulos & Meyer, 2017). Permeabilization of lysosome membranes leads to the binding of galectins to sugars on the inner leaflet of lysosome membranes; this initiates ubiquitination and autophagy of damaged endolysosomes (Koerver et al., 2019; Papadopoulos et al., 2017; Papadopoulos & Meyer, 2017). Relatedly, the term "endo-lysosomal damage response" was used to describe autophagic clearance of damaged lysosomes via p97 and other cofactors (Papadopoulos et al., 2017). Lysophagy may also help with homeostatically-regulated responses. Although, ER and mitochondrial stress responses have defined sensors of stress the sensors for LSR are unclear. It is possible that an increase in lysosome pH can trigger a host of changes,

described above, that can act as stress signals. For example, lysosome biogenesis can be promoted by the release of cations from endolysosomes. Endolysosomes contain levels of calcium approaching those found in ER (Feng & Yang, 2016) and when de-acidified, readily releasable pools of calcium are released from endolysosomes and initiate transcriptional responses to increase lysosome biogenesis via TFEB (Christensen et al., 2002; Hoglinger et al., 2015; Lu, Sung, Lin, Abraham, & Jessen, 2017; Medina et al., 2015; Settembre et al., 2013). One potential LSR stress sensor could be the endolysosome resident transient receptor mucolipin 1 channel (TRPML1). TRPML1 is a divalent cation efflux channel and is implicated in sensing elevated reactive oxygen species (X. Zhang et al., 2016). Upon activation, TRPML1 can release calcium, and this calcium can activate calcineurin and lead to TFEB dephosphorylation (Medina et al., 2015) (Figure 24).

The status of TFEB during LSR might depend on the magnitude and duration of the stressor. Under minor stress conditions, which might occur physiologically, TFEB is phosphorylated by mTORC1 or other kinases, and localized in the cytosol bound to the phospho-binding 14-3-3 protein (Medina et al., 2015; Settembre et al., 2013). Under major stress conditions, which might occur pathologically, TFEB is dephosphorylated and translocates into the nucleus, activates the CLEAR gene network and leads to an up-regulation of genes involved in lysosome functioning (Lu et al., 2017; Martini-Stoica et al., 2016). These responses mirror those of the unfolded protein response (UPR) in the ER, and those in mitochondria (Bravo et al., 2013; Sasaki & Yoshida, 2015)

(Figure 26). Although speculative, such responses may play important roles in LSR. Therefore, LSR can be posited to be a homeostatic control mechanism that functions to protect against and/or rescue stressed lysosomes. In the context of therapeutics, it seems that targeting components of the mTOR-TFEB signaling pathway restores cellular functions in *in vitro* and *in vivo* models of LSD. For example, TFEB nuclear translocation has been suggested as a potential therapeutic target against LSDs. In Gaucher disease (GD), the most prevalent LSD, TFEB overexpression and the restoration of glucocerebrosidase (GCase) restored lysosome function, at least in GD-derived pluripotent stem cells (Awad et al., 2015). Similarly, in a drosophila model of GD, mTOR inhibitor rapamycin is able to partly recover the oxidative stress, locomotor, starvation and stress phenotypes (Kinghorn et al., 2016). In another study, increased expression levels of TFEB rescued GCase activity as well as the activity of -hexosaminidase, both of which are proteins mutated in Tay-Sachs disease (Song et al., 2013). Moreover, TFEB overexpression in *in vitro* and *in vivo* models of Pompe disease caused a decrease in lysosome size, a reduction of aggregated glycogen, and an increase in autophagy (Spampanato et al., 2013). Re-acidification of damaged lysosomes is another potential therapeutic target for LSDs; lysosomal de-acidification could be a central mechanism to target in various LSDs and re-acidification of lysosomes could be a therapeutic target (Folts, Scott-Hewitt, Proschel, Mayer-Proschel, & Noble, 2016). Furthermore, re-acidification of lysosomes was found to have clinical benefits including motor improvement, weight gain, and prolonged survival (Folts et al., 2016).

Inducers of LSR

In this section, we have selected to highlight 5 inducers of LSR based on the literature as well as the work we have completed in our laboratory. We acknowledge that these are not the only LSR inducers, but they are examples of how different molecules induce LSR.

Chloroquine and hydroxychloroquine.

Weak-base compounds following protonation accumulate and are trapped in lysosomes (MacIntyre & Cutler, 1988; Zhitomirsky & Assaraf, 2015); such actions may initiate LSR. Chloroquine (CQ) and hydroxychloroquine (HCQ) are both weak base FDA-approved drugs that appear to induce LSR. However, many other commonly used lysosomotropic agents may also promote LSR (P. M. Chen, Gombart, & Chen, 2011; Jia et al., 2018; Redmann et al., 2017; Settembre et al., 2012; Yoshimori et al., 1991; Zhitomirsky et al., 2018). CQ increases lysosome pH, lysosome size and lysosome membrane permeabilization, as well as inhibits protein degradation (Khan, Halcrow, et al., 2020; Khan, Lakpa, et al., 2019; Lu et al., 2017; Wibo & Poole, 1974). CQ impairment of autophagosome and lysosome fusion results in bioenergetic dysfunction (Redmann et al., 2017). Further, CQ and HCQ inhibit autophagosome-lysosome fusion and increase lysosome size (Mauthe et al., 2018). In an *in vivo* model for age-related macular degeneration, CQ induced lysosome dysfunction; lysosomes size increased and lipid accumulation was observed (P. M. Chen et al., 2011). Moreover, CQ and other lysosomotropic drugs activate TFEB translocation to the nucleus through

the inhibition of mTOR (Lu et al., 2017; Settembre et al., 2012; Zhitomirsky et al., 2018).

HIV-1 proteins.

The HIV-1 proteins, transactivator of transcription (Tat) and glycoprotein 120 (gp120) affect endolysosomes and appear to induce LSR. Tat and gp120 de-acidify endolysosomes, alter their positioning intracellularly, increase lysosome permeabilization, and promote vacuolation (M. Bae et al., 2014; Datta et al., 2019; Hui, Chen, Haughey, et al., 2012; Pietrella et al., 1998); those effects help explain findings that Tat and gp120 increase the release of divalent cations including calcium and iron from endolysosomes (Khan, Chen, & Geiger, 2020; Khan, Halcrow, et al., 2020; Nath et al., 2000; Nath et al., 1995). In the context of LSR, the damaging effects of HIV-1 proteins may be due at least in part to lysosome de-acidification, and the subsequent release of divalent cations from endolysosomes because acidification of lysosomes via activation of endolysosome-resident transient receptor mucolipin 1 (TRPML1) channel protected against gp120-induced changes to lysosomes (M. Bae et al., 2014). TRPML1 is also a reactive oxygen species (ROS)-sensor and calcium efflux channel, which promotes TFEB translocation (M. Bae et al., 2014; X. Zhang et al., 2016). In the context of HIV-1 replication, we studied the escape of HIV-1 Tat from endolysosomes and showed that HIV-1 Tat increases LTR activation only in the presence of CQ (Khan, Datta, Geiger, & Chen, 2018). These findings were interpreted as evidence that CQ-induced de-acidification and lysosome membrane permeabilization precipitated the escape of HIV-1 Tat from lysosomes

(Khan et al., 2018; Khan, Halcrow, et al., 2020). The conclusion that lysosome

pH was centrally involved in that response was supported by findings that

lysosome acidification reduced HIV-1 Tat-induced LTR activation (Khan, Lakpa,

et al., 2019).

In addition to HIV-1 proteins, antiretroviral therapeutic (ART) agents used to treat

people living with HIV-1 can also affect endolysosomes. Antiretrovirals are a

class of drugs that inhibit different stages of HIV-1 infection (Pau & George,

2014) and ARTs have been shown to affect endolysosomes (Festa et al., 2019;

Hui et al., 2019). Weak-base ARTs de-acidified endolysosomes and promoted

amyloidogenesis (Hui et al., 2019). These effects might contribute to the

pathogenesis of HIV-1 associated neurocognitive disorder and Alzheimer's

disease-like pathology in people living with HIV-1 (Afghah, Chen, & Geiger, 2020;

Festa et al., 2019; Hui et al., 2019; Khan, Haughey, Nath, & Geiger, 2019).

Low density lipoprotein (LDL) cholesterol.
Cells internalize exogenous cholesterol through receptor-mediated-endocytosis

and this cholesterol traffics through the endolysosome system. For example, low-

density lipoprotein receptor-related protein 1 (LRP1), part of the low-density

lipoprotein receptor family, mediates endocytosis of LDL cholesterol (Lillis et al.,

2015). Knockdown of LRP1 in mice increases LDL serum levels and increases

cholesterol levels in isolated macrophages. Additionally, LRP1 is linked to

amyloid beta clearance and is shown to be involved in multiple pathways that are

associated with AD reviewed by (Kanekiyo & Bu, 2014). In the context of LSR,

de-acidification of lysosomes promoted amyloidogenesis (X. Chen, Hui, Geiger,

Haughey, & Geiger, 2013; Hui et al., 2019). An interesting question would be to determine the surface levels of LRP1 in *in vitro* and *in vivo* models of AD. Moreover, it might be the case that LRP1 surface level expression is reduced resulting in the extracellular accumulation of senile plaques. Although unexplored, a better understanding of LSR might reveal novel mechanisms underlying AD pathogenesis.

Late endosomes and lysosomes can export cholesterol through lysosomal membrane localized export channels; Niemann Pick C1 and 2 (NPC1/2) (Davies & Ioannou, 2000; Friedland, Liou, Lobel, & Stock, 2003). Endolysosome enlargement and reduction in luminal lysosome calcium levels are evident in Niemann Pick-type C disease, a LSD, where lysosomes are unable to export cholesterol resulting in an accumulation of cholesterol (Jin, Shie, Maezawa, Vincent, & Bird, 2004; Liao et al., 2007; Lloyd-Evans et al., 2008). LDL cholesterol treatment can induce LSR-type responses both *in vitro* and *in vivo*; lysosomes were enlarged in skeletal muscles of rabbits fed a cholesterol-rich diet (X. Chen, Ghribi, & Geiger, 2008). Further, endolysosomes in primary cortical neurons treated with apolipoprotein B-containing LDL were enlarged, de-acidified, and contained increased levels of cholesterol and amyloid beta (Hui, Chen, & Geiger, 2012). Mechanistically, inactivating mTOR and increasing lysosome activity can reduce cholesterol aggregation in NPC cells (W. Wang et al., 2015).

Nanomaterials.

Nanomaterials can traffic into cells via endocytosis (Oh & Park, 2014) and affect the morphology and function of endolysosomes (Jia et al., 2018; Manshian, Pokhrel, Madler, & Soenen, 2018; Y. Ye et al., 2019). While some nanomaterials have been found to be harmful others have protective properties. Silica nanoparticles de-acidified endolysosomes, increased amyloid-beta peptide secretion, and reduced levels of calcium in endolysosomes (Y. Ye et al., 2019). They have also been found to inhibit mTOR activity and increase nuclear TFEB localization (Jia et al., 2018). Silica nanoparticles also increased lysosome activity and degraded more readily compared to gold nanoparticles (Manshian et al., 2018). Gold nanoparticles also seem to cause dysfunction of endolysosomes; they promoted lysosome enlargement and alkalinization, inactivated mTOR, and inhibited fusion of lysosomes with autophagosomes (Ma et al., 2011). Conversely, beneficial effects of acidic nanoparticles on endolysosome function have been observed; carboxyl-modified polystyrene nanoparticles activated the TFEB-mTOR pathway and inhibited ferroptosis (L. Li et al., 2019). Poly (DL-lactide-co-glycolide) (PLGA) acidic nanoparticles (aNP) were found to accumulate in endolysosomes, re-acidify endolysosomes, and restore lysosome functionality (Baltazar et al., 2012). In models of Parkinson's disease, PGLA-aNP re-acidified endolysosomes, decreased lysosome membrane permeabilization, and protected against PD-related neuronal degeneration (Bourdenx et al., 2016). Similarly, in presenilin 1 knock out cells, PGLA-aNP attenuated de-acidification, lysosomal calcium efflux, and autophagy (J. H. Lee et al., 2015).

Drugs of abuse (morphine and methamphetamine).

Several drugs of abuse including opioids and amphetamines may cause LSR;

they are up-taken into endolysosomes, increase luminal pH, cause vacuolization,

permeabilize membranes, and disrupt iron homeostasis (Cubells, Rayport,

Rajendran, & Sulzer, 1994; Funakoshi-Hirose et al., 2013; Liesse, Lhoest,

Trouet, & Tulkens, 1976; Nash et al., 2019; Patierno et al., 2011; E. Xu, Liu, Liu,

Wang, & Xiong, 2018). Methamphetamine increased lysosome size, inhibited

autophagosome-lysosome fusion (Funakoshi-Hirose et al., 2013; Nara, Aki,

Funakoshi, Unuma, & Uemura, 2012), de-acidified lysosomes, impaired

phagocytosis, inhibited antigen presentation, and inhibited macrophage functions

during immune responses (Talloczy et al., 2008). Similarly, the opioid morphine

damaged lysosomes; morphine alone and in combination with HIV-1 increased

lysosome pH, and inhibited fusion between autophagosomes and lysosomes (El-

Hage et al., 2015), induced iron efflux from endolysosomes (Nash et al., 2019),

and increased lysosome pH through mu-opioid receptor-mediated mechanisms

(Nash et al., 2019).

Many clinically used drugs share the physicochemical property of being weakly

or strongly basic. As such and similar to what has been demonstrated for opioids

and methamphetamine, these basic drugs accumulate in acidic endolysosomes

where they would become increasingly charged and where they would be

expected to de-acidify endolysosomes. And recent evidence supports that some

of the following drugs may induce lysosome stress and illicit what we would

characterize as LSR. Commonly used basic drugs (listed in alphabetical order)

include; antipyrine (analgesic), barbiturates (sedative/hypnotics), bupivacaine (local anesthetic), chlorpromazine and olanzapine (antipsychotics), diazepam (anxiolytic), pentazocine (opioid agonist/antagonist), phenylbutazone (NSAID), propranolol (beta blocker), pyrimethamine (anti-parasitic), quinidine (antiarrhythmic), sildenafil citrate (erective dysfunction), telmisartan (anti-hypertensive), tolbutamide (sulfonylurea), valproic acid and phenytoin (anticonvulsants), warfarin (anticoagulant) (Boz, Hu, Yu, & Huang, 2020; Cramb, 1986; Hamaguchi, Haginaka, Tanimoto, & Kuroda, 2014; Jang et al., 2016; Kozako et al., 2016; Pourahmad et al., 2012; Staneva-Stoicheva, Krustev, & Kitova, 1977).

Thus, the possibility exists that any drug, pathogen, or material that enters into the greater endolysosomal system may induce, to varying degrees, lysosome stress and LSR (Figure 2). Of course, the definition of LSR will likely change as new knowledge is added and specific therapeutics are developed, and it is unclear the extent to which LSR might be protective or destructive. Likely, LSR occurs in combination with other intracellular stress responses including those mediated through ER and mitochondria.

Inter-Organellar Signaling

In this era of modern cell biology, there is ever-growing appreciation of the complexities of inter-organellar signaling in health and disease (Afghah et al., 2020; Gottschling & Nystrom, 2017; Khan, Haughey, et al., 2019). Organelles are highly mobile in cells and dynamically form contacts between organelles; as such extensive communications between organelles exists (Deus et al., 2020; Soto-

Heredero, Baixauli, & Mittelbrunn, 2017). Inter-organellar signaling helps maintain cellular functions (Deus et al., 2020; Gottschling & Nystrom, 2017).

Cell stress can cause disrupted crosstalk between organelles (Deus et al., 2020; Guerra et al., 2019; Soto-Heredero et al., 2017; Torres et al., 2017). For example, mitochondria, ER, and endolysosome dysfunction are implicated in multiple diseases and disorders (Annunziata, Sano, & d'Azzo, 2018; Audano et al., 2018; Demers-Lamarche et al., 2016; Plotegher & Duchen, 2017; Soto-Heredero et al., 2017; Torres et al., 2017). Cellular stress signals converge on one common adaptive pathway, termed the integrated stress response (ISR) (Pakos-Zebrucka et al., 2016). The integration point of stress stimuli occurs at the phosphorylation of eukaryotic translation initiation factor 2 alpha (eIF2) and subsequent synthesis of activating transcription factor 4 (ATF4), which is a transcription factor that upregulates genes that promote cellular survival and recovery (Pakos-Zebrucka et al., 2016). ISR can stimulate autophagy pathways and is suggested to promote regulation of cellular fate (Humeau et al., 2020; Kroemer, Marino, & Levine, 2010). The type and duration of a stressor plays an important factor in the outcomes of the ISR. Stress signals from both ER and mitochondrial participate in ISR, although, it remains unclear the degree to which LSR contributes to ISR.

LSR Observed in ER- and Mitochondrial Stress Responses
Endolysosomes dynamically interact physically and chemically with the nucleus, ER and mitochondria (Deus et al., 2020; C. A. Lee & Blackstone, 2020; Settembre et al., 2013) and such inter-organellar signaling might affect organellar

144

stress responses. Indeed, ER and mitochondrial stress can induce LSR

(Table 5). ER stress de-acidifies lysosomes, increases lysosome size, induces

lysosome membrane permeabilization, and leads to lysosome repositioning (D.

Bae, Moore, Mella, Hayashi, & Hollien, 2019; Dauer et al., 2017; Elfrink, Zwart,

Baas, & Scheper, 2013; A. Kim & Cunningham, 2015; Nakashima et al., 2019).

Moreover, it inhibits autophagic flux (Nakashima et al., 2019). Pharmacological

induction of ER stress with tunicamycin causes nuclear translocation of the

transcription factors TFEB and TFE3 (Martina et al., 2016). Further, the lysosome

resident protein mTOR contributes to ER stress, and cell life and death by

regulating expression levels of ER stress response genes (Appenzeller-Herzog &

Hall, 2012; G. Dong et al., 2015). However, there is evidence of mTOR-

independent nuclear translocation of TFEB/3 (Martina et al., 2016).

Similar to ER, LSR is observed in mitochondrial stress such as lysosome

membrane permeabilization, de-acidification, changes in morphology, LDL

cholesterol accumulation, and misfolded protein aggregation (Baixauli et al.,

2015; Butler & Bahr, 2006; Demers-Lamarche et al., 2016; Hwang, Lee, Kim,

Cho, & Koh, 2008; Schieber & Chandel, 2014; X. Zhang et al., 2016). De-

acidification of endolysosomes promotes efflux of redox active iron into the

cytosol which can then generate ROS through the Fenton reaction in the cytosol

and within mitochondria (Uchiyama et al., 2008; Yambire et al., 2019). H_2O_2-

induced oxidative stress suppressed TFEB nuclear translocation and promoted

apoptosis (Q. Su et al., 2018) and TFEB-overexpression was protective; it

Table 5. Comparison of lysosome, mitochondria and ER stress responses. This table highlights the absence or presence of evidence for the observation of LSR in mitochondrial- and ER-stress responses. (+) indicate evidence for LSR, while (-) indicate a lack of evidence for LSR, while (-) indicate a lack of evidence for LSR.

Comparison of Organellar Stress Responses

Lysosome stress responses	Mitochondria stress	Endoplasmic reticulum stress	References
Increased intralysosomal pH	+	+	Lu et al., 2017; khan et al., 2020; Demers-Lamarche et al., 2016; Nakashima et al., 2019
Increased lysosome size	+	+	Ohkuma & Poole, 1981; Hui et al., 2012; Demers-Lamarche et al., 2016; Elfrink et al., 2013
Membrane permeabilization	+	+	Khan et al., 2020; Hwang et al., 2008; Kim & Cunningham, 2015; Dauer et al., 2017
Cationic efflux	+	+	Christensen et al., 2002; Hui et al., 2015; Zhang et al., 2016
Repositioning intracellularly	-	+	Johnson et al., 2016; Bae et al., 2019; Elfrink et al., 2013
Misfolded protein aggregation	+	+	Hui & Ye et al., 2019; Bae et al., 2019; Demers-Lamarche et al., 2016; Baixauli et al., 2015
LDL cholesterol accumulation	-	-	Liao et al., 2007
Redox catastrophe	+	-	Uchiyama et al., 2008; Zhang et al., 2016
Bioenergetic crisis	+	-	Redman et al., 2017; Baixauli et al., 2015

reduced glucose-mediated oxidative stress by increasing the expression of antioxidant enzymes and mitochondrial biogenesis genes (Kang, Li, Zhang, Chi, & Liu, 2019), and increased autophagy (F. Li et al., 2016).

Broader Implications

In comparison to ER and mitochondrial stress responses, relatively little is known about LSR. PubMed and Google Scholar searches for the keywords "ER stress", "unfolded protein response", "mitochondrial stress", "mitochondrial redox catastrophe", and "mitochondrial bioenergetic crisis" generate citations to thousands of manuscripts. Conversely, a search for the keywords "lysosomal stress" or "lysosome stress response" yields less than one dozen manuscript citations; only a few attempted to define lysosome stress. Similar to ER and mitochondria, when presented with excess cargo, lysosomes can undergo stress responses implicated in multiple pathologies (Davidson & Vander Heiden, 2017; Lie & Nixon, 2019; Reuser & Drost, 2006). Thus, establishing a framework for defining LSR is of physiological and pathological importance. Central to the criteria described above for LSR are lysosome de-acidification and lysosome membrane permeabilization. Any drug, protein, virus or insult that affects the endocytic or autophagic pathways may cause lysosome stress and trigger LSR.

Conclusions

Lysosomes are integral to the dynamic endolysosome system and are important for maintaining cellular homeostasis through intracellular degradation of cargo, cytosolic nutrient sensing, and cation homeostasis. Under stressful conditions all organelles including lysosomes, ER and mitochondria exhibit stress responses

147

as they attempt to restore organellar function or promote cell death pathways when stress responses are too great. Few have provided characterizations of LSR and here a framework is presented upon which we can build on the physiological roles and pathological implications for LSR. Through a better understanding of LSR, new and potentially impactful therapeutic interventions might be discovered. In the meantime, LSR might find its place in the vernacular of modern cell biology and might lead to a wave of investigations focused on inter-organellar signaling (Figure 27).

Figure 27.   Organellar stress responses. Resulting from acute and chronic
               stimuli and stressors, lysosomes can exhibit lysosome stress
               responses (LSR). LSR as characterized in the text and in
               Figure 3 is characterized by perinuclear to peripheral
               repositioning of lysosomes, increases in lysosome size,
               reduction in intralysosomal proton concentrations and decreases
               in cytosolic and extracellular pH, intraluminal accumulation of
               LDL cholesterol, increased misfolded protein aggregation,
               lysosomal membrane permeabilization, and efflux of calcium and
               iron from lysosomes. Endoplasmic reticulum (ER) and
               mitochondria exhibit their own stress responses, and these might
               be triggered by LSR. Mitochondria in response to increases in
               cytosolic iron and calcium act as cation sinks; when excessive
               results include increases in reactive oxygen species (ROS)
               leading to redox catastrophe and decreases in adenosine
               triphosphate (ATP) promoting bioenergetic crisis. A vicious cycle
               can result from LSR including (1) increases in ROS can cause
               further lysosome stress, (2) increases in cytosolic calcium can
               trigger calcium-induced calcium release from ER, and (3)
               increases in lipid accumulation and protein aggregation in ER
               can lead to ER stress. Therefore, LSR might be an early and
               upstream event that participates in inter-organellar stress
               responses.

Organelle stress responses
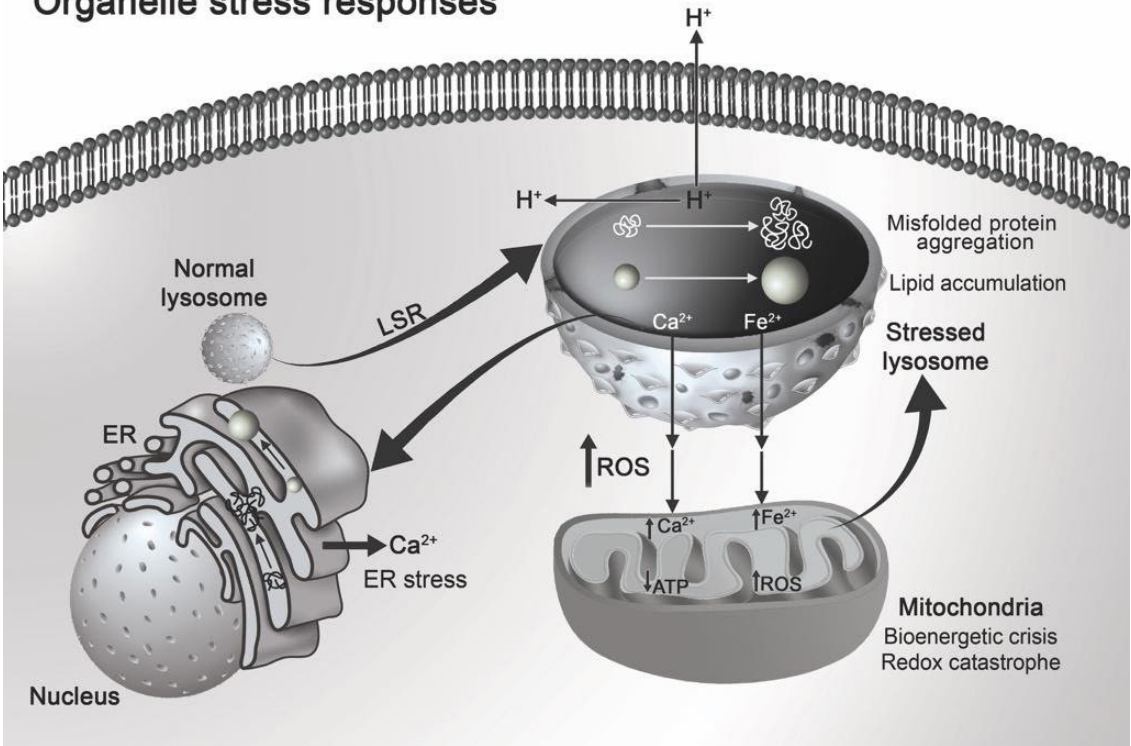
CHAPTER 5

GENERAL DISCUSSION

Conclusions

Iron is both essential and detrimental to cells. It is involved in many life sustaining processes; when levels of free iron increase it leads to the production of radical species that damage DNA, proteins, and lipids (Wallace, 2016). Iron is a redox active metal and is mainly found in either its ferrous (Fe^{2+}) or ferric (Fe^{3+}) form. Ferric iron is redox inactive and is the form that is transported throughout the body. Systemic iron transport is aided by the iron transport glycoprotein, transferrin (TF) (Ponka & Lok, 1999). TF has a high binding affinity for two Fe^{3+} ions which protects the body from the formation of insoluble ferric hydroxides and redox active ferrous form of iron (Muckenthaler et al., 2017; D. R. Richardson et al., 2010). Cells contain transmembrane glycoprotein transferrin receptors (TFR) which allow them to take up iron-bound TF via receptor-mediated endocytosis. This leads to an accumulation of Fe^{3+} within endolysosomes and that accumulated Fe^{3+} can be reduced to Fe^{2+} by ferrireductase protein STEAP3 (Muckenthaler et al., 2017; Ponka & Lok, 1999; Wallace, 2016). After being reduced, Fe^{2+} is released through endolysosome-resident iron permeable channels such as DMT-1 and TRPML1 (Abouhamed et al., 2006; X. P. Dong et al., 2008). It is evident that endolysosomes are critical for cellular iron homeostasis. This is where our study begins.

151

The Geiger/Chen laboratory is interested in understanding the role that endolysosome de-acidification plays in neurogenerative disease pathologies. Over 50% of PLWH develop neurocognitive impairments termed HIV-1 associated neurocognitive disorder (HAND) (Antinori et al., 2007; Clifford & Ances, 2013; McArthur et al., 2010). There is currently no cure for HAND and the underlying mechanisms for its pathogenesis are still under investigation. However, elevated serum iron levels and soluble factors such as HIV-1 protein gp120 have been hypothesized to contribute to HAND pathogenesis (Chang et al., 2015; Kovalevich & Langford, 2012). HIV-1 gp120 induces astrocyte dysfunction, increases ROS production and affects the function and morphology of organelles including endolysosomes (M. Bae et al., 2014; Datta et al., 2019; Lopez et al., 2017; Raber et al., 1996). Thus, in these studies we investigated mechanisms by which HIV-1 gp120 affects cellular iron homeostasis in U87MG cells, an astrocytoma cell line; these cells have been used by others to investigate the cellular effects of HIV-1 gp120 (Lopez et al., 2017; Valentín-Guillama et al., 2018).

In Chapter 2, we determined an intracellular mechanism by which HIV-1 gp120 affects ROS production through endolysosome-based iron release. We observed that HIV-1 gp120 induced, within a 30 min duration, endolysosomal de-acidification which led to a reduction in luminal levels of endolysosome iron and increases in cytosolic and mitochondrial iron levels. Subsequently, an increase of ROS was observed in the cytosol and mitochondria, and these increases were blocked by chelating endolysosome iron with DFO. Interestingly, this

152

phenomenon occurred in the absence of significant cell death even when we extended our treatments to 24 h. Results from other groups confirmed our findings and provide evidence that HIV-1 gp120 treatment increases cell proliferation in U87MG cells through glycolysis and promoting the unfolded protein response (Lopez et al., 2017; Valentín-Guillama et al., 2018).

The study conducted in Chapter 3 is an extension of our first study. HIV-1 gp120 increased cytosolic and mitochondrial ROS levels within 30 min of treatment but did not induce cell death at 24 h. This led us to question whether HIV-1 gp120 had significant effects on iron related proteins in U87MG cells. We first determined the responsiveness of our U87MG cells to changes in intracellular iron levels. DFO and FAC were used to decrease and increase the intracellular liable pool of iron, respectively (Hoepken et al., 2004). We treated our cells at varying time points and concentrations of each compound. Our results demonstrated to us that 24 h treatment with either 100 µM DFO or 100 µM FAC induced a significant increase TFR1 or FTH, respectively. Conversely, 100 µM FAC reduced TFR1, while 100 µM DFO reduced FTH. Thus, moving forward we decided to use a 24 h treatment time point for our studies. We hypothesized that 24 h HIV-1 gp120 would lead to decreases in TFR1 and IRP2 protein, and increases in FTH and FPN protein. To our surprise we did not observe any effect of gp120 on surface or total protein levels of TFR1 and there was no significant changes in IRP2 or FTH protein levels. But, we did observe a significant increase in surface FPN. One explanation for this finding is that U87MG cells might

increase surface levels of FPN in order to release excess iron from the cells and maintain homeostasis.

In Chapter 4, we detailed our definition of lysosomal stress response (LSR) which is a homeostatic regulatory response initiated by lysosomes when they encounter a stressor such as HIV-1 gp120. We have categorized LSR as (1) increased intralysosomal pH, (2) increased lysosome size, (3) membrane permeabilization, (4) cationic efflux, (5) repositioning intracellularly, (6) misfolded protein aggregation, (7) LDL cholesterol accumulation, (8) redox catastrophe, and (9) bioenergetic crisis. The response varies based on the LSR inducer and duration of the stress. In the case of HIV-1 gp120 it is apparent to us that during short term treatments (30 min), HIV-1 gp120 is able to de-acidify endolysosomes, increase endolysosome size and decrease the number of endolysosomes while also inducing the efflux of iron from endolysosomes. Although we didn't test it, this response may be upstream of the UPR response and induce acute ER-stress (Lopez et al., 2017). Thus, inter-organellar signaling maybe a contributor to HAND pathogenesis.

There is far more work to be done and many more questions to asked. Such as, what are the effects of 24 h gp120 treatment on intracellular iron levels; how do endolysosome iron stores contribute to 24 h gp120-induced increases in surface FPN; does inhibition of gp120 internalization into U87MG cells block its de-acidifying effects on endolysosome and the downstream consequences; how does acidifying endolysosomes affect gp120 effect on endolysosome, cytosol

and mitochondrial iron communication; how does HIV-gp120 affect intracellular iron signaling between endolysosomes and mitochondria in primary astrocytes?

Limitations

We appreciate that the experiments conducted and presented in this dissertation have several limitations. Hence, we will briefly discuss some of them in this section. In Chapter 2, we assumed that HIV-1 gp120 was being internalized into the endolysosomes. We did not check whether our cells expressed either receptor, CXCR4 or CCR5, for gp120. Furthermore, we did not conduct any studies with CXCR4 or CCR5 antagonists to determine whether gp120-induced endolysosome de-acidification was a direct or indirect affect. Moreover, our study used only a pharmacological approach to determine the mechanism by which HIV-1 gp120 induced iron release from endolysosomes and how that iron was taken up by mitochondria. To confirm this mechanism, the use of molecular techniques such as knockdown of FPN and TFR1 would be necessary. Another limitation is that at the time that these experiments were carried out we did not have the ability to simultaneously measure iron levels in endolysosomes, cytosol, and mitochondria in live cells.

In Chapter 3, we did not measure levels of endolysosome, cytosol or mitochondrial iron and ROS levels during our treatment 24 h time period. Therefore, we do not know if 24 h HIV-1 gp120 treatment increases cytosolic iron levels. Furthermore, our work did not involve any qPCR analyses to determine changes in mRNA transcripts due to our HIV-1 gp120 treatment. It is possible that HIV-1 gp120 increases the mRNA transcripts of TFR1 and FTH and the time

period we decided on was too short to observe changes in protein levels. We also did not run time course experiments to rule out that 24 h HIV-1 gp120 does not affect the iron related proteins tested in this study. Nonetheless, without these experiments it remains unclear as to how HIV-1 gp120 is affecting these proteins.

Most importantly, our cell model used for this study is limiting. Although U87MG cells have been used to investigate the effects of HIV-1 gp120, these cells are cancer cells, which are reported to have higher levels of ROS compared to non-cancer cells (Liou & Storz, 2010; Schieber & Chandel, 2014); they also proliferate in the presence of ROS due to an elevation of antioxidants to maintain cell survival (Liou & Storz, 2010). Therefore, these cells have modified signaling pathways to promote cell survival and replication and avoid cell death.

Future Directions

Despite these limitations, we think that this work provides a proof of concept for HIV-1 gp120 induced endolysosome iron release which can promote cytosolic and mitochondrial ROS production. Furthermore, our findings demonstrate that HIV-1 gp120 promotes an increase in surface FPN levels in U87MG cells. One way this work can be extended is repeating these studies in human primary astrocytes. We would be able to determine if 1) this endolysosome-mitochondrial iron/ROS mechanism is occurring, 2) does this mechanism induce cell death, and 3) can that cell death be prevented by blocking endolysosome iron release?

Our investigation of changes in iron regulatory proteins due to the presence of HIV-1 gp120 can also be extended using a rodent model; HIV-1 gp120 transgenic mice (Toggas et al., 1994). HIV-1 gp120 transgenic mice express HIV-1 gp120 in astrocytes and is under the control of the glial fibrillary acidic protein promoter (GFAP-gp120tg) (Toggas et al., 1994). The GFAP-gp120tg mice demonstrates reduced autophagy, protein aggregates, hippocampal damage, loss of dendrites and synapses and astrogliosis all of which are involved in HAND neuropathogenesis (J. Fields et al., 2013; Thaney et al., 2018; Toggas et al., 1996). We could set up a study comparing wild-type and GFAP-gp120tg mice in the absence or presence of DFO. The mice would be separated into male and female groups within the WT and gp120 groups. Furthermore, the animals would be raised to maturity (around 3-6 months) and then PBS or DFO (100 mg/kg, twice daily) would be given intraperitoneally for 7 days (Y. Li, K. Pan, et al., 2016). Then, a portion of WT and gp120 mice would be euthanized and brains would be homogenized and the protein levels determined for FPN, IRP2, FTH, and TFR1. The brains of another subset of WT and gp120 would be sliced and stained using, immunohistochemistry to measure levels of the above listed iron-related proteins. The remaining mice would undergo neurocognitive and motor coordination evaluations. There is still much work to be done, but these studies provide a foundation for evidence of intra-organellar iron signaling in the context of HAND.

REFERENCES

Abboud, S., & Haile, D. J. (2000). A novel mammalian iron-regulated protein involved in intracellular iron metabolism. *J Biol Chem, 275*(26), 19906-19912. doi:10.1074/jbc.M000713200

Abouhamed, M., Gburek, J., Liu, W., Torchalski, B., Wilhelm, A., Wolff, N. A., .Smith, C. P. (2006). Divalent metal transporter 1 in the kidney proximal tubule is expressed in late endosomes/lysosomal membranes: implications for renal handling of protein-metal complexes. *Am J Physiol Renal Physiol, 290*(6), F1525-1533. doi:10.1152/ajprenal.00359.2005

Ackerman, C. M., Lee, S., & Chang, C. J. (2017). Analytical Methods for Imaging Metals in Biology: From Transition Metal Metabolism to Transition Metal Signaling. *Anal Chem, 89*(1), 22-41. doi:10.1021/acs.analchem.6b04631

Afghah, Z., Chen, X., & Geiger, J. D. (2020). Role of endolysosomes and inter-organellar signaling in brain disease. *Neurobiol Dis, 134*, 104670. doi:10.1016/j.nbd.2019.104670

Al-Harthi, L., Joseph, J., & Nath, A. (2018). Astrocytes as an HIV CNS reservoir: highlights and reflections of an NIMH-sponsored symposium. *J Neurovirol, 24*(6), 665-669. doi:10.1007/s13365-018-0691-8

Alabduladhem, T. O., & Bordoni, B. (2021). Physiology, Krebs Cycle. In *StatPearls*. Treasure Island (FL).

An, S. F., Groves, M., Gray, F., & Scaravilli, F. (1999). Early entry and widespread cellular involvement of HIV-1 DNA in brains of HIV-1 positive asymptomatic individuals. *J Neuropathol Exp Neurol, 58*(11), 1156-1162. doi:10.1097/00005072-199911000-00005

Anderson, C. P., Shen, M., Eisenstein, R. S., & Leibold, E. A. (2012). Mammalian iron metabolism and its control by iron regulatory proteins. *Biochim Biophys Acta, 1823*(9), 1468-1483. doi:10.1016/j.bbamcr.2012.05.010

Annunziata, I., Sano, R., & d'Azzo, A. (2018). Mitochondria-associated ER membranes (MAMs) and lysosomal storage diseases. *Cell Death Dis, 9*(3), 328. doi:10.1038/s41419-017-0025-4

Antinori, A., Arendt, G., Becker, J. T., Brew, B. J., Byrd, D. A., Cherner, M., Wojna, V. E. (2007). Updated research nosology for HIV-associated neurocognitive disorders. *Neurology, 69*(18), 1789-1799. doi:10.1212/01.WNL.0000287431.88658.8

Antiretroviral Therapy Cohort, C. (2017). Survival of HIV-positive patients starting antiretroviral therapy between 1996 and 2013: a collaborative analysis of cohort studies. *Lancet HIV, 4*(8), e349-e356. doi:10.1016/S2352-3018(17)30066-8

Appenzeller-Herzog, C., & Hall, M. N. (2012). Bidirectional crosstalk between endoplasmic reticulum stress and mTOR signaling. *Trends Cell Biol, 22*(5), 274-282. doi:10.1016/j.tcb.2012.02.006

Arts, E. J., & Hazuda, D. J. (2012). HIV-1 antiretroviral drug therapy. *Cold Spring Harb Perspect Med, 2*(4), a007161. doi:10.1101/cshperspect.a007161

Ashraf, A., Clark, M., & So, P. W. (2018). The Aging of Iron Man. *Front Aging Neurosci, 10*, 65. doi:10.3389/fnagi.2018.00065

Audano, M., Schneider, A., & Mitro, N. (2018). Mitochondria, lysosomes, and dysfunction: their meaning in neurodegeneration. *J Neurochem, 147*(3), 291-309. doi:10.1111/jnc.14471

Avdoshina, V., Fields, J. A., Castellano, P., Dedoni, S., Palchik, G., Trejo, M., Mocchetti, I. (2016). The HIV Protein gp120 Alters Mitochondrial Dynamics in Neurons. *Neurotox Res, 29*(4), 583-593. doi:10.1007/s12640-016-9608-6

Awad, O., Sarkar, C., Panicker, L. M., Miller, D., Zeng, X., Sgambato, J. A., Feldman, R. A. (2015). Altered TFEB-mediated lysosomal biogenesis in Gaucher disease iPSC-derived neuronal cells. *Hum Mol Genet, 24*(20), 5775-5788. doi:10.1093/hmg/ddv297

Bae, D., Moore, K. A., Mella, J. M., Hayashi, S. Y., & Hollien, J. (2019). Degradation of Blos1 mRNA by IRE1 repositions lysosomes and protects cells from stress. *J Cell Biol, 218*(4), 1118-1127. doi:10.1083/jcb.201809027

Bae, M., Patel, N., Xu, H., Lee, M., Tominaga-Yamanaka, K., Nath, A., Haughey, N. J. (2014). Activation of TRPML1 clears intraneuronal Abeta in preclinical models of HIV infection. *J Neurosci, 34*(34), 11485-11503. doi:10.1523/JNEUROSCI.0210-14.2014

Baixauli, F., Acin-Perez, R., Villarroya-Beltri, C., Mazzeo, C., Nunez-Andrade, N., Gabande-Rodriguez, E., Mittelbrunn, M. (2015). Mitochondrial Respiration Controls Lysosomal Function during Inflammatory T Cell Responses. *Cell Metab, 22*(3), 485-498. doi:10.1016/j.cmet.2015.07.020

Ballabio, A. (2016). The awesome lysosome. *EMBO Mol Med, 8*(2), 73-76. doi:10.15252/emmm.201505966

Ballabio, A., & Bonifacino, J. S. (2020). Lysosomes as dynamic regulators of cell and organismal homeostasis. *Nat Rev Mol Cell Biol, 21*(2), 101-118. doi:10.1038/s41580-019-0185-4

Ballabio, A., & Gieselmann, V. (2009). Lysosomal disorders: from storage to cellular damage. *Biochim Biophys Acta, 1793*(4), 684-696. doi:10.1016/j.bbamcr.2008.12.001

Baltazar, G. C., Guha, S., Lu, W., Lim, J., Boesze-Battaglia, K., Laties, A. M., Mitchell, C. H. (2012). Acidic nanoparticles are trafficked to lysosomes and restore an acidic lysosomal pH and degradative function to compromised ARPE-19 cells. *PLOS one, 7*(12), e49635. doi:10.1371/journal.pone.0049635

Barre-Sinoussi, F., Chermann, J. C., Rey, F., Nugeyre, M. T., Chamaret, S., Gruest, J., Montagnier, L. (1983). Isolation of a T-lymphotropic retrovirus from a patient at risk for acquired immune deficiency syndrome (AIDS). *Science, 220*(4599), 868-871. doi:10.1126/science.6189183

Bi, X., Haque, T. S., Zhou, J., Skillman, A. G., Lin, B., Lee, C. E., Lynch, G. (2000). Novel cathepsin D inhibitors block the formation of hyperphosphorylated tau fragments in hippocampus. *J Neurochem, 74*(4), 1469-1477. doi:10.1046/j.1471-4159.2000.0741469.x

Bindoli, A., Fukuto, J. M., & Forman, H. J. (2008). Thiol chemistry in peroxidase catalysis and redox signaling. *Antioxid Redox Signal, 10*(9), 1549-1564. doi:10.1089/ars.2008.2063

Bird, P. I., Trapani, J. A., & Villadangos, J. A. (2009). Endolysosomal proteases and their inhibitors in immunity. *Nat Rev Immunol, 9*(12), 871-882. doi:10.1038/nri2671

Bonam, S. R., Wang, F., & Muller, S. (2019). Lysosomes as a therapeutic target. *Nat Rev Drug Discov, 18*(12), 923-948. doi:10.1038/s41573-019-0036-1

Bourdenx, M., Daniel, J., Genin, E., Soria, F. N., Blanchard-Desce, M., Bezard, E., & Dehay, B. (2016). Nanoparticles restore lysosomal acidification defects: Implications for Parkinson and other lysosomal-related diseases. *Autophagy, 12*(3), 472-483. doi:10.1080/15548627.2015.1136769

Boz, Z., Hu, M., Yu, Y., & Huang, X. F. (2020). N-acetylcysteine prevents olanzapine-induced oxidative stress in mHypoA-59 hypothalamic neurons. *Sci Rep, 10*(1), 19185. doi:10.1038/s41598-020-75356-3

Brailoiu, E., Churamani, D., Cai, X., Schrlau, M. G., Brailoiu, G. C., Gao, X., Patel, S. (2009). Essential requirement for two-pore channel 1 in NAADP-mediated calcium signaling. *J Cell Biol, 186*(2), 201-209. doi:10.1083/jcb.200904073

Brand, M. D. (2005). The efficiency and plasticity of mitochondrial energy transduction. *Biochem Soc Trans, 33*(Pt 5), 897-904. doi:10.1042/BST0330897

Braulke, T., & Bonifacino, J. S. (2009). Sorting of lysosomal proteins. *Biochim Biophys Acta, 1793*(4), 605-614. doi:10.1016/j.bbamcr.2008.10.016

Bravo, R., Parra, V., Gatica, D., Rodriguez, A. E., Torrealba, N., Paredes, F., Lavandero, S. (2013). Endoplasmic reticulum and the unfolded protein response: dynamics and metabolic integration. *Int Rev Cell Mol Biol, 301*, 215-290. doi:10.1016/B978-0-12-407704-1.00005-1

Brew, B. J., Pemberton, L., Blennow, K., Wallin, A., & Hagberg, L. (2005). CSF amyloid beta42 and tau levels correlate with AIDS dementia complex. *Neurology, 65*(9), 1490-1492. doi:10.1212/01.wnl.0000183293.95787.b7

Bridges, K. R., & Cudkowicz, A. (1984). Effect of iron chelators on the transferrin receptor in K562 cells. *J Biol Chem, 259*(21), 12970-12977. Retrieved from https://www.ncbi.nlm.nih.gov/pubmed/6092356

Brookes, P. S., Yoon, Y., Robotham, J. L., Anders, M. W., & Sheu, S. S. (2004). Calcium, ATP, and ROS: a mitochondrial love-hate triangle. *Am J Physiol Cell Physiol, 287*(4), C817-833. doi:10.1152/ajpcell.00139.2004

Butler, D., & Bahr, B. A. (2006). Oxidative stress and lysosomes: CNS-related consequences and implications for lysosomal enhancement strategies and induction of autophagy. *Antioxid Redox Signal, 8*(1-2), 185-196. doi:10.1089/ars.2006.8.185

Cable, H., & Lloyd, J. B. (1999). Cellular uptake and release of two contrasting iron chelators. *J Pharm Pharmacol, 51*(2), 131-134. Retrieved from https://www.ncbi.nlm.nih.gov/pubmed/10217310

Cabukusta, B., & Neefjes, J. (2018). Mechanisms of lysosomal positioning and movement. *Traffic, 19*(10), 761-769. doi:10.1111/tra.12587

Calcraft, P. J., Ruas, M., Pan, Z., Cheng, X., Arredouani, A., Hao, X., Zhu, M. X. (2009). NAADP mobilizes calcium from acidic organelles through two-pore channels. *Nature, 459*(7246), 596-600. doi:10.1038/nature08030

Cao, Y., Espinola, J. A., Fossale, E., Massey, A. C., Cuervo, A. M., MacDonald, M. E., & Cotman, S. L. (2006). Autophagy is disrupted in a knock-in mouse model of juvenile neuronal ceroid lipofuscinosis. *J Biol Chem, 281*(29), 20483-20493. doi:10.1074/jbc.M602180200

Cataldo, A. M., Barnett, J. L., Berman, S. A., Li, J., Quarless, S., Bursztajn, S., Nixon, R. A. (1995). Gene expression and cellular content of cathepsin D in Alzheimer's disease brain: evidence for early up-regulation of the endosomal-lysosomal system. *Neuron, 14*(3), 671-680. doi:10.1016/0896-6273(95)90324-0

Cataldo, A. M., Paskevich, P. A., Kominami, E., & Nixon, R. A. (1991). Lysosomal hydrolases of different classes are abnormally distributed in brains of patients with Alzheimer disease. *Proc Natl Acad Sci U S A, 88*(24), 10998-11002. doi:10.1073/pnas.88.24.10998

Chang, H. C., Bayeva, M., Taiwo, B., Palella, F. J., Jr., Hope, T. J., & Ardehali, H. (2015). Short communication: high cellular iron levels are associated with increased HIV infection and replication. *AIDS Res Hum Retroviruses, 31*(3), 305-312. doi:10.1089/aid.2014.0169

Chauhan, A., Mehla, R., Vijayakumar, T. S., & Handy, I. (2014). Endocytosis-mediated HIV-1 entry and its significance in the elusive behavior of the virus in astrocytes. *Virology, 456-457*, 1-19. doi:10.1016/j.virol.2014.03.002

Chen, C., Liu, P., Duan, X., Cheng, M., & Xu, L. X. (2019). Deferoxamine-induced high expression of TfR1 and DMT1 enhanced iron uptake in triple-negative breast cancer cells by activating IL-6/PI3K/AKT pathway. *Onco Targets Ther, 12*, 4359-4377. doi:10.2147/OTT.S193507

Chen, D., Xie, J., Fiskesund, R., Dong, W., Liang, X., Lv, J., Huang, B. (2018). Chloroquine modulates antitumor immune response by resetting tumor-associated macrophages toward M1 phenotype. *Nat Commun, 9*(1), 873. doi:10.1038/s41467-018-03225-9

Chen, L., Liu, J., Xu, C., Keblesh, J., Zang, W., & Xiong, H. (2011). HIV-1gp120 induces neuronal apoptosis through enhancement of 4-aminopyridine-senstive outward K+ currents. *PLOS one, 6*(10), e25994. doi:10.1371/journal.pone.0025994

Chen, P. M., Gombart, Z. J., & Chen, J. W. (2011). Chloroquine treatment of ARPE-19 cells leads to lysosome dilation and intracellular lipid accumulation: possible implications of lysosomal dysfunction in macular degeneration. *Cell Biosci, 1*(1), 10. doi:10.1186/2045-3701-1-10

Chen, X., Ghribi, O., & Geiger, J. D. (2008). Rabbits fed cholesterol-enriched diets exhibit pathological features of inclusion body myositis. *Am J Physiol Regul Integr Comp Physiol, 294*(3), R829-835. doi:10.1152/ajpregu.00639.2007

Chen, X., Hui, L., Geiger, N. H., Haughey, N. J., & Geiger, J. D. (2013). Endolysosome involvement in HIV-1 transactivator protein-induced neuronal amyloid beta production. *Neurobiol Aging, 34*(10), 2370-2378. doi:10.1016/j.neurobiolaging.2013.04.015

Chino, H., & Mizushima, N. (2020). ER-Phagy: Quality Control and Turnover of Endoplasmic Reticulum. *Trends Cell Biol, 30*(5), 384-398. doi:10.1016/j.tcb.2020.02.001

Christensen, K. A., Myers, J. T., & Swanson, J. A. (2002). pH-dependent regulation of lysosomal calcium in macrophages. *J Cell Sci, 115*(Pt 3), 599-607. Retrieved from https://www.ncbi.nlm.nih.gov/pubmed/11861766

Claude, A. (1946a). Fractionation of Mammalian Liver Cells by Differential Centrifugation : I. Problems, Methods, and Preparation of Extract. *J Exp Med, 84*(1), 51-59. Retrieved from https://www.ncbi.nlm.nih.gov/pubmed/19871553

Claude, A. (1946b). Fractionation of Mammalian Liver Cells by Differential Centrifugation : Ii. Experimental Procedures and Results. *J Exp Med, 84*(1), 61-89. Retrieved from https://www.ncbi.nlm.nih.gov/pubmed/19871554

Clifford, D. B., & Ances, B. M. (2013). HIV-Associated Neurocognitive Disorder (HAND). *Lancet Infect Dis, 13*(11), 976-986. doi:10.1016/s1473-3099(13)70269-x

Colacurcio, D. J., & Nixon, R. A. (2016). Disorders of lysosomal acidification-The emerging role of v-ATPase in aging and neurodegenerative disease. *Ageing Res Rev, 32*, 75-88. doi:10.1016/j.arr.2016.05.004

Connor, R. I., Sheridan, K. E., Ceradini, D., Choe, S., & Landau, N. R. (1997). Change in coreceptor use correlates with disease progression in HIV-1--infected individuals. *J Exp Med, 185*(4), 621-628. doi:10.1084/jem.185.4.621

Cramb, G. (1986). Selective lysosomal uptake and accumulation of the beta-adrenergic antagonist propranolol in cultured and isolated cell systems. *Biochem Pharmacol, 35*(8), 1365-1372. doi:10.1016/0006-2952(86)90283-2

Crichton, R. R., Wilmet, S., Legssyer, R., & Ward, R. J. (2002). Molecular and cellular mechanisms of iron homeostasis and toxicity in mammalian cells. *J Inorg Biochem, 91*(1), 9-18. doi:10.1016/s0162-0134(02)00461-0

Crowley, L. C., Scott, A. P., Marfell, B. J., Boughaba, J. A., Chojnowski, G., & Waterhouse, N. J. (2016). Measuring Cell Death by Propidium Iodide Uptake and Flow Cytometry. *Cold Spring Harb Protoc, 2016*(7). doi:10.1101/pdb.prot087163

Cubells, J. F., Rayport, S., Rajendran, G., & Sulzer, D. (1994). Methamphetamine neurotoxicity involves vacuolation of endocytic organelles and dopamine-dependent intracellular oxidative stress. *J Neurosci, 14*(4), 2260-2271. Retrieved from https://www.ncbi.nlm.nih.gov/pubmed/8158268

Daneman, R., & Prat, A. (2015). The blood-brain barrier. *Cold Spring Harb Perspect Biol, 7*(1), a020412. doi:10.1101/cshperspect.a020412

Danzer, K. M., Kranich, L. R., Ruf, W. P., Cagsal-Getkin, O., Winslow, A. R., Zhu, L., McLean, P. J. (2012). Exosomal cell-to-cell transmission of alpha synuclein oligomers. *Mol Neurodegener, 7*, 42. doi:10.1186/1750-1326-7-42

Das, A., Nag, S., Mason, A. B., & Barroso, M. M. (2016). Endosome-mitochondria interactions are modulated by iron release from transferrin. *J Cell Biol, 214*(7), 831-845. doi:10.1083/jcb.201602069

Datta, G., Miller, N. M., Afghah, Z., Geiger, J. D., & Chen, X. (2019). HIV-1 gp120 Promotes Lysosomal Exocytosis in Human Schwann Cells. *Front Cell Neurosci, 13*, 329. doi:10.3389/fncel.2019.00329

Dauer, P., Gupta, V. K., McGinn, O., Nomura, A., Sharma, N. S., Arora, N., Banerjee, S. (2017). Inhibition of Sp1 prevents ER homeostasis and causes cell death by lysosomal membrane permeabilization in pancreatic cancer. *Sci Rep, 7*(1), 1564. doi:10.1038/s41598-017-01696-2

Davidson, S. M., & Vander Heiden, M. G. (2017). Critical Functions of the Lysosome in Cancer Biology. *Annu Rev Pharmacol Toxicol, 57*, 481-507. doi:10.1146/annurev-pharmtox-010715-103101

Davies, J. P., & Ioannou, Y. A. (2000). Topological analysis of Niemann-Pick C1 protein reveals that the membrane orientation of the putative sterol-sensing domain is identical to those of 3-hydroxy-3-methylglutaryl-CoA reductase and sterol regulatory element binding protein cleavage-activating protein. *J Biol Chem, 275*(32), 24367-24374. doi:10.1074/jbc.M002184200

Dawson, V. L., Dawson, T. M., Uhl, G. R., & Snyder, S. H. (1993). Human immunodeficiency virus type 1 coat protein neurotoxicity mediated by nitric oxide in primary cortical cultures. *Proc Natl Acad Sci U S A, 90*(8), 3256-3259. doi:10.1073/pnas.90.8.3256

de Duve, C. (2005). The lysosome turns fifty. *Nat Cell Biol, 7*(9), 847-849. doi:10.1038/ncb0905-847

Debebe, Z., Ammosova, T., Jerebtsova, M., Kurantsin-Mills, J., Niu, X., Charles, S., Nekhai, S. (2007). Iron chelators ICL670 and 311 inhibit HIV-1 transcription. *Virology, 367*(2), 324-333. doi:10.1016/j.virol.2007.06.011

Deeks, S. G., Overbaugh, J., Phillips, A., & Buchbinder, S. (2015). HIV infection. *Nat Rev Dis Primers, 1*, 15035. doi:10.1038/nrdp.2015.35

del Toro, D., Alberch, J., Lazaro-Dieguez, F., Martin-Ibanez, R., Xifro, X., Egea, G., & Canals, J. M. (2009). Mutant huntingtin impairs post-Golgi trafficking to lysosomes by delocalizing optineurin/Rab8 complex from the Golgi apparatus. *Mol Biol Cell, 20*(5), 1478-1492. doi:10.1091/mbc.E08-07-0726

Demers-Lamarche, J., Guillebaud, G., Tlili, M., Todkar, K., Belanger, N., Grondin, M., Germain, M. (2016). Loss of Mitochondrial Function Impairs Lysosomes. *J Biol Chem, 291*(19), 10263-10276. doi:10.1074/jbc.M115.695825

Deus, C. M., Yambire, K. F., Oliveira, P. J., & Raimundo, N. (2020). Mitochondria-Lysosome Crosstalk: From Physiology to Neurodegeneration. *Trends Mol Med, 26*(1), 71-88. doi:10.1016/j.molmed.2019.10.009

Di Meo, S., Reed, T. T., Venditti, P., & Victor, V. M. (2016). Role of ROS and RNS Sources in Physiological and Pathological Conditions. *Oxid Med Cell Longev, 2016*, 1245049. doi:10.1155/2016/1245049

Diebold, L., & Chandel, N. S. (2016). Mitochondrial ROS regulation of proliferating cells. *Free Radic Biol Med, 100*, 86-93. doi:10.1016/j.freeradbiomed.2016.04.198

Dikalov, S. I., & Harrison, D. G. (2014). Methods for detection of mitochondrial and cellular reactive oxygen species. *Antioxid Redox Signal, 20*(2), 372-382. doi:10.1089/ars.2012.4886

Dixon, S. J., Lemberg, K. M., Lamprecht, M. R., Skouta, R., Zaitsev, E. M., Gleason, C. E., Stockwell, B. R. (2012). Ferroptosis: an iron-dependent form of nonapoptotic cell death. *Cell, 149*(5), 1060-1072. doi:10.1016/j.cell.2012.03.042

Doherty, J., & Baehrecke, E. H. (2018). Life, death and autophagy. *Nat Cell Biol, 20*(10), 1110-1117. doi:10.1038/s41556-018-0201-5

Dong, G., Liu, Y., Zhang, L., Huang, S., Ding, H. F., & Dong, Z. (2015). mTOR contributes to ER stress and associated apoptosis in renal tubular cells. *Am J Physiol Renal Physiol, 308*(3), F267-274. doi:10.1152/ajprenal.00629.2014

Dong, X. P., Cheng, X., Mills, E., Delling, M., Wang, F., Kurz, T., & Xu, H. (2008). The type IV mucolipidosis-associated protein TRPML1 is an endolysosomal iron release channel. *Nature, 455*(7215), 992-996. doi:10.1038/nature07311

Dong, X. P., Shen, D., Wang, X., Dawson, T., Li, X., Zhang, Q., Xu, H. (2010). PI(3,5)P(2) controls membrane trafficking by direct activation of mucolipin Ca(2+) release channels in the endolysosome. *Nat Commun, 1*, 38. doi:10.1038/ncomms1037

Donovan, A., Lima, C. A., Pinkus, J. L., Pinkus, G. S., Zon, L. I., Robine, S., & Andrews, N. C. (2005). The iron exporter ferroportin/Slc40a1 is essential for iron homeostasis. *Cell Metab, 1*(3), 191-200. doi:10.1016/j.cmet.2005.01.003

Dore, G. J., Correll, P. K., Li, Y., Kaldor, J. M., Cooper, D. A., & Brew, B. J. (1999). Changes to AIDS dementia complex in the era of highly active antiretroviral therapy. *AIDS, 13*(10), 1249-1253. doi:10.1097/00002030-199907090-00015

Dore, G. J., McDonald, A., Li, Y., Kaldor, J. M., Brew, B. J., & National, H. I. V. S. C. (2003). Marked improvement in survival following AIDS dementia complex in the era of highly active antiretroviral therapy. *AIDS, 17*(10), 1539-1545. doi:10.1097/00002030-200307040-00015

Dringen, R., Bishop, G. M., Koeppe, M., Dang, T. N., & Robinson, S. R. (2007). The pivotal role of astrocytes in the metabolism of iron in the brain. *Neurochem Res, 32*(11), 1884-1890. doi:10.1007/s11064-007-9375-0

Dunn, L. L., Suryo Rahmanto, Y., & Richardson, D. R. (2007). Iron uptake and metabolism in the new millennium. *Trends Cell Biol, 17*(2), 93-100. doi:10.1016/j.tcb.2006.12.003

Eaton, J. W., & Qian, M. (2002). Molecular bases of cellular iron toxicity. *Free Radic Biol Med, 32*(9), 833-840. Retrieved from https://www.ncbi.nlm.nih.gov/pubmed/11978485

El-Amine, R., Germini, D., Zakharova, V. V., Tsfasman, T., Sheval, E. V., Louzada, R. A. N., Vassetzky, Y. S. (2018). HIV-1 Tat protein induces DNA damage in human peripheral blood B-lymphocytes via mitochondrial ROS production. *Redox Biol, 15*, 97-108. doi:10.1016/j.redox.2017.11.024

El-Hage, N., Podhaizer, E. M., Sturgill, J., & Hauser, K. F. (2011). Toll-like receptor expression and activation in astroglia: differential regulation by HIV-1 Tat, gp120, and morphine. *Immunol Invest, 40*(5), 498-522. doi:10.3109/08820139.2011.561904

El-Hage, N., Rodriguez, M., Dever, S. M., Masvekar, R. R., Gewirtz, D. A., & Shacka, J. J. (2015). HIV-1 and morphine regulation of autophagy in microglia: limited interactions in the context of HIV-1 infection and opioid abuse. *J Virol, 89*(2), 1024-1035. doi:10.1128/JVI.02022-14

Elfrink, H. L., Zwart, R., Baas, F., & Scheper, W. (2013). Inhibition of endoplasmic reticulum associated degradation reduces endoplasmic reticulum stress and alters lysosomal morphology and distribution. *Mol Cells, 35*(4), 291-297. doi:10.1007/s10059-013-2286-9

Ellis, R. J., Deutsch, R., Heaton, R. K., Marcotte, T. D., McCutchan, J. A., Nelson, J. A., Grant, I. (1997). Neurocognitive impairment is an independent risk factor for death in HIV infection. San Diego HIV Neurobehavioral Research Center Group. *Arch Neurol, 54*(4), 416-424. doi:10.1001/archneur.1997.00550160054016

Endo, T., Yamano, K., & Kawano, S. (2011). Structural insight into the mitochondrial protein import system. *Biochim Biophys Acta, 1808*(3), 955-970. doi:10.1016/j.bbamem.2010.07.018

Erie, C., Sacino, M., Houle, L., Lu, M. L., & Wei, J. (2015). Altered lysosomal positioning affects lysosomal functions in a cellular model of Huntington's disease. *Eur J Neurosci, 42*(3), 1941-1951. doi:10.1111/ejn.12957

Ernster, L., & Schatz, G. (1981). Mitochondria: a historical review. *J Cell Biol, 91*(3 Pt 2), 227s-255s. doi:10.1083/jcb.91.3.227s

Everall, I. P., Heaton, R. K., Marcotte, T. D., Ellis, R. J., McCutchan, J. A., Atkinson, J. H., Masliah, E. (1999). Cortical synaptic density is reduced in mild to moderate human immunodeficiency virus neurocognitive disorder. HNRC Group. HIV Neurobehavioral Research Center. *Brain Pathol, 9*(2), 209-217. Retrieved from https://onlinelibrary.wiley.com/doi/abs/10.1111/j.1750-3639.1999.tb00219.x?sid=nlm%3Apubmed

Fais, S., O'Driscoll, L., Borras, F. E., Buzas, E., Camussi, G., Cappello, F., Giebel, B. (2016). Evidence-Based Clinical Use of Nanoscale Extracellular Vesicles in Nanomedicine. *ACS Nano, 10*(4), 3886-3899. doi:10.1021/acsnano.5b08015

Fan, Y., & He, J. J. (2016). HIV-1 Tat Induces Unfolded Protein Response and Endoplasmic Reticulum Stress in Astrocytes and Causes Neurotoxicity through Glial Fibrillary Acidic Protein (GFAP) Activation and Aggregation. *J Biol Chem, 291*(43), 22819-22829. doi:10.1074/jbc.M116.731828

Feng, X., & Yang, J. (2016). Lysosomal Calcium in Neurodegeneration. *Messenger (Los Angel), 5*(1-2), 56-66. doi:10.1166/msr.2016.1055

Fernández, B., Fdez, E., Gómez-Suaga, P., Gil, F., Molina-Villalba, I., Ferrer, I., . . . Hilfiker, S. (2016). Iron overload causes endolysosomal deficits modulated by NAADP-regulated 2-pore channels and RAB7A. In *Autophagy* (Vol. 12, pp. 1487-1506).

Festa, L., Gutoskey, C. J., Graziano, A., Waterhouse, B. D., & Meucci, O. (2015). Induction of Interleukin-1beta by Human Immunodeficiency Virus-1 Viral Proteins Leads to Increased Levels of Neuronal Ferritin Heavy Chain, Synaptic Injury, and Deficits in Flexible Attention. *J Neurosci, 35*(29), 10550-10561. doi:10.1523/JNEUROSCI.4403-14.2015

Festa, L., Roth, L. M., B, K. J., Geiger, J. D., Jordan-Sciutto, K. L., & Grinspan, J. B. (2019). Protease Inhibitors, Saquinavir and Darunavir, Inhibit Oligodendrocyte Maturation: Implications for Lysosomal Stress. *J Neuroimmune Pharmacol*. doi:10.1007/s11481-019-09893-8

Fiandra, L., Capetti, A., Sorrentino, L., & Corsi, F. (2017). Nanoformulated Antiretrovirals for Penetration of the Central Nervous System: State of the Art. *J Neuroimmune Pharmacol, 12*(1), 17-30. doi:10.1007/s11481-016-9716-3

Fields, J., Dumaop, W., Rockenstein, E., Mante, M., Spencer, B., Grant, I., Masliah, E. (2013). Age-dependent molecular alterations in the autophagy pathway in HIVE patients and in a gp120 tg mouse model: reversal with beclin-1 gene transfer. *J Neurovirol, 19*(1), 89-101. doi:10.1007/s13365-012-0145-7

Fields, J. A., Serger, E., Campos, S., Divakaruni, A. S., Kim, C., Smith, K., Masliah, E. (2016). HIV alters neuronal mitochondrial fission/fusion in the brain during HIV-associated neurocognitive disorders. *Neurobiol Dis, 86*, 154-169. doi:10.1016/j.nbd.2015.11.015

Fitting, S., Ignatowska-Jankowska, B. M., Bull, C., Skoff, R. P., Lichtman, A. H., Wise, L. E., Hauser, K. F. (2013). Synaptic dysfunction in the hippocampus accompanies learning and memory deficits in human immunodeficiency virus type-1 Tat transgenic mice. *Biol Psychiatry, 73*(5), 443-453. doi:10.1016/j.biopsych.2012.09.026

Foga, I. O., Nath, A., Hasinoff, B. B., & Geiger, J. D. (1997). Antioxidants and dipyridamole inhibit HIV-1 gp120-induced free radical-based oxidative damage to human monocytoid cells. *J Acquir Immune Defic Syndr Hum Retrovirol, 16*(4), 223-229. Retrieved from http://dx.doi.org/

Folts, C. J., Scott-Hewitt, N., Proschel, C., Mayer-Proschel, M., & Noble, M. (2016). Lysosomal Re-acidification Prevents Lysosphingolipid-Induced Lysosomal Impairment and Cellular Toxicity. *PLoS Biol, 14*(12), e1002583. doi:10.1371/journal.pbio.1002583

Fossale, E., Wolf, P., Espinola, J. A., Lubicz-Nawrocka, T., Teed, A. M., Gao, H., . . . Cotman, S. L. (2004). Membrane trafficking and mitochondrial abnormalities precede subunit c deposition in a cerebellar cell model of juvenile neuronal ceroid lipofuscinosis. *BMC Neurosci, 5*, 57. doi:10.1186/1471-2202-5-57

Friedland, N., Liou, H. L., Lobel, P., & Stock, A. M. (2003). Structure of a cholesterol-binding protein deficient in Niemann-Pick type C2 disease. *Proc Natl Acad Sci U S A, 100*(5), 2512-2517. doi:10.1073/pnas.0437840100

Fukuda, T., Ahearn, M., Roberts, A., Mattaliano, R. J., Zaal, K., Ralston, E., Raben, N. (2006). Autophagy and mistargeting of therapeutic enzyme in skeletal muscle in Pompe disease. *Mol Ther, 14*(6), 831-839. doi:10.1016/j.ymthe.2006.08.009

Funakoshi-Hirose, I., Aki, T., Unuma, K., Funakoshi, T., Noritake, K., & Uemura, K. (2013). Distinct effects of methamphetamine on autophagy-lysosome and ubiquitin-proteasome systems in HL-1 cultured mouse atrial cardiomyocytes. *Toxicology, 312*, 74-82. doi:10.1016/j.tox.2013.07.016

Gallo, R. C., Salahuddin, S. Z., Popovic, M., Shearer, G. M., Kaplan, M., Haynes, B. F., et al. (1984). Frequent detection and isolation of cytopathic retroviruses (HTLV-III) from patients with AIDS and at risk for AIDS. *Science, 224*(4648), 500-503. doi:10.1126/science.6200936

Galluzzi, L., Baehrecke, E. H., Ballabio, A., Boya, P., Bravo-San Pedro, J. M., Cecconi, F., Kroemer, G. (2017). Molecular definitions of autophagy and related processes. *EMBO J, 36*(13), 1811-1836. doi:10.15252/embj.201796697

Gelman, B. B., Soukup, V. M., Holzer, C. E., 3rd, Fabian, R. H., Schuenke, K. W., Keherly, M. J., Lahart, C. J. (2005). Potential role for white matter lysosome expansion in HIV-associated dementia. *J Acquir Immune Defic Syndr, 39*(4), 422-425. Retrieved from https://www.ncbi.nlm.nih.gov/pubmed/16010164

German Advisory Committee Blood, S. A. o. P. T. b. B. (2016). Human Immunodeficiency Virus (HIV). *Transfus Med Hemother, 43*(3), 203-222. doi:10.1159/000445852

Gottlieb, M. S., Schroff, R., Schanker, H. M., Weisman, J. D., Fan, P. T., Wolf, R. A., & Saxon, A. (1981). Pneumocystis carinii pneumonia and mucosal candidiasis in previously healthy homosexual men: evidence of a new acquired cellular immunodeficiency. *N Engl J Med, 305*(24), 1425-1431. doi:10.1056/NEJM198112103052401

Gottschling, D. E., & Nystrom, T. (2017). The Upsides and Downsides of Organelle Interconnectivity. *Cell, 169*(1), 24-34. doi:10.1016/j.cell.2017.02.030

Gowrishankar, S., Yuan, P., Wu, Y., Schrag, M., Paradise, S., Grutzendler, J., Ferguson, S. M. (2015). Massive accumulation of luminal protease-deficient axonal lysosomes at Alzheimer's disease amyloid plaques. *Proc Natl Acad Sci U S A, 112*(28), E3699-3708. doi:10.1073/pnas.1510329112

Gray, L. R., Roche, M., Flynn, J. K., Wesselingh, S. L., Gorry, P. R., & Churchill, M. J. (2014). Is the central nervous system a reservoir of HIV-1? *Curr Opin HIV AIDS, 9*(6), 552-558. doi:10.1097/COH.0000000000000108

Gruenheid, S., Canonne-Hergaux, F., Gauthier, S., Hackam, D. J., Grinstein, S., & Gros, P. (1999). The iron transport protein NRAMP2 is an integral membrane glycoprotein that colocalizes with transferrin in recycling endosomes. *J Exp Med, 189*(5), 831-841. doi:10.1084/jem.189.5.831

Guerra, F., Girolimetti, G., Beli, R., Mitruccio, M., Pacelli, C., Ferretta, A., Bucci, C. (2019). Synergistic Effect of Mitochondrial and Lysosomal Dysfunction in Parkinson's Disease. *Cells, 8*(5). doi:10.3390/cells8050452

Guix, F. X. (2020). The interplay between aging-associated loss of protein homeostasis and extracellular vesicles in neurodegeneration. *J Neurosci Res, 98*(2), 262-283. doi:10.1002/jnr.24526

Gulec, S., Anderson, G. J., & Collins, J. F. (2014). Mechanistic and regulatory aspects of intestinal iron absorption. *Am J Physiol Gastrointest Liver Physiol, 307*(4), G397-409. doi:10.1152/ajpgi.00348.2013

Halcrow, P., Khan, N., Datta, G., Ohm, J. E., Chen, X., & Geiger, J. D. (2019). Importance of measuring endolysosome, cytosolic, and extracellular pH in understanding the pathogenesis of and possible treatments for glioblastoma multiforme. *Cancer Rep, 2*(6). doi:10.1002/cnr2.1193

Hamaguchi, R., Haginaka, J., Tanimoto, T., & Kuroda, Y. (2014). Maintenance of luminal pH and protease activity in lysosomes/late endosomes by vacuolar ATPase in chlorpromazine-treated RAW264 cells accumulating phospholipids. *Cell Biol Toxicol, 30*(1), 67-77. doi:10.1007/s10565-014-9269-2

Hamdi, A., Roshan, T. M., Kahawita, T. M., Mason, A. B., Sheftel, A. D., & Ponka, P. (2016). Erythroid cell mitochondria receive endosomal iron by a "kiss-and-run" mechanism. *Biochim Biophys Acta, 1863*(12), 2859-2867. doi:10.1016/j.bbamcr.2016.09.008

Harding, H. P., Novoa, I., Zhang, Y., Zeng, H., Wek, R., Schapira, M., & Ron, D. (2000). Regulated translation initiation controls stress-induced gene expression in mammalian cells. *Mol Cell, 6*(5), 1099-1108. doi:10.1016/s1097-2765(00)00108-8

Harding, H. P., Zhang, Y., Bertolotti, A., Zeng, H., & Ron, D. (2000). Perk is essential for translational regulation and cell survival during the unfolded protein response. *Mol Cell, 5*(5), 897-904. doi:10.1016/s1097-2765(00)80330-5

Harding, H. P., Zhang, Y., & Ron, D. (1999). Protein translation and folding are coupled by an endoplasmic-reticulum-resident kinase. *Nature, 397*(6716), 271-274. doi:10.1038/16729

Harding, H. P., Zhang, Y., Zeng, H., Novoa, I., Lu, P. D., Calfon, M., Ron, D. (2003). An integrated stress response regulates amino acid metabolism and resistance to oxidative stress. *Mol Cell, 11*(3), 619-633. doi:10.1016/s1097-2765(03)00105-9

Haughey, N. J., Holden, C. P., Nath, A., & Geiger, J. D. (1999). Involvement of inositol 1,4,5-trisphosphate-regulated stores of intracellular calcium in calcium dysregulation and neuron cell death caused by HIV-1 protein tat. *J Neurochem, 73*(4), 1363-1374. doi:10.1046/j.1471-4159.1999.0731363.x

Haughey, N. J., Nath, A., Mattson, M. P., Slevin, J. T., & Geiger, J. D. (2001). HIV-1 Tat through phosphorylation of NMDA receptors potentiates glutamate excitotoxicity. *J Neurochem, 78*(3), 457-467. Retrieved from https://www.ncbi.nlm.nih.gov/pubmed/11483648

He, B., Shi, Y., Liang, Y., Yang, A., Fan, Z., Yuan, L., Zhang, Q. (2018). Single-walled carbon-nanohorns improve biocompatibility over nanotubes by triggering less protein-initiated pyroptosis and apoptosis in macrophages. *Nat Commun, 9*(1), 2393. doi:10.1038/s41467-018-04700-z

Heaton, R. K., Franklin, D. R., Ellis, R. J., McCutchan, J. A., Letendre, S. L., Leblanc, S., Group, H. (2011). HIV-associated neurocognitive disorders before and during the era of combination antiretroviral therapy: differences in rates, nature, and predictors. *J Neurovirol, 17*(1), 3-16. doi:10.1007/s13365-010-0006-1

Hetz, C. (2012). The unfolded protein response: controlling cell fate decisions under ER stress and beyond. *Nat Rev Mol Cell Biol, 13*(2), 89-102. doi:10.1038/nrm3270

Heuser, J. (1989). Changes in lysosome shape and distribution correlated with changes in cytoplasmic pH. *J Cell Biol, 108*(3), 855-864. doi:10.1083/jcb.108.3.855

High, K. P., Brennan-Ing, M., Clifford, D. B., Cohen, M. H., Currier, J., Deeks, S. G., Aging. (2012). HIV and aging: state of knowledge and areas of critical need for research. A report to the NIH Office of AIDS Research by the HIV and Aging Working Group. *J Acquir Immune Defic Syndr, 60 Suppl 1*, S1-18. doi:10.1097/QAI.0b013e31825a3668

Hill, S., Sataranatarajan, K., & Van Remmen, H. (2018). Role of Signaling Molecules in Mitochondrial Stress Response. *Front Genet, 9*, 225. doi:10.3389/fgene.2018.00225

Hirayama, T. (2018). Development of Chemical Tools for Imaging of Fe(II) Ions in Living Cells: A Review. *Acta Histochem Cytochem, 51*(5), 137-143. doi:10.1267/ahc.18015

Hoepken, H. H., Korten, T., Robinson, S. R., & Dringen, R. (2004). Iron accumulation, iron-mediated toxicity and altered levels of ferritin and transferrin receptor in cultured astrocytes during incubation with ferric ammonium citrate. *J Neurochem, 88*(5), 1194-1202. doi:10.1046/j.1471-4159.2003.02236.x

Hoffmann, A. C., Minakaki, G., Menges, S., Salvi, R., Savitskiy, S., Kazman, A., . . . Xiang, W. (2019). Extracellular aggregated alpha synuclein primarily triggers lysosomal dysfunction in neural cells prevented by trehalose. *Sci Rep, 9*(1), 544. doi:10.1038/s41598-018-35811-8

Hoglinger, D., Haberkant, P., Aguilera-Romero, A., Riezman, H., Porter, F. D., Platt, F. M., Schultz, C. (2015). Intracellular sphingosine releases calcium from lysosomes. *Elife, 4*. doi:10.7554/eLife.10616

Holopainen, J. M., Saarikoski, J., Kinnunen, P. K., & Jarvela, I. (2001). Elevated lysosomal pH in neuronal ceroid lipofuscinoses (NCLs). *Eur J Biochem, 268*(22), 5851-5856. doi:10.1046/j.0014-2956.2001.02530.x

Holtzman, E. (1989). *Lysosomes*. New York: Plenum Press

Hsu, C. L., Lee, E. X., Gordon, K. L., Paz, E. A., Shen, W. C., Ohnishi, K., La Spada, A. R. (2018). MAP4K3 mediates amino acid-dependent regulation of autophagy via phosphorylation of TFEB. *Nat Commun, 9*(1), 942. doi:10.1038/s41467-018-03340-7

Huang, H., Chen, J., Lu, H., Zhou, M., Chai, Z., & Hu, Y. (2017). Iron-induced generation of mitochondrial ROS depends on AMPK activity. *Biometals, 30*(4), 623-628. doi:10.1007/s10534-017-0023-0

Huang, M. L., Chiang, S., Kalinowski, D. S., Bae, D. H., Sahni, S., & Richardson, D. R. (2019). The Role of the Antioxidant Response in Mitochondrial Dysfunction in Degenerative Diseases: Cross-Talk between Antioxidant Defense, Autophagy, and Apoptosis. *Oxid Med Cell Longev, 2019*, 6392763. doi:10.1155/2019/6392763

Hui, L., Chen, X., & Geiger, J. D. (2012). Endolysosome involvement in LDL cholesterol-induced Alzheimer's disease-like pathology in primary cultured neurons. *Life Sci, 91*(23-24), 1159-1168. doi:10.1016/j.lfs.2012.04.039

Hui, L., Chen, X., Haughey, N. J., & Geiger, J. D. (2012). Role of endolysosomes in HIV-1 Tat-induced neurotoxicity. *ASN Neuro, 4*(4), 243-252. doi:10.1042/AN20120017

Hui, L., Geiger, N. H., Bloor-Young, D., Churchill, G. C., Geiger, J. D., & Chen, X. (2015). Release of calcium from endolysosomes increases calcium influx through N-type calcium channels: Evidence for acidic store-operated calcium entry in neurons. *Cell Calcium, 58*(6), 617-627. doi:10.1016/j.ceca.2015.10.001

Hui, L., Ye, Y., Soliman, M. L., Lakpa, K. L., Miller, N. M., Afghah, Z., Chen, X. (2019). Antiretroviral Drugs Promote Amyloidogenesis by De-Acidifying Endolysosomes. *J Neuroimmune Pharmacol*. doi:10.1007/s11481-019-09862-1

Humeau, J., Leduc, M., Cerrato, G., Loos, F., Kepp, O., & Kroemer, G. (2020). Phosphorylation of eukaryotic initiation factor-2alpha (eIF2alpha) in autophagy. *Cell Death Dis, 11*(6), 433. doi:10.1038/s41419-020-2642-6

Huotari, J., & Helenius, A. (2011). Endosome maturation. *EMBO J, 30*(17), 3481-3500. doi:10.1038/emboj.2011.286

Hwang, J. J., Lee, S. J., Kim, T. Y., Cho, J. H., & Koh, J. Y. (2008). Zinc and 4-hydroxy-2-nonenal mediate lysosomal membrane permeabilization induced by H2O2 in cultured hippocampal neurons. *J Neurosci, 28*(12), 3114-3122. doi:10.1523/JNEUROSCI.0199-08.2008

Iwai, K., Drake, S. K., Wehr, N. B., Weissman, A. M., LaVaute, T., Minato, N., Rouault, T. A. (1998). Iron-dependent oxidation, ubiquitination, and degradation of iron regulatory protein 2: implications for degradation of oxidized proteins. *Proc Natl Acad Sci U S A, 95*(9), 4924-4928. doi:10.1073/pnas.95.9.4924

Jaiswal, J. K., Andrews, N. W., & Simon, S. M. (2002). Membrane proximal lysosomes are the major vesicles responsible for calcium-dependent exocytosis in nonsecretory cells. *J Cell Biol, 159*(4), 625-635. doi:10.1083/jcb.200208154

Jang, J. W., Song, Y., Kim, K. M., Kim, J. S., Choi, E. K., Kim, J., & Seo, H. (2016). Hepatocellular carcinoma-targeted drug discovery through image-based phenotypic screening in co-cultures of HCC cells with hepatocytes. *BMC Cancer, 16*(1), 810. doi:10.1186/s12885-016-2816-x

Jia, J., Abudu, Y. P., Claude-Taupin, A., Gu, Y., Kumar, S., Choi, S. W., Deretic, V. (2018). Galectins Control mTOR in Response to Endomembrane Damage. *Mol Cell, 70*(1), 120-135 e128. doi:10.1016/j.molcel.2018.03.009

Jin, L. W., Shie, F. S., Maezawa, I., Vincent, I., & Bird, T. (2004). Intracellular accumulation of amyloidogenic fragments of amyloid-beta precursor protein in neurons with Niemann-Pick type C defects is associated with endosomal abnormalities. *Am J Pathol, 164*(3), 975-985. doi:10.1016/s0002-9440(10)63185-9

Johnson, D. E., Ostrowski, P., Jaumouille, V., & Grinstein, S. (2016). The position of lysosomes within the cell determines their luminal pH. *J Cell Biol, 212*(6), 677-692. doi:10.1083/jcb.201507112

Johnson, T. P., Patel, K., Johnson, K. R., Maric, D., Calabresi, P. A., Hasbun, R., & Nath, A. (2013). Induction of IL-17 and nonclassical T-cell activation by HIV-Tat protein. *Proc Natl Acad Sci U S A, 110*(33), 13588-13593. doi:10.1073/pnas.1308673110

Kallianpur, A. R., Gittleman, H., Letendre, S., Ellis, R., Barnholtz-Sloan, J. S., Bush, W. S., Group, C. S. (2019). Cerebrospinal Fluid Ceruloplasmin, Haptoglobin, and Vascular Endothelial Growth Factor Are Associated with Neurocognitive Impairment in Adults with HIV Infection. *Mol Neurobiol, 56*(5), 3808-3818. doi:10.1007/s12035-018-1329-9

Kanekiyo, T., & Bu, G. (2014). The low-density lipoprotein receptor-related protein 1 and amyloid-beta clearance in Alzheimer's disease. *Front Aging Neurosci, 6*, 93. doi:10.3389/fnagi.2014.00093

Kang, Y., Li, Y., Zhang, T., Chi, Y., & Liu, M. (2019). Effects of transcription factor EB on oxidative stress and apoptosis induced by high glucose in podocytes. *Int J Mol Med, 44*(2), 447-456. doi:10.3892/ijmm.2019.4209

Kausar, S., Wang, F., & Cui, H. (2018). The Role of Mitochondria in Reactive Oxygen Species Generation and Its Implications for Neurodegenerative Diseases. *Cells, 7*(12). doi:10.3390/cells7120274

Kawabata, H., Germain, R. S., Ikezoe, T., Tong, X., Green, E. M., Gombart, A. F., & Koeffler, H. P. (2001). Regulation of expression of murine transferrin receptor 2. *Blood, 98*(6), 1949-1954. doi:10.1182/blood.v98.6.1949

Ke, Y., & Qian, Z. M. (2007). Brain iron metabolism: neurobiology and neurochemistry. *Prog Neurobiol, 83*(3), 149-173. doi:10.1016/j.pneurobio.2007.07.009

Khan, N., Chen, X., & Geiger, J. D. (2020). Role of Divalent Cations in HIV-1 Replication and Pathogenicity. *Viruses, 12*(4). doi:10.3390/v12040471

Khan, N., Datta, G., Geiger, J. D., & Chen, X. (2018). Apolipoprotein E isoform dependently affects Tat-mediated HIV-1 LTR transactivation. *J Neuroinflammation, 15*(1), 91. doi:10.1186/s12974-018-1129-1

Khan, N., Halcrow, P. W., Lakpa, K. L., Afghah, Z., Miller, N. M., Dowdy, S. F., Chen, X. (2020). Two-pore channels regulate Tat endolysosome escape and Tat-mediated HIV-1 LTR transactivation. *FASEB J, 34*(3), 4147-4162. doi:10.1096/fj.201902534R

Khan, N., Haughey, N. J., Nath, A., & Geiger, J. D. (2019). Involvement of organelles and inter-organellar signaling in the pathogenesis of HIV-1 associated neurocognitive disorder and Alzheimer's disease. *Brain Res, 1722*, 146389. doi:10.1016/j.brainres.2019.146389

Khan, N., Lakpa, K. L., Halcrow, P. W., Afghah, Z., Miller, N. M., Geiger, J. D., & Chen, X. (2019). BK channels regulate extracellular Tat-mediated HIV-1 LTR transactivation. *Sci Rep, 9*(1), 12285. doi:10.1038/s41598-019-48777-y

Kim, A., & Cunningham, K. W. (2015). A LAPF/phafin1-like protein regulates TORC1 and lysosomal membrane permeabilization in response to endoplasmic reticulum membrane stress. *Mol Biol Cell, 26*(25), 4631-4645. doi:10.1091/mbc.E15-08-0581

Kim, S. H., Smith, A. J., Tan, J., Shytle, R. D., & Giunta, B. (2015). MSM ameliorates HIV-1 Tat induced neuronal oxidative stress via rebalance of the glutathione cycle. *Am J Transl Res, 7*(2), 328-338. Retrieved from https://www.ncbi.nlm.nih.gov/pubmed/25893035

Kinghorn, K. J., Gronke, S., Castillo-Quan, J. I., Woodling, N. S., Li, L., Sirka, E., Partridge, L. (2016). A Drosophila Model of Neuronopathic Gaucher Disease Demonstrates Lysosomal-Autophagic Defects and Altered mTOR Signalling and Is Functionally Rescued by Rapamycin. *J Neurosci, 36*(46), 11654-11670. doi:10.1523/JNEUROSCI.4527-15.2016

Kiselyov, K., Colletti, G. A., Terwilliger, A., Ketchum, K., Lyons, C. W., Quinn, J., & Muallem, S. (2011). TRPML: transporters of metals in lysosomes essential for cell survival? *Cell Calcium, 50*(3), 288-294. doi:10.1016/j.ceca.2011.04.009

Koerver, L., Papadopoulos, C., Liu, B., Kravic, B., Rota, G., Brecht, L., Meyer, H. (2019). The ubiquitin-conjugating enzyme UBE2QL1 coordinates lysophagy in response to endolysosomal damage. *EMBO Rep, 20*(10), e48014. doi:10.15252/embr.201948014

Kohen, R., & Nyska, A. (2002). Oxidation of biological systems: oxidative stress phenomena, antioxidants, redox reactions, and methods for their quantification. *Toxicol Pathol, 30*(6), 620-650. doi:10.1080/01926230290166724

Kohno, K., Normington, K., Sambrook, J., Gething, M. J., & Mori, K. (1993). The promoter region of the yeast KAR2 (BiP) gene contains a regulatory domain that responds to the presence of unfolded proteins in the endoplasmic reticulum. *Mol Cell Biol, 13*(2), 877-890. doi:10.1128/mcb.13.2.877

Koike, M., Shibata, M., Waguri, S., Yoshimura, K., Tanida, I., Kominami, E., Uchiyama, Y. (2005). Participation of autophagy in storage of lysosomes in neurons from mouse models of neuronal ceroid-lipofuscinoses (Batten disease). *Am J Pathol, 167*(6), 1713-1728. doi:10.1016/S0002-9440(10)61253-9

Konijn, A. M., Glickstein, H., Vaisman, B., Meyron-Holtz, E. G., Slotki, I. N., & Cabantchik, Z. I. (1999). The cellular labile iron pool and intracellular ferritin in K562 cells. *Blood, 94*(6), 2128-2134. Retrieved from https://www.ncbi.nlm.nih.gov/pubmed/10477743

Kornfeld, S., & Mellman, I. (1989). The biogenesis of lysosomes. *Annu Rev Cell Biol, 5*, 483-525. doi:10.1146/annurev.cb.05.110189.002411

Korolchuk, V. I., Saiki, S., Lichtenberg, M., Siddiqi, F. H., Roberts, E. A., Imarisio, S., Rubinsztein, D. C. (2011). Lysosomal positioning coordinates cellular nutrient responses. *Nat Cell Biol, 13*(4), 453-460. doi:10.1038/ncb2204

Kovalevich, J., & Langford, D. (2012). Neuronal toxicity in HIV CNS disease. *Future Virol, 7*(7), 687-698. doi:10.2217/fvl.12.57

Kozako, T., Soeda, S., Yoshimitsu, M., Arima, N., Kuroki, A., Hirata, S., Soeda, S. (2016). Angiotensin II type 1 receptor blocker telmisartan induces apoptosis and autophagy in adult T-cell leukemia cells. *FEBS Open Bio, 6*(5), 442-460. doi:10.1002/2211-5463.12055

Kozutsumi, Y., Segal, M., Normington, K., Gething, M. J., & Sambrook, J. (1988). The presence of malfolded proteins in the endoplasmic reticulum signals the induction of glucose-regulated proteins. *Nature, 332*(6163), 462-464. doi:10.1038/332462a0

Kroemer, G., Marino, G., & Levine, B. (2010). Autophagy and the integrated stress response. *Mol Cell, 40*(2), 280-293. doi:10.1016/j.molcel.2010.09.023

Kubli, D. A., & Gustafsson, A. B. (2012). Mitochondria and mitophagy: the yin and yang of cell death control. *Circ Res, 111*(9), 1208-1221. doi:10.1161/CIRCRESAHA.112.265819

Kuijpers, M., Azarnia Tehran, D., Haucke, V., & Soykan, T. (2020). The axonal endo-lysosomal and autophagic systems. *J Neurochem*. doi:10.1111/jnc.15287

Kumari, N., Ammosova, T., Diaz, S., Lin, X., Niu, X., Ivanov, A., Nekhai, S. (2016). Increased iron export by ferroportin induces restriction of HIV-1 infection in sickle cell disease. *Blood Adv, 1*(3), 170-183. doi:10.1182/bloodadvances.2016000745

Kurz, T., Eaton, J. W., & Brunk, U. T. (2011). The role of lysosomes in iron metabolism and recycling. *Int J Biochem Cell Biol, 43*(12), 1686-1697. doi:10.1016/j.biocel.2011.08.016

La Spina, M., Contreras, P. S., Rissone, A., Meena, N. K., Jeong, E., & Martina, J. A. (2020). MiT/TFE Family of Transcription Factors: An Evolutionary Perspective. *Front Cell Dev Biol, 8*, 609683. doi:10.3389/fcell.2020.609683

Lakpa, K. L., Halcrow, P. W., Chen, X., & Geiger, J. D. (2020). Readily Releasable Stores of Calcium in Neuronal Endolysosomes: Physiological and Pathophysiological Relevance. *Adv Exp Med Biol, 1131*, 681-697. doi:10.1007/978-3-030-12457-1_27

Lee, A. H., Iwakoshi, N. N., & Glimcher, L. H. (2003). XBP-1 regulates a subset of endoplasmic reticulum resident chaperone genes in the unfolded protein response. *Mol Cell Biol, 23*(21), 7448-7459. doi:10.1128/mcb.23.21.7448-7459.2003

Lee, C. A., & Blackstone, C. (2020). ER morphology and endo-lysosomal crosstalk: Functions and disease implications. *Biochim Biophys Acta Mol Cell Biol Lipids, 1865*(1), 158544. doi:10.1016/j.bbalip.2019.158544

Lee, J. H., McBrayer, M. K., Wolfe, D. M., Haslett, L. J., Kumar, A., Sato, Y., Nixon, R. A. (2015). Presenilin 1 Maintains Lysosomal Ca(2+) Homeostasis via TRPML1 by Regulating vATPase-Mediated Lysosome Acidification. *Cell Rep, 12*(9), 1430-1444. doi:10.1016/j.celrep.2015.07.050

Lee, S., Sato, Y., & Nixon, R. A. (2011). Lysosomal proteolysis inhibition selectively disrupts axonal transport of degradative organelles and causes an Alzheimer's-like axonal dystrophy. *J Neurosci, 31*(21), 7817-7830. doi:10.1523/JNEUROSCI.6412-10.2011

Lener, T., Gimona, M., Aigner, L., Borger, V., Buzas, E., Camussi, G., Giebel, B. (2015). Applying extracellular vesicles based therapeutics in clinical trials - an ISEV position paper. *J Extracell Vesicles, 4*, 30087. doi:10.3402/jev.v4.30087

Letendre, S., Marquie-Beck, J., Capparelli, E., Best, B., Clifford, D., Collier, A. C., Group, C. (2008). Validation of the CNS Penetration-Effectiveness rank for quantifying antiretroviral penetration into the central nervous system. *Arch Neurol, 65*(1), 65-70. doi:10.1001/archneurol.2007.31

Li, F., Lang, F., Zhang, H., Xu, L., Wang, Y., & Hao, E. (2016). Role of TFEB Mediated Autophagy, Oxidative Stress, Inflammation, and Cell Death in Endotoxin Induced Myocardial Toxicity of Young and Aged Mice. *Oxid Med Cell Longev, 2016*, 5380319. doi:10.1155/2016/5380319

Li, L., Sun, S., Tan, L., Wang, Y., Wang, L., Zhang, Z., & Zhang, L. (2019). Polystyrene Nanoparticles Reduced ROS and Inhibited Ferroptosis by Triggering Lysosome Stress and TFEB Nucleus Translocation in a Size-Dependent Manner. *Nano Lett, 19*(11), 7781-7792. doi:10.1021/acs.nanolett.9b02795

Li, L. B., Chai, R., Zhang, S., Xu, S. F., Zhang, Y. H., Li, H. L., Guo, C. (2019). Iron Exposure and the Cellular Mechanisms Linked to Neuron Degeneration in Adult Mice. *Cells, 8*(2). doi:10.3390/cells8020198

Li, Y., Pan, K., Chen, L., Ning, J. L., Li, X., Yang, T., . . . Tao, G. (2016). Deferoxamine regulates neuroinflammation and iron homeostasis in a mouse model of postoperative cognitive dysfunction. *J Neuroinflammation, 13*(1), 268. doi:10.1186/s12974-016-0740-2

Li, Y., Xu, M., Ding, X., Yan, C., Song, Z., Chen, L., Yang, C. (2016). Protein kinase C controls lysosome biogenesis independently of mTORC1. *Nat Cell Biol, 18*(10), 1065-1077. doi:10.1038/ncb3407

Liang, J. R., Lingeman, E., Luong, T., Ahmed, S., Muhar, M., Nguyen, T., Corn, J. E. (2020). A Genome-wide ER-phagy Screen Highlights Key Roles of Mitochondrial Metabolism and ER-Resident UFMylation. *Cell, 180*(6), 1160-1177 e1120. doi:10.1016/j.cell.2020.02.017

Liang, Q., Ouyang, X., Schneider, L., & Zhang, J. (2011). Reduction of mutant huntingtin accumulation and toxicity by lysosomal cathepsins D and B in neurons. *Mol Neurodegener, 6*, 37. doi:10.1186/1750-1326-6-37

Liao, G., Yao, Y., Liu, J., Yu, Z., Cheung, S., Xie, A., Bi, X. (2007). Cholesterol accumulation is associated with lysosomal dysfunction and autophagic stress in Npc1 -/- mouse brain. *Am J Pathol, 171*(3), 962-975. doi:10.2353/ajpath.2007.070052

Lie, P. P. Y., & Nixon, R. A. (2019). Lysosome trafficking and signaling in health and neurodegenerative diseases. *Neurobiol Dis, 122*, 94-105. doi:10.1016/j.nbd.2018.05.015

Liesse, M., Lhoest, G., Trouet, A., & Tulkens, P. (1976). Uptake and intracellular localization of morphine in lysosomes and cell sap of cultured fibroblasts. *Arch Int Physiol Biochim, 84*(3), 638-639. Retrieved from https://www.ncbi.nlm.nih.gov/pubmed/64204

Lillis, A. P., Muratoglu, S. C., Au, D. T., Migliorini, M., Lee, M. J., Fried, S. K., Strickland, D. K. (2015). LDL Receptor-Related Protein-1 (LRP1) Regulates Cholesterol Accumulation in Macrophages. *PLOS one, 10*(6), e0128903. doi:10.1371/journal.pone.0128903

Lin, J., Shi, S. S., Zhang, J. Q., Zhang, Y. J., Zhang, L., Liu, Y., .Wen, L. P. (2016). Giant Cellular Vacuoles Induced by Rare Earth Oxide Nanoparticles are Abnormally Enlarged Endo/Lysosomes and Promote mTOR-Dependent TFEB Nucleus Translocation. *Small, 12*(41), 5759-5768. doi:10.1002/smll.201601903

Lindl, K. A., Akay, C., Wang, Y., White, M. G., & Jordan-Sciutto, K. L. (2007). Expression of the endoplasmic reticulum stress response marker, BiP, in the central nervous system of HIV-positive individuals. *Neuropathol Appl Neurobiol, 33*(6), 658-669. doi:10.1111/j.1365-2990.2007.00866.x

Liou, G. Y., & Storz, P. (2010). Reactive oxygen species in cancer. *Free Radic Res, 44*(5), 479-496. doi:10.3109/10715761003667554

Lloyd-Evans, E., Morgan, A. J., He, X., Smith, D. A., Elliot-Smith, E., Sillence, D. J., Platt, F. M. (2008). Niemann-Pick disease type C1 is a sphingosine storage disease that causes deregulation of lysosomal calcium. *Nat Med, 14*(11), 1247-1255. doi:10.1038/nm.1876

Lloyd, J. B., Cable, H., & Rice-Evans, C. (1991). Evidence that desferrioxamine cannot enter cells by passive diffusion. *Biochem Pharmacol, 41*(9), 1361-1363. Retrieved from https://www.ncbi.nlm.nih.gov/pubmed/2018567

Lopez, S. N., Rodriguez-Valentin, M., Rivera, M., Rodriguez, M., Babu, M., Cubano, L. A., Boukli, N. M. (2017). HIV-1 Gp120 clade B/C induces a GRP78 driven cytoprotective mechanism in astrocytoma. *Oncotarget, 8*(40), 68415-68438. doi:10.18632/oncotarget.19474

Louboutin, J. P., & Strayer, D. (2014). Role of Oxidative Stress in HIV-1-Associated Neurocognitive Disorder and Protection by Gene Delivery of Antioxidant Enzymes. *Antioxidants (Basel), 3*(4), 770-797. doi:10.3390/antiox3040770

Lu, S., Sung, T., Lin, N., Abraham, R. T., & Jessen, B. A. (2017). Lysosomal adaptation: How cells respond to lysosomotropic compounds. *PLOS one, 12*(3), e0173771. doi:10.1371/journal.pone.0173771

Lutgen, V., Narasipura, S. D., Barbian, H. J., Richards, M., Wallace, J., Razmpour, R., Al-Harthi, L. (2020). HIV infects astrocytes in vivo and egresses from the brain to the periphery. *PLoS Pathog, 16*(6), e1008381. doi:10.1371/journal.ppat.1008381

Luzio, J. P., Hackmann, Y., Dieckmann, N. M., & Griffiths, G. M. (2014). The biogenesis of lysosomes and lysosome-related organelles. *Cold Spring Harb Perspect Biol, 6*(9), a016840. doi:10.1101/cshperspect.a016840

Lv, H., & Shang, P. (2018). The significance, trafficking and determination of labile iron in cytosol, mitochondria and lysosomes. *Metallomics, 10*(7), 899-916. doi:10.1039/c8mt00048d

Ma, X., Wu, Y., Jin, S., Tian, Y., Zhang, X., Zhao, Y., Liang, X. J. (2011). Gold nanoparticles induce autophagosome accumulation through size-dependent nanoparticle uptake and lysosome impairment. *ACS Nano, 5*(11), 8629-8639. doi:10.1021/nn202155y

MacIntyre, A. C., & Cutler, D. J. (1988). The potential role of lysosomes in tissue distribution of weak bases. *Biopharm Drug Dispos, 9*(6), 513-526. doi:10.1002/bod.2510090602

MacKenzie, E. L., Iwasaki, K., & Tsuji, Y. (2008). Intracellular iron transport and storage: from molecular mechanisms to health implications. *Antioxid Redox Signal, 10*(6), 997-1030. doi:10.1089/ars.2007.1893

Maia, J., Caja, S., Strano Moraes, M. C., Couto, N., & Costa-Silva, B. (2018). Exosome-Based Cell-Cell Communication in the Tumor Microenvironment. *Front Cell Dev Biol, 6*, 18. doi:10.3389/fcell.2018.00018

Manoli, I., Alesci, S., Blackman, M. R., Su, Y. A., Rennert, O. M., & Chrousos, G. P. (2007). Mitochondria as key components of the stress response. *Trends Endocrinol Metab, 18*(5), 190-198. doi:10.1016/j.tem.2007.04.004

Manshian, B. B., Pokhrel, S., Madler, L., & Soenen, S. J. (2018). The impact of nanoparticle-driven lysosomal alkalinization on cellular functionality. *J Nanobiotechnology, 16*(1), 85. doi:10.1186/s12951-018-0413-7

Marques, A. R. A., & Saftig, P. (2019). Lysosomal storage disorders - challenges, concepts and avenues for therapy: beyond rare diseases. *J Cell Sci, 132*(2). doi:10.1242/jcs.221739

Martina, J. A., Diab, H. I., Brady, O. A., & Puertollano, R. (2016). TFEB and TFE3 are novel components of the integrated stress response. *EMBO J, 35*(5), 479-495. doi:10.15252/embj.201593428

Martina, J. A., & Puertollano, R. (2018). Protein phosphatase 2A stimulates activation of TFEB and TFE3 transcription factors in response to oxidative stress. *J Biol Chem, 293*(32), 12525-12534. doi:10.1074/jbc.RA118.003471

Martini-Stoica, H., Xu, Y., Ballabio, A., & Zheng, H. (2016). The Autophagy-Lysosomal Pathway in Neurodegeneration: A TFEB Perspective. *Trends Neurosci, 39*(4), 221-234. doi:10.1016/j.tins.2016.02.002

Martinus, R. D., Garth, G. P., Webster, T. L., Cartwright, P., Naylor, D. J., Hoj, P. B., & Hoogenraad, N. J. (1996). Selective induction of mitochondrial chaperones in response to loss of the mitochondrial genome. *Eur J Biochem, 240*(1), 98-103. doi:10.1111/j.1432-1033.1996.0098h.x

Masliah, E., Achim, C. L., Ge, N., DeTeresa, R., Terry, R. D., & Wiley, C. A. (1992). Spectrum of human immunodeficiency virus-associated neocortical damage. *Ann Neurol, 32*(3), 321-329. doi:10.1002/ana.410320304

Masliah, E., Heaton, R. K., Marcotte, T. D., Ellis, R. J., Wiley, C. A., Mallory, M., . . . Grant, I. (1997). Dendritic injury is a pathological substrate for human immunodeficiency virus-related cognitive disorders. HNRC Group. The HIV Neurobehavioral Research Center. *Ann Neurol, 42*(6), 963-972. doi:10.1002/ana.410420618

Masur, H., Michelis, M. A., Greene, J. B., Onorato, I., Stouwe, R. A., Holzman, R. S., Cunningham-Rundles, S. (1981). An outbreak of community-acquired Pneumocystis carinii pneumonia: initial manifestation of cellular immune dysfunction. *N Engl J Med, 305*(24), 1431-1438. doi:10.1056/NEJM198112103052402

Matteoni, R., & Kreis, T. E. (1987). Translocation and clustering of endosomes and lysosomes depends on microtubules. *J Cell Biol, 105*(3), 1253-1265. doi:10.1083/jcb.105.3.1253

Mauthe, M., Orhon, I., Rocchi, C., Zhou, X., Luhr, M., Hijlkema, K. J., Reggiori, F. (2018). Chloroquine inhibits autophagic flux by decreasing autophagosome-lysosome fusion. *Autophagy, 14*(8), 1435-1455. doi:10.1080/15548627.2018.1474314

McArthur, J. C., Steiner, J., Sacktor, N., & Nath, A. (2010). Human immunodeficiency virus-associated neurocognitive disorders: Mind the gap. *Ann Neurol, 67*(6), 699-714. doi:10.1002/ana.22053

Medina, D. L., Di Paola, S., Peluso, I., Armani, A., De Stefani, D., Venditti, R., . . . Ballabio, A. (2015). Lysosomal calcium signalling regulates autophagy through calcineurin and TFEB. *Nat Cell Biol, 17*(3), 288-299. doi:10.1038/ncb3114

Meyron-Holtz, E. G., Ghosh, M. C., Iwai, K., LaVaute, T., Brazzolotto, X., Berger, U. V., Rouault, T. A. (2004). Genetic ablations of iron regulatory proteins 1 and 2 reveal why iron regulatory protein 2 dominates iron homeostasis. *EMBO J, 23*(2), 386-395. doi:10.1038/sj.emboj.7600041

Mills, E., Dong, X. P., Wang, F., & Xu, H. (2010). Mechanisms of brain iron transport: insight into neurodegeneration and CNS disorders. *Future Med Chem, 2*(1), 51-64. Retrieved from https://www.ncbi.nlm.nih.gov/pubmed/20161623

Mindell, J. A. (2012). Lysosomal acidification mechanisms. *Annu Rev Physiol, 74*, 69-86. doi:10.1146/annurev-physiol-012110-142317

Miranda, A. M., Lasiecka, Z. M., Xu, Y., Neufeld, J., Shahriar, S., Simoes, S., Di Paolo, G. (2018). Neuronal lysosomal dysfunction releases exosomes harboring APP C-terminal fragments and unique lipid signatures. *Nat Commun, 9*(1), 291. doi:10.1038/s41467-017-02533-w

Montalbetti, N., Simonin, A., Dalghi, M. G., Kovacs, G., & Hediger, M. A. (2014). Development and Validation of a Fast and Homogeneous Cell-Based Fluorescence Screening Assay for Divalent Metal Transporter 1 (DMT1/SLC11A2) Using the FLIPR Tetra. *J Biomol Screen, 19*(6), 900-908. doi:10.1177/1087057114521663

Mony, V. K., Benjamin, S., & O'Rourke, E. J. (2016). A lysosome-centered view of nutrient homeostasis. *Autophagy, 12*(4), 619-631. doi:10.1080/15548627.2016.1147671

Moos, T., Rosengren Nielsen, T., Skjorringe, T., & Morgan, E. H. (2007). Iron trafficking inside the brain. *J Neurochem, 103*(5), 1730-1740. doi:10.1111/j.1471-4159.2007.04976.x

Mori, K. (2015). The unfolded protein response: the dawn of a new field. *Proc Jpn Acad Ser B Phys Biol Sci, 91*(9), 469-480. doi:10.2183/pjab.91.469

Muckenthaler, M. U., Rivella, S., Hentze, M. W., & Galy, B. (2017). A Red Carpet for Iron Metabolism. *Cell, 168*(3), 344-361. doi:10.1016/j.cell.2016.12.034

Muller, F. L., Liu, Y., & Van Remmen, H. (2004). Complex III releases superoxide to both sides of the inner mitochondrial membrane. *J Biol Chem, 279*(47), 49064-49073. doi:10.1074/jbc.M407715200

Myers, B. M., Prendergast, F. G., Holman, R., Kuntz, S. M., & LaRusso, N. F. (1991). Alterations in the structure, physicochemical properties, and pH of hepatocyte lysosomes in experimental iron overload. *J Clin Invest, 88*(4), 1207-1215. doi:10.1172/JCI115423

Nakashima, A., Cheng, S. B., Kusabiraki, T., Motomura, K., Aoki, A., Ushijima, A., Saito, S. (2019). Endoplasmic reticulum stress disrupts lysosomal homeostasis and induces blockade of autophagic flux in human trophoblasts. *Sci Rep, 9*(1), 11466. doi:10.1038/s41598-019-47607-5

Napolitano, G., & Ballabio, A. (2016). TFEB at a glance. *J Cell Sci, 129*(13), 2475-2481. doi:10.1242/jcs.146365

Nara, A., Aki, T., Funakoshi, T., Unuma, K., & Uemura, K. (2012). Hyperstimulation of macropinocytosis leads to lysosomal dysfunction during exposure to methamphetamine in SH-SY5Y cells. *Brain Res, 1466*, 1-14. doi:10.1016/j.brainres.2012.05.017

Nash, B., Tarn, K., Irollo, E., Luchetta, J., Festa, L., Halcrow, P., Meucci, O. (2019). Morphine-Induced Modulation of Endolysosomal Iron Mediates Upregulation of Ferritin Heavy Chain in Cortical Neurons. *eNeuro, 6*(4). doi:10.1523/ENEURO.0237-19.2019

Nath, A., Haughey, N. J., Jones, M., Anderson, C., Bell, J. E., & Geiger, J. D. (2000). Synergistic neurotoxicity by human immunodeficiency virus proteins Tat and gp120: protection by memantine. *Ann Neurol, 47*(2), 186-194. Retrieved from https://www.ncbi.nlm.nih.gov/pubmed/10665489

Nath, A., Padua, R. A., & Geiger, J. D. (1995). HIV-1 coat protein gp120-induced increases in levels of intrasynaptosomal calcium. *Brain Res, 678*(1-2), 200-206. Retrieved from https://www.ncbi.nlm.nih.gov/pubmed/7620888

Navia, B. A., Cho, E. S., Petito, C. K., & Price, R. W. (1986). The AIDS dementia complex: II. Neuropathology. *Ann Neurol, 19*(6), 525-535. doi:10.1002/ana.410190603

Navia, B. A., Jordan, B. D., & Price, R. W. (1986). The AIDS dementia complex: I. Clinical features. *Ann Neurol, 19*(6), 517-524. doi:10.1002/ana.410190602

Nekhai, S., Kumari, N., & Dhawan, S. (2013). Role of cellular iron and oxygen in the regulation of HIV-1 infection. *Future Virol, 8*(3), 301-311. doi:10.2217/fvl.13.6

Nguyen, M., Wong, Y. C., Ysselstein, D., Severino, A., & Krainc, D. (2019). Synaptic, Mitochondrial, and Lysosomal Dysfunction in Parkinson's Disease. *Trends Neurosci, 42*(2), 140-149. doi:10.1016/j.tins.2018.11.001

Nickel, A., Kohlhaas, M., & Maack, C. (2014). Mitochondrial reactive oxygen species production and elimination. *J Mol Cell Cardiol, 73*, 26-33. doi:10.1016/j.yjmcc.2014.03.011

Nie, G., Sheftel, A. D., Kim, S. F., & Ponka, P. (2005). Overexpression of mitochondrial ferritin causes cytosolic iron depletion and changes cellular iron homeostasis. *Blood, 105*(5), 2161-2167. doi:10.1182/blood-2004-07-2722

Oakes, S. A., & Papa, F. R. (2015). The role of endoplasmic reticulum stress in human pathology. *Annu Rev Pathol, 10*, 173-194. doi:10.1146/annurev-pathol-012513-104649

Oh, N., & Park, J. H. (2014). Endocytosis and exocytosis of nanoparticles in mammalian cells. *Int J Nanomedicine, 9 Suppl 1*, 51-63. doi:10.2147/IJN.S26592

Ohkuma, S., & Poole, B. (1981). Cytoplasmic vacuolation of mouse peritoneal macrophages and the uptake into lysosomes of weakly basic substances. *J Cell Biol, 90*(3), 656-664. doi:10.1083/jcb.90.3.656

Oikawa, N., & Walter, J. (2019). Presenilins and gamma-Secretase in Membrane Proteostasis. *Cells, 8*(3). doi:10.3390/cells8030209

Pagliarini, D. J., & Rutter, J. (2013). Hallmarks of a new era in mitochondrial biochemistry. *Genes Dev, 27*(24), 2615-2627. doi:10.1101/gad.229724.113

Pakos-Zebrucka, K., Koryga, I., Mnich, K., Ljujic, M., Samali, A., & Gorman, A. M. (2016). The integrated stress response. *EMBO Rep, 17*(10), 1374-1395. doi:10.15252/embr.201642195

Palmieri, M., Pal, R., Nelvagal, H. R., Lotfi, P., Stinnett, G. R., Seymour, M. L., Sardiello, M. (2017). mTORC1-independent TFEB activation via Akt inhibition promotes cellular clearance in neurodegenerative storage diseases. *Nat Commun, 8*, 14338. doi:10.1038/ncomms14338

Pan, H. Y., Alamri, A. H., & Valapala, M. (2019). Nutrient deprivation and lysosomal stress induce activation of TFEB in retinal pigment epithelial cells. *Cell Mol Biol Lett, 24*, 33. doi:10.1186/s11658-019-0159-8

Pantaleo, G., & Fauci, A. S. (1996). Immunopathogenesis of HIV infection. *Annu Rev Microbiol, 50*, 825-854. doi:10.1146/annurev.micro.50.1.825

Papadopoulos, C., Kirchner, P., Bug, M., Grum, D., Koerver, L., Schulze, N., Meyer, H. (2017). VCP/p97 cooperates with YOD1, UBXD1 and PLAA to drive clearance of ruptured lysosomes by autophagy. *EMBO J, 36*(2), 135-150. doi:10.15252/embj.201695148

Papadopoulos, C., & Meyer, H. (2017). Detection and Clearance of Damaged Lysosomes by the Endo-Lysosomal Damage Response and Lysophagy. *Curr Biol, 27*(24), R1330-R1341. doi:10.1016/j.cub.2017.11.012

Partaledis, J. A., & Berlin, V. (1993). The FKB2 gene of Saccharomyces cerevisiae, encoding the immunosuppressant-binding protein FKBP-13, is regulated in response to accumulation of unfolded proteins in the endoplasmic reticulum. *Proc Natl Acad Sci U S A, 90*(12), 5450-5454. doi:10.1073/pnas.90.12.5450

Parton, R. G., Dotti, C. G., Bacallao, R., Kurtz, I., Simons, K., & Prydz, K. (1991). pH-induced microtubule-dependent redistribution of late endosomes in neuronal and epithelial cells. *J Cell Biol, 113*(2), 261-274. doi:10.1083/jcb.113.2.261

Patierno, S., Anselmi, L., Jaramillo, I., Scott, D., Garcia, R., & Sternini, C. (2011). Morphine induces mu opioid receptor endocytosis in guinea pig enteric neurons following prolonged receptor activation. *Gastroenterology, 140*(2), 618-626. doi:10.1053/j.gastro.2010.11.005

Patton, S. M., Wang, Q., Hulgan, T., Connor, J. R., Jia, P., Zhao, Z., Kallianpur, A. R. (2017). Cerebrospinal fluid (CSF) biomarkers of iron status are associated with CSF viral load, antiretroviral therapy, and demographic factors in HIV-infected adults. *Fluids Barriers CNS, 14*(1), 11. doi:10.1186/s12987-017-0058-1

Pau, A. K., & George, J. M. (2014). Antiretroviral therapy: current drugs. *Infect Dis Clin North Am, 28*(3), 371-402. doi:10.1016/j.idc.2014.06.001

Perera, R. M., & Zoncu, R. (2016). The Lysosome as a Regulatory Hub. *Annu Rev Cell Dev Biol, 32*, 223-253. doi:10.1146/annurev-cellbio-111315-125125

Perez-Gonzalez, R., Gauthier, S. A., Kumar, A., & Levy, E. (2012). The exosome secretory pathway transports amyloid precursor protein carboxyl-terminal fragments from the cell into the brain extracellular space. *J Biol Chem, 287*(51), 43108-43115. doi:10.1074/jbc.M112.404467

Persellin, R. H. (1969). Lysosome stabilization by leukocyte granule membrane antiserum. *J Immunol, 103*(1), 29-44. Retrieved from https://www.ncbi.nlm.nih.gov/pubmed/5796858

Petrat, F., Rauen, U., & de Groot, H. (1999). Determination of the chelatable iron pool of isolated rat hepatocytes by digital fluorescence microscopy using the fluorescent probe, phen green SK. *Hepatology, 29*(4), 1171-1179. doi:10.1002/hep.510290435

Pietrella, D., Monari, C., Retini, C., Palazzetti, B., Bistoni, F., & Vecchiarelli, A. (1998). Human immunodeficiency virus type 1 envelope protein gp120 impairs intracellular antifungal mechanisms in human monocytes. *J Infect Dis, 177*(2), 347-354. doi:10.1086/514195

Platt, F. M. (2018). Emptying the stores: lysosomal diseases and therapeutic strategies. *Nat Rev Drug Discov, 17*(2), 133-150. doi:10.1038/nrd.2017.214

Plotegher, N., & Duchen, M. R. (2017). Mitochondrial Dysfunction and Neurodegeneration in Lysosomal Storage Disorders. *Trends Mol Med, 23*(2), 116-134. doi:10.1016/j.molmed.2016.12.003

Ponka, P. (1997). Tissue-specific regulation of iron metabolism and heme synthesis: distinct control mechanisms in erythroid cells. *Blood, 89*(1), 1-25. Retrieved from https://www.ncbi.nlm.nih.gov/pubmed/8978272

Ponka, P., & Lok, C. N. (1999). The transferrin receptor: role in health and disease. *Int J Biochem Cell Biol, 31*(10), 1111-1137. doi:10.1016/s1357-2725(99)00070-9

Popovic, M., Tenner-Racz, K., Pelser, C., Stellbrink, H. J., van Lunzen, J., Lewis, G., Racz, P. (2005). Persistence of HIV-1 structural proteins and glycoproteins in lymph nodes of patients under highly active antiretroviral therapy. *Proc Natl Acad Sci U S A, 102*(41), 14807-14812. doi:10.1073/pnas.0506857102

Pourahmad, J., Eskandari, M. R., Kaghazi, A., Shaki, F., Shahraki, J., & Fard, J. K. (2012). A new approach on valproic acid induced hepatotoxicity: involvement of lysosomal membrane leakiness and cellular proteolysis. *Toxicol In Vitro, 26*(4), 545-551. doi:10.1016/j.tiv.2012.01.020

Price, R. W., & Brew, B. J. (1988). The AIDS dementia complex. *J Infect Dis, 158*(5), 1079-1083. doi:10.1093/infdis/158.5.1079

Pu, J., Guardia, C. M., Keren-Kaplan, T., & Bonifacino, J. S. (2016). Mechanisms and functions of lysosome positioning. *J Cell Sci, 129*(23), 4329-4339. doi:10.1242/jcs.196287

Qian, Z. M., To, Y., Tang, P. L., & Feng, Y. M. (1999). Transferrin receptors on the plasma membrane of cultured rat astrocytes. *Exp Brain Res, 129*(3), 473-476. doi:10.1007/s002210050916

Quinlan, C. L., Perevoshchikova, I. V., Hey-Mogensen, M., Orr, A. L., & Brand, M. D. (2013). Sites of reactive oxygen species generation by mitochondria oxidizing different substrates. *Redox Biol, 1*, 304-312. doi:10.1016/j.redox.2013.04.005

Rabanal-Ruiz, Y., & Korolchuk, V. I. (2018). mTORC1 and Nutrient Homeostasis: The Central Role of the Lysosome. *Int J Mol Sci, 19*(3). doi:10.3390/ijms19030818

Raben, N., Roberts, A., & Plotz, P. H. (2007). Role of autophagy in the pathogenesis of Pompe disease. *Acta Myol, 26*(1), 45-48. Retrieved from https://www.ncbi.nlm.nih.gov/pubmed/17915569

Raber, J., Toggas, S. M., Lee, S., Bloom, F. E., Epstein, C. J., & Mucke, L. (1996). Central nervous system expression of HIV-1 Gp120 activates the hypothalamic-pituitary-adrenal axis: evidence for involvement of NMDA receptors and nitric oxide synthase. *Virology, 226*(2), 362-373. doi:10.1006/viro.1996.0664

Ratovitski, T., Chighladze, E., Waldron, E., Hirschhorn, R. R., & Ross, C. A. (2011). Cysteine proteases bleomycin hydrolase and cathepsin Z mediate N-terminal proteolysis and toxicity of mutant huntingtin. *J Biol Chem, 286*(14), 12578-12589. doi:10.1074/jbc.M110.185348

Rauen, U., Springer, A., Weisheit, D., Petrat, F., Korth, H. G., de Groot, H., & Sustmann, R. (2007). Assessment of chelatable mitochondrial iron by using mitochondrion-selective fluorescent iron indicators with different iron-binding affinities. *Chembiochem, 8*(3), 341-352. doi:10.1002/cbic.200600311

Ravikumar, B., Duden, R., & Rubinsztein, D. C. (2002). Aggregate-prone proteins with polyglutamine and polyalanine expansions are degraded by autophagy. *Hum Mol Genet, 11*(9), 1107-1117. doi:10.1093/hmg/11.9.1107

Ravikumar, B., Sarkar, S., Davies, J. E., Futter, M., Garcia-Arencibia, M., Green-Thompson, Z. W., Rubinsztein, D. C. (2010). Regulation of mammalian autophagy in physiology and pathophysiology. *Physiol Rev, 90*(4), 1383-1435. doi:10.1152/physrev.00030.2009

Ravikumar, B., Vacher, C., Berger, Z., Davies, J. E., Luo, S., Oroz, L. G., Rubinsztein, D. C. (2004). Inhibition of mTOR induces autophagy and reduces toxicity of polyglutamine expansions in fly and mouse models of Huntington disease. *Nat Genet, 36*(6), 585-595. doi:10.1038/ng1362

Reddy, P. H., & Oliver, D. M. (2019). Amyloid Beta and Phosphorylated Tau-Induced Defective Autophagy and Mitophagy in Alzheimer's Disease. *Cells, 8*(5). doi:10.3390/cells8050488

Redmann, M., Benavides, G. A., Berryhill, T. F., Wani, W. Y., Ouyang, X., Johnson, M. S., Zhang, J. (2017). Inhibition of autophagy with bafilomycin and chloroquine decreases mitochondrial quality and bioenergetic function in primary neurons. *Redox Biol, 11*, 73-81. doi:10.1016/j.redox.2016.11.004

Rehli, M., Den Elzen, N., Cassady, A. I., Ostrowski, M. C., & Hume, D. A. (1999). Cloning and characterization of the murine genes for bHLH-ZIP transcription factors TFEC and TFEB reveal a common gene organization for all MiT subfamily members. *Genomics, 56*(1), 111-120. doi:10.1006/geno.1998.5588

Reuser, A. J., & Drost, M. R. (2006). Lysosomal dysfunction, cellular pathology and clinical symptoms: basic principles. *Acta Paediatr Suppl, 95*(451), 77-82. doi:10.1080/08035320600618957

Richardson, D., & Baker, E. (1992). Two mechanisms of iron uptake from transferrin by melanoma cells. The effect of desferrioxamine and ferric ammonium citrate. *J Biol Chem, 267*(20), 13972-13979. Retrieved from https://www.ncbi.nlm.nih.gov/pubmed/1629195

Richardson, D. R., Lane, D. J., Becker, E. M., Huang, M. L., Whitnall, M., Suryo Rahmanto, Y., Ponka, P. (2010). Mitochondrial iron trafficking and the integration of iron metabolism between the mitochondrion and cytosol. *Proc Natl Acad Sci U S A, 107*(24), 10775-10782. doi:10.1073/pnas.0912925107

Richardson, D. R., & Ponka, P. (1995). Identification of a mechanism of iron uptake by cells which is stimulated by hydroxyl radicals generated via the iron-catalysed Haber-Weiss reaction. *Biochim Biophys Acta, 1269*(2), 105-114. doi:10.1016/0167-4889(95)00096-b

Roczniak-Ferguson, A., Petit, C. S., Froehlich, F., Qian, S., Ky, J., Angarola, B., Ferguson, S. M. (2012). The transcription factor TFEB links mTORC1 signaling to transcriptional control of lysosome homeostasis. *Sci Signal, 5*(228), ra42. doi:10.1126/scisignal.2002790

Ru, W., & Tang, S. J. (2017). HIV-associated synaptic degeneration. *Mol Brain, 10*(1), 40. doi:10.1186/s13041-017-0321-z

Rubinsztein, D. C. (2006). The roles of intracellular protein-degradation pathways in neurodegeneration. *Nature, 443*(7113), 780-786. doi:10.1038/nature05291

Ruggiano, A., Foresti, O., & Carvalho, P. (2014). Quality control: ER-associated degradation: protein quality control and beyond. *J Cell Biol, 204*(6), 869-879. doi:10.1083/jcb.201312042

Russo, R., Navarra, M., Maiuolo, J., Rotiroti, D., Bagetta, G., & Corasaniti, M. T. (2005). 17beta-estradiol protects SH-SY5Y Cells against HIV-1 gp120-induced cell death: evidence for a role of estrogen receptors. *Neurotoxicology, 26*(5), 905-913. doi:10.1016/j.neuro.2005.01.009

Ryan, M. T., & Hoogenraad, N. J. (2007). Mitochondrial-nuclear communications. *Annu Rev Biochem, 76*, 701-722. doi:10.1146/annurev.biochem.76.052305.091720

Saftig, P., & Klumperman, J. (2009). Lysosome biogenesis and lysosomal membrane proteins: trafficking meets function. *Nat Rev Mol Cell Biol, 10*(9), 623-635. doi:10.1038/nrm2745

Sanchez, A. B., & Kaul, M. (2017). Neuronal Stress and Injury Caused by HIV-1, cART and Drug Abuse: Converging Contributions to HAND. *Brain Sci, 7*(3). doi:10.3390/brainsci7030025

Sardar Sinha, M., Ansell-Schultz, A., Civitelli, L., Hildesjo, C., Larsson, M., Lannfelt, L., Hallbeck, M. (2018). Alzheimer's disease pathology propagation by exosomes containing toxic amyloid-beta oligomers. *Acta Neuropathol, 136*(1), 41-56. doi:10.1007/s00401-018-1868-1

Sardiello, M., Palmieri, M., di Ronza, A., Medina, D. L., Valenza, M., Gennarino, V. A., Ballabio, A. (2009). A gene network regulating lysosomal biogenesis and function. *Science, 325*(5939), 473-477. doi:10.1126/science.1174447

Sasaki, K., & Yoshida, H. (2015). Organelle autoregulation-stress responses in the ER, Golgi, mitochondria and lysosome. *J Biochem, 157*(4), 185-195. doi:10.1093/jb/mvv010

Saylor, D., Dickens, A. M., Sacktor, N., Haughey, N., Slusher, B., Pletnikov, M., McArthur, J. C. (2016). HIV-associated neurocognitive disorder--pathogenesis and prospects for treatment. *Nat Rev Neurol, 12*(4), 234-248. doi:10.1038/nrneurol.2016.27

Schieber, M., & Chandel, N. S. (2014). ROS function in redox signaling and oxidative stress. *Curr Biol, 24*(10), R453-462. doi:10.1016/j.cub.2014.03.034

Scutari, R., Alteri, C., Perno, C. F., Svicher, V., & Aquaro, S. (2017). The Role of HIV Infection in Neurologic Injury. *Brain Sci, 7*(4). doi:10.3390/brainsci7040038

Settembre, C., & Ballabio, A. (2014). Lysosomal adaptation: how the lysosome responds to external cues. *Cold Spring Harb Perspect Biol, 6*(6). doi:10.1101/cshperspect.a016907

Settembre, C., Di Malta, C., Polito, V. A., Garcia Arencibia, M., Vetrini, F., Erdin, S., Ballabio, A. (2011). TFEB links autophagy to lysosomal biogenesis. *Science, 332*(6036), 1429-1433. doi:10.1126/science.1204592

Settembre, C., Fraldi, A., Medina, D. L., & Ballabio, A. (2013). Signals from the lysosome: a control centre for cellular clearance and energy metabolism. *Nat Rev Mol Cell Biol, 14*(5), 283-296. doi:10.1038/nrm3565

Settembre, C., Zoncu, R., Medina, D. L., Vetrini, F., Erdin, S., Erdin, S., Ballabio, A. (2012). A lysosome-to-nucleus signalling mechanism senses and regulates the lysosome via mTOR and TFEB. *EMBO J, 31*(5), 1095-1108. doi:10.1038/emboj.2012.32

Sha, Y., Rao, L., Settembre, C., Ballabio, A., & Eissa, N. T. (2017). STUB1 regulates TFEB-induced autophagy-lysosome pathway. *EMBO J, 36*(17), 2544-2552. doi:10.15252/embj.201796699

Shah, A., Kumar, S., Simon, S. D., Singh, D. P., & Kumar, A. (2013). HIV gp120- and methamphetamine-mediated oxidative stress induces astrocyte apoptosis via cytochrome P450 2E1. *Cell Death Dis, 4*, e850. doi:10.1038/cddis.2013.374

Sharma, B. (2014). Oxidative stress in HIV patients receiving antiretroviral therapy. *Curr HIV Res, 12*(1), 13-21. doi:10.2174/1570162x12666140402100959

Shen, J., Chen, X., Hendershot, L., & Prywes, R. (2002). ER stress regulation of ATF6 localization by dissociation of BiP/GRP78 binding and unmasking of Golgi localization signals. *Dev Cell, 3*(1), 99-111. doi:10.1016/s1534-5807(02)00203-4

Shi, H., Bencze, K. Z., Stemmler, T. L., & Philpott, C. C. (2008). A cytosolic iron chaperone that delivers iron to ferritin. *Science, 320*(5880), 1207-1210. doi:10.1126/science.1157643

Shin, A. H., & Thayer, S. A. (2013). Human immunodeficiency virus-1 protein Tat induces excitotoxic loss of presynaptic terminals in hippocampal cultures. *Mol Cell Neurosci, 54*, 22-29. doi:10.1016/j.mcn.2012.12.005

Siman, R., Mistretta, S., Durkin, J. T., Savage, M. J., Loh, T., Trusko, S., & Scott, R. W. (1993). Processing of the beta-amyloid precursor. Multiple proteases generate and degrade potentially amyloidogenic fragments. *J Biol Chem, 268*(22), 16602-16609. Retrieved from https://www.ncbi.nlm.nih.gov/pubmed/8344942

Snider, W. D., Simpson, D. M., Nielsen, S., Gold, J. W., Metroka, C. E., & Posner, J. B. (1983). Neurological complications of acquired immune deficiency syndrome: analysis of 50 patients. *Ann Neurol, 14*(4), 403-418. doi:10.1002/ana.410140404

Song, W., Wang, F., Savini, M., Ake, A., di Ronza, A., Sardiello, M., & Segatori, L. (2013). TFEB regulates lysosomal proteostasis. *Hum Mol Genet, 22*(10), 1994-2009. doi:10.1093/hmg/ddt052

Soto-Heredero, G., Baixauli, F., & Mittelbrunn, M. (2017). Interorganelle Communication between Mitochondria and the Endolysosomal System. *Front Cell Dev Biol, 5*, 95. doi:10.3389/fcell.2017.00095

Spampanato, C., Feeney, E., Li, L., Cardone, M., Lim, J. A., Annunziata, F., Raben, N. (2013). Transcription factor EB (TFEB) is a new therapeutic target for Pompe disease. *EMBO Mol Med, 5*(5), 691-706. doi:10.1002/emmm.201202176

Staneva-Stoicheva, D., Krustev, L., & Kitova, E. (1977). [Morphological changes in the liver of rats treated with phenobarbital, methylphenobarbital and their N-substituted morpholinoethyl derivatives]. *Eksp Med Morfol, 16*(2), 90-96. Retrieved from https://www.ncbi.nlm.nih.gov/pubmed/891455

Steinberg, B. E., Huynh, K. K., Brodovitch, A., Jabs, S., Stauber, T., Jentsch, T. J., & Grinstein, S. (2010). A cation counterflux supports lysosomal acidification. *J Cell Biol, 189*(7), 1171-1186. doi:10.1083/jcb.200911083

Steingrimsson, E., Copeland, N. G., & Jenkins, N. A. (2004). Melanocytes and the microphthalmia transcription factor network. *Annu Rev Genet, 38*, 365-411. doi:10.1146/annurev.genet.38.072902.092717

Su, L. J., Zhang, J. H., Gomez, H., Murugan, R., Hong, X., Xu, D., Peng, Z. Y. (2019). Reactive Oxygen Species-Induced Lipid Peroxidation in Apoptosis, Autophagy, and Ferroptosis. *Oxid Med Cell Longev, 2019*, 5080843. doi:10.1155/2019/5080843

Su, Q., Zheng, B., Wang, C. Y., Yang, Y. Z., Luo, W. W., Ma, S. M., Liu, Z. X. (2018). Oxidative Stress Induces Neuronal Apoptosis Through Suppressing Transcription Factor EB Phosphorylation at Ser467. *Cell Physiol Biochem, 46*(4), 1536-1554. doi:10.1159/000489198

Sun, A. (2018). Lysosomal storage disease overview. *Ann Transl Med, 6*(24), 476. doi:10.21037/atm.2018.11.39

Talloczy, Z., Martinez, J., Joset, D., Ray, Y., Gacser, A., Toussi, S., Santambrogio, L. (2008). Methamphetamine inhibits antigen processing, presentation, and phagocytosis. *PLoS Pathog, 4*(2), e28. doi:10.1371/journal.ppat.0040028

Tanaka, Y., Guhde, G., Suter, A., Eskelinen, E. L., Hartmann, D., Lullmann-Rauch, R., Saftig, P. (2000). Accumulation of autophagic vacuoles and cardiomyopathy in LAMP-2-deficient mice. *Nature, 406*(6798), 902-906. doi:10.1038/35022595

Tancini, B., Buratta, S., Sagini, K., Costanzi, E., Delo, F., Urbanelli, L., & Emiliani, C. (2019). Insight into the Role of Extracellular Vesicles in Lysosomal Storage Disorders. *Genes (Basel), 10*(7). doi:10.3390/genes10070510

Thaney, V. E., Sanchez, A. B., Fields, J. A., Minassian, A., Young, J. W., Maung, R., & Kaul, M. (2018). Transgenic mice expressing HIV-1 envelope protein gp120 in the brain as an animal model in neuroAIDS research. *J Neurovirol, 24*(2), 156-167. doi:10.1007/s13365-017-0584-2

Toggas, S. M., Masliah, E., & Mucke, L. (1996). Prevention of HIV-1 gp120-induced neuronal damage in the central nervous system of transgenic mice by the NMDA receptor antagonist memantine. *Brain Res, 706*(2), 303-307. Retrieved from https://www.sciencedirect.com/science/article/abs/pii/0006899395011978?via%3Dihub

Toggas, S. M., Masliah, E., Rockenstein, E. M., Rall, G. F., Abraham, C. R., & Mucke, L. (1994). Central nervous system damage produced by expression of the HIV-1 coat protein gp120 in transgenic mice. *Nature, 367*(6459), 188-193. doi:10.1038/367188a0

Torrano, V., Royo, F., Peinado, H., Loizaga-Iriarte, A., Unda, M., Falcon-Perez, J. M., & Carracedo, A. (2016). Vesicle-MaNiA: extracellular vesicles in liquid biopsy and cancer. *Curr Opin Pharmacol, 29*, 47-53. doi:10.1016/j.coph.2016.06.003

Torres, S., Balboa, E., Zanlungo, S., Enrich, C., Garcia-Ruiz, C., & Fernandez-Checa, J. C. (2017). Lysosomal and Mitochondrial Liaisons in Niemann-Pick Disease. *Front Physiol, 8*, 982. doi:10.3389/fphys.2017.00982

Torti, F. M., & Torti, S. V. (2002). Regulation of ferritin genes and protein. *Blood, 99*(10), 3505-3516. doi:10.1182/blood.v99.10.3505

Trajkovic, K., Jeong, H., & Krainc, D. (2017). Mutant Huntingtin Is Secreted via a Late Endosomal/Lysosomal Unconventional Secretory Pathway. *J Neurosci, 37*(37), 9000-9012. doi:10.1523/JNEUROSCI.0118-17.2017

Traore, H. N., & Meyer, D. (2004). The effect of iron overload on in vitro HIV-1 infection. *J Clin Virol, 31 Suppl 1*, S92-98. doi:10.1016/j.jcv.2004.09.011

Trinder, D., Batey, R. G., Morgan, E. H., & Baker, E. (1990). Effect of cellular iron concentration on iron uptake by hepatocytes. *Am J Physiol, 259*(4 Pt 1), G611-617. doi:10.1152/ajpgi.1990.259.4.G611

Trivedi, P. C., Bartlett, J. J., & Pulinilkunnil, T. (2020). Lysosomal Biology and Function: Modern View of Cellular Debris Bin. *Cells, 9*(5). doi:10.3390/cells9051131

Turchan, J., Pocernich, C. B., Gairola, C., Chauhan, A., Schifitto, G., Butterfield, D. A., Nath, A. (2003). Oxidative stress in HIV demented patients and protection ex vivo with novel antioxidants. *Neurology, 60*(2), 307-314. Retrieved from https://www.ncbi.nlm.nih.gov/pubmed/12552050

Turrens, J. F. (2003). Mitochondrial formation of reactive oxygen species. *J Physiol, 552*(Pt 2), 335-344. doi:10.1113/jphysiol.2003.049478

Uchiyama, A., Kim, J. S., Kon, K., Jaeschke, H., Ikejima, K., Watanabe, S., & Lemasters, J. J. (2008). Translocation of iron from lysosomes into mitochondria is a key event during oxidative stress-induced hepatocellular injury. *Hepatology, 48*(5), 1644-1654. doi:10.1002/hep.22498

Valentín-Guillama, G., López, S., Kucheryavykh, Y. V., Chorna, N. E., Pérez, J., Ortiz-Rivera, J., Kucheryavykh, L. Y. (2018). HIV-1 Envelope Protein gp120 Promotes Proliferation and the Activation of Glycolysis in Glioma Cell. In *Cancers (Basel)* (Vol. 10).

Valera-Alberni, M., & Canto, C. (2018). Mitochondrial stress management: a dynamic journey. *Cell Stress, 2*(10), 253-274. doi:10.15698/cst2018.10.158

van Niel, G., D'Angelo, G., & Raposo, G. (2018). Shedding light on the cell biology of extracellular vesicles. *Nat Rev Mol Cell Biol, 19*(4), 213-228. doi:10.1038/nrm.2017.125

Varghese, J., James, J., Vaulont, S., McKie, A., & Jacob, M. (2018). Increased intracellular iron in mouse primary hepatocytes in vitro causes activation of the Akt pathway but decreases its response to insulin. *Biochim Biophys Acta Gen Subj, 1862*(9), 1870-1882. doi:10.1016/j.bbagen.2018.05.022

Vega-Rubin-de-Celis, S., Pena-Llopis, S., Konda, M., & Brugarolas, J. (2017). Multistep regulation of TFEB by MTORC1. *Autophagy, 13*(3), 464-472. doi:10.1080/15548627.2016.1271514

Vesce, S., Bezzi, P., Rossi, D., Meldolesi, J., & Volterra, A. (1997). HIV-1 gp120 glycoprotein affects the astrocyte control of extracellular glutamate by both inhibiting the uptake and stimulating the release of the amino acid. *FEBS Lett, 411*(1), 107-109. Retrieved from https://febs.onlinelibrary.wiley.com/doi/full/10.1016/S0014-5793%2897%2900674-1?sid=nlm%3Apubmed

Vijaykumar, T. S., Nath, A., & Chauhan, A. (2008). Chloroquine mediated molecular tuning of astrocytes for enhanced permissiveness to HIV infection. *Virology, 381*(1), 1-5. doi:10.1016/j.virol.2008.07.039

Viviani, B., Corsini, E., Binaglia, M., Galli, C. L., & Marinovich, M. (2001). Reactive oxygen species generated by glia are responsible for neuron death induced by human immunodeficiency virus-glycoprotein 120 in vitro. *Neuroscience, 107*(1), 51-58. Retrieved from https://www.ncbi.nlm.nih.gov/pubmed/11744246

Wallace, D. F. (2016). The Regulation of Iron Absorption and Homeostasis. *Clin Biochem Rev, 37*(2), 51-62. Retrieved from https://www.ncbi.nlm.nih.gov/pubmed/28303071

Wallander, M. L., Leibold, E. A., & Eisenstein, R. S. (2006). Molecular control of vertebrate iron homeostasis by iron regulatory proteins. *Biochim Biophys Acta, 1763*(7), 668-689. doi:10.1016/j.bbamcr.2006.05.004

Wallings, R. L., Humble, S. W., Ward, M. E., & Wade-Martins, R. (2019). Lysosomal Dysfunction at the Centre of Parkinson's Disease and Frontotemporal Dementia/Amyotrophic Lateral Sclerosis. *Trends Neurosci, 42*(12), 899-912. doi:10.1016/j.tins.2019.10.002

Wang, F., Gomez-Sintes, R., & Boya, P. (2018). Lysosomal membrane permeabilization and cell death. *Traffic, 19*(12), 918-931. doi:10.1111/tra.12613

Wang, H., Li, Z., Niu, J., Xu, Y., Ma, L., Lu, A., Meng, G. (2018). Antiviral effects of ferric ammonium citrate. *Cell Discov, 4*, 14. doi:10.1038/s41421-018-0013-6

Wang, W., Di, X., D'Agostino, R. B., Jr., Torti, S. V., & Torti, F. M. (2007). Excess capacity of the iron regulatory protein system. *J Biol Chem, 282*(34), 24650-24659. doi:10.1074/jbc.M703167200

Wang, W., Gao, Q., Yang, M., Zhang, X., Yu, L., Lawas, M., Xu, H. (2015). Up-regulation of lysosomal TRPML1 channels is essential for lysosomal adaptation to nutrient starvation. *Proc Natl Acad Sci U S A, 112*(11), E1373-1381. doi:10.1073/pnas.1419669112

Wartosch, L., Bright, N. A., & Luzio, J. P. (2015). Lysosomes. *Curr Biol, 25*(8), R315-316. doi:10.1016/j.cub.2015.02.027

Weisiger, R. A., & Fridovich, I. (1973). Mitochondrial superoxide simutase. Site of synthesis and intramitochondrial localization. *J Biol Chem, 248*(13), 4793-4796. Retrieved from https://www.ncbi.nlm.nih.gov/pubmed/4578091

Wibo, M., & Poole, B. (1974). Protein degradation in cultured cells. II. The uptake of chloroquine by rat fibroblasts and the inhibition of cellular protein degradation and cathepsin B1. *J Cell Biol, 63*(2 Pt 1), 430-440. doi:10.1083/jcb.63.2.430

Winslow, A. R., Chen, C. W., Corrochano, S., Acevedo-Arozena, A., Gordon, D. E., Peden, A. A., Rubinsztein, D. C. (2010). alpha-Synuclein impairs macroautophagy: implications for Parkinson's disease. *J Cell Biol, 190*(6), 1023-1037. doi:10.1083/jcb.201003122

Winterbourn, C. C. (2013). The biological chemistry of hydrogen peroxide. *Methods Enzymol, 528*, 3-25. doi:10.1016/B978-0-12-405881-1.00001-X

Wolfe, D. M., Lee, J. H., Kumar, A., Lee, S., Orenstein, S. J., & Nixon, R. A. (2013). Autophagy failure in Alzheimer's disease and the role of defective lysosomal acidification. *Eur J Neurosci, 37*(12), 1949-1961. doi:10.1111/ejn.12169

Wolff, N. A., Garrick, L. M., Zhao, L., Garrick, M. D., & Thevenod, F. (2014). Mitochondria represent another locale for the divalent metal transporter 1 (DMT1). *Channels (Austin), 8*(5), 458-466. doi:10.4161/19336950.2014.956564

Wolff, N. A., Garrick, M. D., Zhao, L., Garrick, L. M., Ghio, A. J., & Thevenod, F. (2018). A role for divalent metal transporter (DMT1) in mitochondrial uptake of iron and manganese. *Sci Rep, 8*(1), 211. doi:10.1038/s41598-017-18584-4

Xiong, J., & Zhu, M. X. (2016). Regulation of lysosomal ion homeostasis by channels and transporters. *Sci China Life Sci, 59*(8), 777-791. doi:10.1007/s11427-016-5090-x

Xu, E., Liu, J., Liu, H., Wang, X., & Xiong, H. (2018). Inflammasome Activation by Methamphetamine Potentiates Lipopolysaccharide Stimulation of IL-1beta Production in Microglia. *J Neuroimmune Pharmacol, 13*(2), 237-253. doi:10.1007/s11481-018-9780-y

Xu, H., & Ren, D. (2015). Lysosomal physiology. *Annu Rev Physiol, 77*, 57-80. doi:10.1146/annurev-physiol-021014-071649

Xu, M., Kashanchi, F., Foster, A., Rotimi, J., Turner, W., Gordeuk, V. R., & Nekhai, S. (2010). Hepcidin induces HIV-1 transcription inhibited by ferroportin. *Retrovirology, 7*, 104. doi:10.1186/1742-4690-7-104

Yambire, K. F., Rostosky, C., Watanabe, T., Pacheu-Grau, D., Torres-Odio, S., Sanchez-Guerrero, A., Raimundo, N. (2019). Impaired lysosomal acidification triggers iron deficiency and inflammation in vivo. *Elife, 8*. doi:10.7554/eLife.51031

Yanagawa, M., Tsukuba, T., Nishioku, T., Okamoto, Y., Okamoto, K., Takii, R., Yamamoto, K. (2007). Cathepsin E deficiency induces a novel form of lysosomal storage disorder showing the accumulation of lysosomal membrane sialoglycoproteins and the elevation of lysosomal pH in macrophages. *J Biol Chem, 282*(3), 1851-1862. doi:10.1074/jbc.M604143200

Yang, Y., Yao, H., Lu, Y., Wang, C., & Buch, S. (2010). Cocaine potentiates astrocyte toxicity mediated by human immunodeficiency virus (HIV-1) protein gp120. *PLOS one, 5*(10), e13427. doi:10.1371/journal.pone.0013427

Ye, J., Rawson, R. B., Komuro, R., Chen, X., Dave, U. P., Prywes, R., Goldstein, J. L. (2000). ER stress induces cleavage of membrane-bound ATF6 by the same proteases that process SREBPs. *Mol Cell, 6*(6), 1355-1364. doi:10.1016/s1097-2765(00)00133-7

Ye, Y., Hui, L., Lakpa, K. L., Xing, Y., Wollenzien, H., Chen, X., Geiger, J. D. (2019). Effects of silica nanoparticles on endolysosome function in primary cultured neurons (1). *Can J Physiol Pharmacol, 97*(4), 297-305. doi:10.1139/cjpp-2018-0401

Yogalingam, G., Lee, A. R., Mackenzie, D. S., Maures, T. J., Rafalko, A., Prill, H., LeBowitz, J. H. (2017). Cellular Uptake and Delivery of Myeloperoxidase to Lysosomes Promote Lipofuscin Degradation and Lysosomal Stress in Retinal Cells. *J Biol Chem, 292*(10), 4255-4265. doi:10.1074/jbc.M116.739441

Yoneda, T., Benedetti, C., Urano, F., Clark, S. G., Harding, H. P., & Ron, D. (2004). Compartment-specific perturbation of protein handling activates genes encoding mitochondrial chaperones. *J Cell Sci, 117*(Pt 18), 4055-4066. doi:10.1242/jcs.01275

Yoshida, H., Matsui, T., Hosokawa, N., Kaufman, R. J., Nagata, K., & Mori, K. (2003). A time-dependent phase shift in the mammalian unfolded protein response. *Dev Cell, 4*(2), 265-271. doi:10.1016/s1534-5807(03)00022-4

Yoshimori, T., Yamamoto, A., Moriyama, Y., Futai, M., & Tashiro, Y. (1991). Bafilomycin A1, a specific inhibitor of vacuolar-type H(+)-ATPase, inhibits acidification and protein degradation in lysosomes of cultured cells. *J Biol Chem, 266*(26), 17707-17712. Retrieved from https://www.ncbi.nlm.nih.gov/pubmed/1832676

Yu, L., Chen, Y., & Tooze, S. A. (2018). Autophagy pathway: Cellular and molecular mechanisms. *Autophagy, 14*(2), 207-215. doi:10.1080/15548627.2017.1378838

Zhang, J., Liu, J., Katafiasz, B., Fox, H., & Xiong, H. (2011). HIV-1 gp120-induced axonal injury detected by accumulation of beta-amyloid precursor protein in adult rat corpus callosum. *J Neuroimmune Pharmacol, 6*(4), 650-657. doi:10.1007/s11481-011-9259-6

Zhang, X., Cheng, X., Yu, L., Yang, J., Calvo, R., Patnaik, S., Xu, H. (2016). MCOLN1 is a ROS sensor in lysosomes that regulates autophagy. *Nat Commun, 7*, 12109. doi:10.1038/ncomms12109

Zhao, G. Y., Di, D. H., Wang, B., Zhang, P., & Xu, Y. J. (2014). Iron regulates the expression of ferroportin 1 in the cultured hFOB 1.19 osteoblast cell line. *Exp Ther Med, 8*(3), 826-830. doi:10.3892/etm.2014.1823

Zhao, Q., Wang, J., Levichkin, I. V., Stasinopoulos, S., Ryan, M. T., & Hoogenraad, N. J. (2002). A mitochondrial specific stress response in mammalian cells. *EMBO J, 21*(17), 4411-4419. doi:10.1093/emboj/cdf445

Zhitomirsky, B., & Assaraf, Y. G. (2015). Lysosomal sequestration of hydrophobic weak base chemotherapeutics triggers lysosomal biogenesis and lysosome-dependent cancer multidrug resistance. *Oncotarget, 6*(2), 1143-1156. doi:10.18632/oncotarget.2732

Zhitomirsky, B., Yunaev, A., Kreiserman, R., Kaplan, A., Stark, M., & Assaraf, Y. G. (2018). Lysosomotropic drugs activate TFEB via lysosomal membrane fluidization and consequent inhibition of mTORC1 activity. *Cell Death Dis, 9*(12), 1191. doi:10.1038/s41419-018-1227-0

Zigdon, H., Meshcheriakova, A., Farfel-Becker, T., Volpert, G., Sabanay, H., & Futerman, A. H. (2017). Altered lysosome distribution is an early neuropathological event in neurological forms of Gaucher disease. *FEBS Lett, 591*(5), 774-783. doi:10.1002/1873-3468.12591

Zucchini, S., Pittaluga, A., Brocca-Cofano, E., Summa, M., Fabris, M., De Michele, R., Simonato, M. (2013). Increased excitability in tat-transgenic mice: role of tat in HIV-related neurological disorders. *Neurobiol Dis, 55*, 110-119. doi:10.1016/j.nbd.2013.02.004